



Javaheri, A., Kruse, T., Moones, K., Mejías-Luque, R., Debraekeleer, A., Asche, I., ... Gerhard, M. (2016). *Helicobacter pylori* adhesin HopQ engages in a virulence-enhancing interaction with human CEACAMs. *Nature Microbiology*, 2, [16189]. DOI: 10.1038/nmicrobiol.2016.189

Peer reviewed version

Link to published version (if available):
[10.1038/nmicrobiol.2016.189](https://doi.org/10.1038/nmicrobiol.2016.189)

[Link to publication record in Explore Bristol Research](#)
PDF-document

This is the author accepted manuscript (AAM). The final published version (version of record) is available online via Nature at <http://www.nature.com/articles/nmicrobiol2016189>. Please refer to any applicable terms of use of the publisher.

University of Bristol - Explore Bristol Research

General rights

This document is made available in accordance with publisher policies. Please cite only the published version using the reference above. Full terms of use are available:
<http://www.bristol.ac.uk/pure/about/ebr-terms.html>

1 ***H. pylori* adhesin HopQ engages in a virulence-enhancing interaction with**
2 **human CEACAMs**
3
4
5

6 Anahita Javaheri^{1,15,‡}, Tobias Kruse^{2,‡}, Kristof Moonens^{3,4,‡}, Ayla Debraekeleer^{3,4}, Raquel
7 Mejías-Luque^{1,15}, Isabell Asche⁵, Nicole Tegtmeyer⁵, Behnam Kalali^{1,2}, Nina C. Bach⁶,
8 Stephan A. Sieber⁶, Darryl J. Hill⁷, Verena Königer⁸, Christof R. Hauck⁹, Roman
9 Moskalenko¹⁰, Rainer Haas⁸, Dirk H. Busch¹, Esther Klaile^{11,12}, Hortense Slevogt¹¹, Alexej
10 Schmidt^{13,14}, Steffen Backert⁵, Han Remaut^{3,4,‡}, Bernhard B. Singer^{12‡} and Markus
11 Gerhard^{1,2,15‡*}

12
13
14
15 **Affiliations:**

16 ¹Institute for Medical Microbiology, Immunology and Hygiene; Technische Universität
17 München; Munich, 81675, Germany,

18 ²Imevax GmbH, 81675 Munich

19 ³Structural and Molecular Microbiology, Structural Biology Research Center, VIB, Pleinlaan 2, 1050
20 Brussels, Belgium

21 ⁴Structural Biology Brussels, Vrije Universiteit Brussel, Pleinlaan 2, 1050 Brussels, Belgium

22 ⁵Friedrich Alexander University Erlangen, Department of Biology, Division of Microbiology,
23 Erlangen, Germany

24 ⁶Center for Integrated Protein Science Munich, Department Chemie, Institute of Advanced Studies,
25 Technische Universität München, 85747 Garching, Germany

26 ⁷School of Cellular & Molecular Medicine, University of Bristol, BS8 ITD, Bristol, UK

27 ⁸Max von Pettenkofer-Institut für Hygiene und Medizinische Mikrobiologie, Department of
28 Bacteriology, Ludwig-Maximilians-Universität, D-80336 Munich, Germany

29 ⁹Lehrstuhl für Zellbiologie, Universität Konstanz, Konstanz, Germany

30 ¹⁰Department of Pathology, Sumy State University, Sumy 40000, Ukraine

31 ¹¹Septomics Research Centre, Jena University Hospital, 07745 Jena, Germany.

32 ¹²Center for Sepsis Control and Care (CSCC), Jena University Hospital, 07747 Jena, Germany

33 ¹³Institute of Anatomy, Medical Faculty, University Duisburg-Essen, 45122 Essen, Germany

34 ¹⁴Department of Medical Biosciences, Pathology, Umeå University, SE-901 85 Umeå, Sweden

35 ¹⁵German Center for Infection Research, Partner Site Munich, Munich, Germany

36 *Correspondence to: markus.gerhard@tum.de

37 ‡ These authors contributed equally to this work

38 **Summary:** *Helicobacter pylori* specifically colonizes the human gastric epithelium and is the
39 major causative agent for ulcer disease and gastric cancer development. Here we identified
40 members of the carcinoembryonic antigen-related cell adhesion molecule (CEACAM) family
41 as novel receptors of *H. pylori* and show that HopQ is the surface-exposed adhesin that
42 specifically binds human CEACAM1, CEACAM3, CEACAM5 and CEACAM6. HopQ -
43 CEACAM binding is glycan-independent and targeted to the N-domain. *H. pylori* binding
44 induces CEACAM1 mediated signaling, and the HopQ-CEACAM1 interaction enables
45 translocation of the virulence factor CagA into host cells, and enhances the release of pro-
46 inflammatory mediators such as interleukin-8. Based on the crystal structure of HopQ, we
47 found that a β -hairpin insertion (HopQ-ID) in HopQ's extracellular 3+4 helix bundle domain
48 is important for CEACAM binding. A peptide derived from this domain competitively
49 inhibits HopQ-mediated activation of the Cag virulence pathway, as genetic or antibody-
50 mediated abrogation of the HopQ function shows. Together, our data imply the HopQ-
51 CEACAM1 interaction as potentially promising novel therapeutic target to combat *H. pylori*-
52 associated diseases.

53

54 *Helicobacter pylori* (*H. pylori*) is one of the most prevalent human pathogens,
55 colonizing half of the world's population. Chronic inflammation elicited by this bacterium is
56 the main cause of gastric cancer¹. During co-evolution with its human host over more than
57 60,000 years², the bacterium has acquired numerous adaptations for the long-term survival
58 within its unique niche, the stomach. This includes the ability to buffer the extreme acidity of
59 this environment, the interference with cellular signaling pathways, the evasion of the human
60 immune response and a strong adhesive property to host cells³. Specifically, *H. pylori*
61 persistence is facilitated by the binding of BabA and SabA adhesins to the human blood group
62 antigen Leb and the sLex antigen, respectively⁴⁻⁶. However, adhesion to blood group antigens
63 is not universal, is dynamically regulated during the course of infection and can also be turned
64 off⁷. We observed that *H. pylori* was capable of binding to human gastric epithelium of non-
65 secretors. Therefore, we hypothesized that the bacterium might be able to interact with other
66 cell surface receptors to ensure persistent colonization.

67 We here show that the *H. pylori* adhesin HopQ specifically interacts with human
68 carcinoembryonic antigen-related cell adhesion molecules (CEACAMs). CEACAMs embrace
69 a group of immunoglobulin superfamily-related glycoproteins with a wide tissue distribution.
70 CEACAM1 can be expressed in leukocytes, endothelial and epithelial cells, CEACAM3 and
71 CEACAM8 in granulocytes, CEACAM5 and CEACAM7 in epithelial cells and CEACAM6
72 in epithelia and granulocytes. In epithelial cells, transmembrane anchored CEACAM1 as well
73 as glycosylphosphatidylinositol-linked CEACAM5, CEACAM6 and CEACAM7 localize to
74 the apical membrane⁸. CEACAMs modulate diverse cellular functions such as cell adhesion,
75 differentiation, proliferation, and cell survival. Some CEACAMs were recognized as valuable
76 tumor markers due to their enlarged expression in the malignant tissue and increased sera
77 level⁹. In recent years, CEACAMs have also emerged as immunomodulatory mediators¹⁰.
78 Interestingly, in humans, several CEACAMs have been found to specifically interact with
79 bacteria such as *Neisseria*, *Haemophilus influenzae*, *Moraxella catarrhalis*, and *Escherichia*
80 *coli*¹¹.

81

82 ***H. pylori* binds to CEACAMs expressed in human stomach**

83 Based on the observation that *H. pylori* efficiently colonizes individuals in the absence of
84 Lewis blood group antigens¹² on the one hand, and the increased expression of members of
85 the carcinoembryonic antigen-related cell adhesion molecule family (CEACAMs) in gastric
86 tumors, we hypothesized that *H. pylori* may employ CEACAMs as receptors. Using pull
87 down and flow cytometric approaches we found a robust interaction of the *H. pylori* strain

88 G27 with recombinant human CEACAM1-Fc (Fig. 1a), comparable to that of *Moraxella*
89 *catarrhalis* (Extended Data Fig. 1a and b). As negative control, *Moraxella lacunata* did not
90 bind to human CEACAM1, nor did *Campylobacter jejuni*, a pathogen closely related to *H.*
91 *pylori* (Extended Data Fig. 1a and b). When testing for CEACAM specificity, we observed a
92 clear interaction of *H. pylori* also with CEACAM3, 5 and 6, but not with CEACAM8 (Fig.1b
93 and Extended Data Fig. 1c and d). Importantly, all *H. pylori* strains tested bound to these
94 CEACAMs (Extended Data Fig.1f and g) including well-characterized reference strains
95 (26695, J99) and the mouse-adapted strain SS1. However, binding strength differed among
96 strains, with some preferentially binding to CEACAM1, and others to CEACAM5 and/or
97 CEACAM6 (Extended Data Fig. 1f and g). We then analyzed the expression profiles of
98 CEACAM1, CEACAM5 and CEACAM6 in normal and inflamed human stomach tissues and
99 gastric cancer. If at all low levels of CEACAM1 and CEACAM5 were expressed at the apical
100 side of epithelial cells, and their expression, as well as that of CEACAM6, was up-regulated
101 upon gastritis and in gastric tumors (Fig. 1c and Extended Data Fig. 1e). During infection, *H.*
102 *pylori*-induced responses may thus lead to increased expression of its CEACAM-receptors.
103 Adhesins from other bacteria were shown to specifically bind to the N-domain of human
104 CEACAM1^{13,14}. Similarly, we found that lack of the CEACAM1 N-domain abolished *H.*
105 *pylori* binding completely (Fig. 1d). While for the interaction of *Neisseria meningitidis* with
106 CEACAM1 the N-domain was necessary but not sufficient for binding¹⁵, we observed binding
107 of *H. pylori* to all tested CEACAM1 isoforms containing the N-domain, as well as to the N-
108 domain alone (Fig. 1e). However, binding to the N-domain alone was weaker than to the N-
109 A1-B CEACAM1 variant, which bound less than the N-A1-B-A2 variant (Fig. 1e and
110 Extended Data Fig.1j), suggesting that these domains stabilize the CEACAM1-*H.pylori*
111 interaction. Comparison of the respective N-domains indicated several residues conserved in
112 CEACAM1, 5, and 6 but not in CEACAM8 (Extended Data Fig. 1h).

113

114 **Species specificity of *Helicobacter* – CEACAM interaction**

115 Although, murine and Mongolian gerbil models are routinely used to study gastric infection
116 with *H. pylori*, the bacterium has been described so far to be naturally transmitted to only
117 humans and non-human primates. Although CEACAMs are found in most mammalian
118 species, and have a high degree of conservation, we found *H. pylori* to bind selectively to
119 human, but not to mouse, bovine or canine CEACAM1 orthologues (Fig. 2a). However, we
120 were surprised to find a strong interaction of *H. pylori* with rat-CEACAM1 (Fig. 2b and d).
121 This interaction was also mediated through the N-domain of rat-CEACAM1 (Fig. 2c and d).

122 To substantiate these findings, we transfected human, mouse or rat-CEACAM1 into CHO
123 cells, to which *H. pylori* does not adhere otherwise. Using confocal laser scanning
124 microscopy, we observed *de novo* adhesion of *H. pylori* to CHO cells expressing human and
125 rat, but not mouse CEACAM1 (Fig. 2e), which could be confirmed by pull down and Western
126 blotting of lysates from transfected cells (Fig. 2f and Extended Data Fig. 2d). This finding
127 makes *H. pylori* the first pathogen for which its CEACAM binding is not restricted to one
128 species. Comparing the protein sequences of the CEACAM1-N domains, several amino acids
129 conserved in human and rat differ in mouse (i.e. asn10, glu26, asn42, tyr48, pro59, thr66,
130 asn77, val79, val89, ile90, glu103, tyr108) (Extended Data Fig. 2a). In addition, our findings
131 of the lack of binding to mouse CEACAM1 may explain the differences seen in pathology
132 between infected mice and humans¹⁶.

133 The genus *Helicobacter* comprises several other spp. i.e. *H. felis*, *suis*, and *bizzozeronii* as
134 well as the human pathogenic *H. bilis* and *H. heilmannii*. When assessing the interaction of
135 these *Helicobacters* with human CEACAMs, only *H. bilis* bound to human CEACAM1, 5 and
136 6 (Extended Data Fig.2b and c). As *H. pylori*, *H. bilis* interacted with the N-domain of hu-
137 CEACAM1 (Extended Data Fig.2b and c). This interaction may explain how *H. bilis* manages
138 to colonize human bile ducts, where high levels of constitutively expressed CEACAM1 are
139 present.

140

141 **HopQ is the *Helicobacter* adhesin interacting with CEACAMs**

142 In order to identify the CEACAM-binding partner in *Helicobacter*, we initially screened a
143 number of *Helicobacter* mutants devoid of defined virulence factors that have been shown to
144 be implicated in various modes of host cell interaction (BabA, SabA, AlpA/B, VacA, gGT,
145 urease and the *cagPAI*)^{5,6,17}. All of these mutants still bound to hu-CEACAM1 (Fig. 3a).
146 Therefore we established an immunoprecipitation approach (Extended Data Fig. 3a) using *H.*
147 *pylori* lysate and recombinant hu-CEACAM1-Fc coupled to protein G. Mass spectrometric
148 analysis of the co-precipitate identified two highly conserved *H. pylori* outer membrane
149 proteins as candidate CEACAM1 adhesins: HopQ and HopZ (Fig. 3b). Unlike a *hopZ* mutant,
150 a *hopQ* deletion mutant was devoid of CEACAM1 binding (Fig. 3c). Importantly, the *hopQ*
151 mutant was also unable to bind to CEACAM5 and 6 (Fig.3c).

152 Next we tested the binding of recombinant HopQ to different gastric cancer cell lines and
153 found that HopQ interacted with AGS and MKN45 both endogenously expressing
154 CEACAMs (Extended Data Fig.3b). HopQ did not bind to the CEACAM negative cell line
155 MKN28. Utilizing our CHO transfectants, we found that the recombinant HopQ interacted

156 preferentially with CEACAM1 and 5, and to lesser extent to CEACAM3 and 6. No binding
157 was observed to CHO cells expressing either CEACAM4, 7, or 8 (Extended Data Fig. 3c).
158 HopQ is a member of a *H. pylori*-specific family of outer membrane proteins, and shows no
159 significant homology to other CEACAM-binding adhesins from other Gram-negative
160 bacteria, i.e. Opa proteins or UspA1 from *Neisseria meningitidis* and *Neisseria gonorrhoeae*
161 or *Moraxella catarrhalis*, respectively, and is therefore a novel bacterial factor hijacking
162 CEACAMs. Like Opa and UspA1^{13,14}, HopQ targets the N-terminal domain in CEACAMs,
163 an interaction we found to require folded protein (see below) and was dependent on
164 CEACAM sequence, resulting in specificity for human CEACAM1, 3, 5 and 6. The *H. pylori*
165 *hopQ* gene (*omp27*; HP1177 in the *H. pylori* reference strain 26695) exhibits genetic diversity
166 that represents two allelic families¹⁸, type-I and type-II (Extended Data Fig. 3d), of which the
167 type-I allele is found more frequently in *cag*(+)/*s1-vacA* type strains. Both alleles share 75 to
168 80% nucleotide sequences and exhibit a homology of 70% at the amino acid level¹⁸.
169 Importantly, *hopQ* genotype shows a geographic variation, with the *hopQ* type-I alleles more
170 prevalent in Asian compared to Western strains; and was also found to correlate with strain
171 virulence, with type-I alleles associated with higher inflammation and gastric atrophy¹⁹.

172

173 **Structure and binding properties of the HopQ adhesin domain**

174 HopQ belongs to a paralogous family of *H. pylori* outer membrane proteins (Hop's), to which
175 also the blood group antigen binding adhesins BabA and SabA belong^{5,6,17,20}. To gain insight
176 into its structure-function relationship we determined the binding properties and X-ray
177 structure of a HopQ fragment corresponding to its predicted extracellular domain (residues
178 17-444 of the mature protein; HopQ^{AD}; Fig. 4a). HopQ^{AD} showed strong, dose dependent
179 binding to the N-terminal domain of human CEACAM1 (C1ND; residues 35-142) in ELISA
180 (Fig. 4b) and isothermal titration calorimetry (ITC) revealed a 1:1 stoichiometry with a
181 dissociation constant of 296±40 nM (Extended Data Fig. 4a). The HopQ^{AD} X-ray structure
182 shows that, like BabA and SabA, the HopQ ectodomain adopts a 3+4-helix bundle topology,
183 though lacks the extended coiled-coil “stem” domain that connects the ectodomain to the
184 transmembrane region (Fig. 4a and Extended Data Fig.4d). In BabA, the carbohydrate binding
185 site resides fully in a 4-stranded β-domain that is inserted between helices 4 and 5²¹ (Extended
186 Data Fig.4d). In HopQ, a 2-stranded β-hairpin is found in this position (residues 180-218).
187 Removal of the β-hairpin resulted in a soluble protein that showed a ~10 fold reduction of
188 CEACAM1 binding affinity (Fig. 4b and Extended Data Fig. 4c), indicating that although the

189 HopQ insertion domain is implicated in binding, it does not comprise the full binding site as
190 found in BabA (Fig. 4b).

191 The hitherto characterized Hop adhesins are lectins^{5,6,17,22}. Instead, *H. pylori* was seen to
192 retain binding to CEACAM1 upon enzymatic deglycosylation, and Far Western analysis
193 revealed that HopQ^{AD} specifically bound folded, but not denatured C1ND (Fig. 4c),
194 suggesting HopQ-CEACAM binding relies on protein-protein rather than glycan-dependent
195 interactions. Indeed, ITC binding profiles of HopQ^{AD} titrated with non-glycosylated *E. coli*
196 expressed C1ND (Ec-C1ND) revealed an equimolar interaction with a dissociation constant of
197 417±48 nM (Extended Data Fig. 4b), showing that CEACAM N-glycosylation only provides
198 a minor stabilizing contribution to the HopQ-CEACAM interaction. To further map the HopQ
199 binding site, we pre-incubated CEACAM1 with the *M. catarrhalis* adhesin UspA1, and found
200 that this prevented binding by *H. pylori* (Fig. 4d), suggesting that both adhesins have
201 overlapping binding epitopes. In further support, mutation of CEACAM1 residues Y34 or I91
202 within the UspA1 binding epitope reduced or nearly abrogated CEACAM1 binding by *H.*
203 *pylori* (Fig. 4e). Interestingly, I91 is conserved in rat but mutated to T in mouse CEACAM1,
204 possibly explaining the observed species specificity in HopQ binding (Extended Data Fig. 2a,
205 see above).

206

207 **HopQ – CEACAM1 interaction triggers cell responses**

208 Available animal models only partially replicate the *H. pylori* pathogenesis observed in its
209 human host and mouse CEACAMs did not support HopQ binding. Therefore, to further
210 investigate how HopQ may influence adhesion and cellular responses, we sought to establish
211 cellular pathogenesis models in which the HopQ-CEACAM mediated adhesion could be
212 analyzed. According to Singer et al.²³, we characterized various gastric cell lines typically
213 employed for *H. pylori in vitro* experiments regarding their expression of CEACAMs, and
214 observed that MKN45, KatoIII and AGS did express CEACAM1, CEACAM5 and
215 CEACAM6, whereas MKN28 showed no presence of CEACAMs (Extended Data Fig.5a and
216 b). In parallel, CHO cells were stably transfected with CEACAM1-L (containing the
217 immunoreceptor tyrosine-based inhibition motif (ITIM). Upon infection with *H. pylori* wild-
218 type strain P12 and its isogenic *hopQ* deletion mutant, we observed a significantly reduced
219 adherence to CHO-CEACAM1-L, MKN45 and AGS cells when *hopQ* was not present, while
220 strains deficient in the adhesins BabA and SabA showed only slightly reduced adhesion (Fig.
221 5a and Extended Data Fig.5c). HopQ binding was also studied in human gastric biopsies from
222 *H. pylori* infected individuals. Here, we detected that HopQ bound to the apical side human

223 gastric epithelium and co-localized with CEACAM in biopsies from *H. pylori* infected
224 individuals (Fig. 5b and Extended Data Fig. 5d), while no binding was observed in
225 CEACAM1 negative samples from normal stomach (not shown). In CHO-CEACAM1-L
226 cells, we observed tyrosine-phosphorylation of the CEACAM1 ITIM domain upon exposure
227 to *H. pylori*, which was apparent within 5 minutes, and was maintained for up to 1 hour
228 (Fig.5c). Phosphorylation of the CEACAM1 ITIM domain is a well-known initial event
229 triggering SHP1/2 recruitment inducing downstream signaling cascades^{24,25}. Contact-
230 dependent signaling through CEACAMs is a common means of modulating immune
231 responses related to infection, inflammation and cancer¹⁰, and these immune-dampening
232 cascades likely reflect the multiple independent emergence of non-homologous CEACAM-
233 interacting proteins in diverse mucosal Gram-negative pathogens including *Neisseria*,
234 *Haemophilus*, *Escherichia*, *Salmonella*, *Moraxella* sp.^{13,14}. For *H. pylori*, interaction with
235 human CEACAM1 through HopQ may represent a critical parameter for immuno-modulatory
236 signaling during colonization and chronic infection of man.

237 Additionally, *hopQ* mutant *H. pylori* strains showed an almost complete loss of *cagPAI*-
238 dependent CagA translocation (Fig. 5d) and strongly reduced IL-8 induction (Fig.5e), while
239 loss of other known adhesins had no effect on CagA delivery (Extended Data Fig.5e and f).
240 This is in line with a previous study showing that in AGS gastric cancer cells, a *hopQ* mutant
241 *H. pylori* strain exhibited reduced ability to activate NF- κ B and altered translocation of
242 CagA²⁶. In contrast to our findings, Belogolova et al. did not observe reduced adherence of a
243 *hopQ* mutant *H. pylori* P12 strain, which could be due to the observed growth dependent
244 expression of CEACAMs in these cells.

245 To corroborate our data in an independent model and compensate for potential clonal effects
246 in stably transfected cells, we transiently transfected HEK293 cells with human CEACAM (1-
247 L,3,4,5,6,7,8) expression plasmids. Infection of these cells confirmed the defect in CagA
248 translocation observed in CHO-CEACAM1-L cells, which was restored upon
249 complementation of the *hopQ* mutant strain (P12 Δ *hopQ**hopQ*⁺) (Fig.5f and Extended Data
250 Fig.5g). Also, cellular elongation, the so called “hummingbird phenotype”, was significantly
251 reduced upon deletion of *hopQ* (Fig. 5g and h). Further, we observed that *H. pylori* modulates
252 important host transcription factors such as Myc or STAT3, in a *hopQ*-dependent fashion
253 (Extended Data Fig. 5h). Our results reveal that HopQ-CEACAM binding leads to direct and
254 indirect alterations in host cell signaling cascades, and start to shed light on these HopQ-
255 associated virulence landscapes. Given the importance of these signaling events for gastric
256 carcinogenesis, we explored if the CEACAM-HopQ interaction could be targeted in order to

257 prevent CagA translocation and downstream effects. Indeed, incubation of the cells with an α -
258 CEACAM1 antibody, α -HopQ antiserum or a HopQ-derived peptide corresponding to the
259 Hop-ID (aa 189-220) reduced CagA translocation in a dose dependent manner (Fig. 5i-k), but
260 not corresponding controls (Extended Data Fig. 5h). These data demonstrate that the HopQ-
261 CEACAM1 interaction is necessary for successful translocation of the oncoprotein CagA into
262 epithelial cells as well as modulation of inflammatory signaling, and that interference with
263 this interaction can prevent CagA translocation, giving an indication of the translational
264 potential of HopQ targeting for *H. pylori* vaccination or immunotherapy.

265

266 **Deletion of *hopQ* abrogates colonization in a rat model of *H. pylori* infection**

267 As we have found binding of HopQ to human and rat, but not to mouse CEACAM, we finally
268 determined the role of HopQ *in vivo*, using a rat model of *H. pylori* infection. Having
269 observed that CEACAM1 was expressed in normal rat stomach (Fig. 6a and Extended Data
270 Fig. 6b), we infected rats with the mouse adapted strain SS1, able to bind human and rat
271 CEACAM1 (Extended Data Fig. 6a). While the wild type SS1 was able to efficiently colonize
272 rats, albeit at lower levels compared to the mouse, (Fig. 6b) , the *hopQ* deficient SS1 strain
273 was not able to colonize rats at detectable levels, and could not induce an inflammatory
274 response in comparison to the wild type SS1 strain (Fig. 6b and c). Therefore, in this model,
275 HopQ seems also to serve as an important factor to mediate *H. pylori* colonization. While
276 infection of rats with *H. pylori* has been described²⁷, our finding may allow the establishment
277 of an animal model for studying *H. pylori* infection that better replicates the prevailing
278 virulence pathways.

279

280 **Discussion**

281 The here identified CEACAM-binding property provides *H. pylori* a means of
282 epithelial adherence in addition to the Lewis antigens used by the BabA and SabA
283 adhesins^{5,6,17}. While over-expression of CEACAMs in gastrointestinal tumors is well
284 described, their up-regulation during *H. pylori*-induced inflammation in the stomach has not
285 been reported so far, suggesting the pathogen has the ability to shape its own adhesive niche.
286 A similar phenomenon has also been observed for the inflammation-induced up-regulation of
287 sialylated antigens that form the receptors for the SabA adhesin⁶. A plausible route to
288 CEACAM modulation is through the transcription factors NF- κ B and AP1, both of which are
289 induced during *H. pylori* infection²⁸ and are known to regulate CEACAM expression²⁹.
290 Though HopQ-dependent adherence may appear redundant to that of other adhesins like
291 BabA, SabA or LabA, HopQ specializes on human CEACAMs and is required for *cagPAI*
292 functionality. From the perspective of host-pathogen (i.e. human-*H. pylori*) co-evolution, the
293 primary function of HopQ may lie in immune-modulation through CEACAM binding, and
294 HopQ's indirect effects on other virulence cascades elicited by *H. pylori* such as that induced
295 by increased CagA delivery may not have been initially "intended". The *cagPAI* was acquired
296 by ancestral *H. pylori* in a single event that occurred before modern humans migrated out of
297 East Africa around 58,000 years ago³⁰. Thus, it is likely that the employment of CEACAM1
298 ligation by *H. pylori* occurred much earlier to support colonization and to modulate immune
299 responses. This assumption is supported by the fact that all fully sequenced *H. pylori* strains
300 bear *hopQ* (Extended Data Fig.3d), indicating that this is an essential outer membrane protein
301 of *H. pylori*. Upon occurrence of type-I *H. pylori* strains by *cagPAI* acquisition more than
302 60,000 years ago³⁰ this ancient survival strategy was further implemented into a mechanism
303 supporting pathogenicity, and thus may have contributed to the switch from commensal to
304 pathogenic *H. pylori*³¹. Pathogenicity might even be further aggravated by our observation
305 that CEACAMs are strongly up-regulated during gastritis, which further potentiates binding
306 of *H. pylori* to epithelial cells and specifically facilitates CagA/*cagPAI* interaction with the
307 host cells.

308 Taken together, the finding that *H. pylori* employs CEACAMs not only for bacterial
309 adherence but also to induce cellular signaling may lead to a better understanding of the
310 pathogenic mechanisms of these bacteria and might lead to novel therapeutic approaches to
311 more effectively combat this highly prevalent infection and the associated gastric pathology.

312
313

314

315 **Materials and Methods**

316

317 **Bacteria and bacterial growth conditions**

318 The *H. pylori* strains G27³², PMSS1³³, SS1³⁴, J99 (ATCC, 700824), 2808³⁵, 26695 (ATCC,
319 70039), TX30³⁶, 60190³⁷, P12³⁸, NCTC11637 (ATCC, 43504), Ka89 and *H. bilis*
320 (ATCC43879) were grown on Wilkins–Chalgren blood agar plates under microaerobic
321 conditions (10% CO₂, 5% O₂, 8.5% N₂, and 37°C). *H. suis*³⁹ and *H. heilmannii*⁴⁰ were grown
322 on Brucella agar and *H. felis* (ATCC 49179) and *H. bizzozeronii*⁴¹ on brain-heart infusion
323 (BHI) agar supplemented with 10% horse blood. *Moraxella catarrhalis* (ATCC, 25238)
324 provided by C. R. Hauck (Konstanz Research School Chemical Biology, University of
325 Konstanz, Germany), *Moraxella Lacunata* (ATCC 17967) and *Campylobacter jejuni* (ATCC,
326 33560) were cultured on brain–heart infusion (BHI) agar supplemented with 5% heated horse
327 blood overnight at 37°C in a CO₂ incubator. The generation of an isogenic Δ *hopQ* mutant has
328 been done by replacement of the entire gene by a chloramphenicol resistance cassette. For
329 genetic complementation of *hopQ*, the 1,926 bp gene fragment of *H. pylori* strain P12 was
330 amplified by PCR. This fragment was cloned into the complementation vector pSB1001 using
331 the AphA3 cassette for selection. This fusion construct was introduced in the plasticity region
332 of strain P12 Δ *hopQ* (between ORFs HP0999 and HP1000) using a strategy as described⁴².

333 **Production of CEACAM proteins**

334 The cDNA, which encodes the extracellular domains of human CEACAM1-Fc (consisting of
335 N-A1-B1-A2 domains), human CEACAM1dN-Fc (consisting of A1-B1-A2, lacking the first
336 143 amino acids of the N-terminal IgV-like domain), rat CEACAM1-Fc (consisting of N-A1-
337 B1-A2), rat CEACAM1dN-Fc (consisting of A1-B1-A2), human CEACAM3-Fc (consisting
338 of N), human CEACAM6-Fc (consisting of N-A-B), human CEACAM8-Fc (consisting of N-
339 A-B), respectively, were fused to a human heavy chain Fc-domain and cloned into the
340 pcDNA3.1(+) expression vector (Invitrogen, San Diego, CA), sequenced and stably
341 transfected into HEK293 (ATCC CRL-1573) cells as described⁴³. The Fc chimeric CEACAM-
342 Fc proteins were accumulated in serum-free Pro293s-CDM medium (Lonza) and were
343 recovered by Protein A/G-Sepharose affinity Chromatography (Pierce). Proteins were
344 analyzed by SDS-PAGE and stained by Coomassie blue demonstrating an equal amount and
345 integrity of the produced fusion proteins (Extended Data Fig. 1i). Recombinant-human
346 CEACAM5-Fc was ordered from Sino Biological Inc. The GFP-tagged CEACAMs (human-
347 CEACAM1 and its variants, mouse-CEACAM1, bovine-CEACAM1 and canine-CEACAM1)

348 were provided by Dr. C. R. Hauck (University Konstanz, Germany). For production of the
349 recombinant human CEACAM1 N-Domain (C1ND), the annotated domain (residues 35-142
350 of CEACAM1, Uniprot ID: P13688) was first backtranslated using the Gene
351 Optimizer[®] (LifeTechnologies) and the leader sequence of the Igk-chain as well as a C-
352 terminal Strep-Tag II was added. The gene was synthesized and seamlessly cloned into
353 pCDNA3.4-TOPO (LifeTechnologies). Protein was produced in a 2 L culture of Expi293
354 cells according to the Expi293 expression system instructions (LifeTechnologies).
355 The resulting supernatant was concentrated and diafiltered against ten volumes of 1x
356 SAC buffer (100 mM Tris-HCl, 140 mM NaCl, 1 mM EDTA, pH 8.0) by crossflow-
357 filtration, using a Hydrosart 5 kDa molecular-weight cutoff membrane (Sartorius). The
358 retentate was loaded onto a StrepTrap HP column (GE Healthcare) and eluted with 1x SAC
359 supplemented with 2.5 mM D-Desthiobiotin (IBA). The protein was stored at +4°C.

360 For the bacterial expression of the C1ND (Ec-C1ND) the amino acid sequence (residues 35-
361 142 of CEACAM1, Uniprot ID: P13688) was codon optimized for expression in *E. coli*,
362 synthesized by GeneArt *de novo* gene synthesis (Life Technologies), and cloned with a C-
363 terminal His6 tag in the pDEST[™]14 vector using Gateway technology (Invitrogen). *E. coli*
364 C43(DE3) cells were transformed with the resulting construct and grown in LB supplemented
365 with 100 µg/mL ampicillin at 37°C while shaking. At OD₆₀₀=1 Ec-C1ND expression was
366 induced with 1 mM IPTG overnight at 30°C. Cells were collected by centrifugation at 6.238 g
367 for 15 minutes at 4°C and resuspended in 50mM Tris-HCl pH 7.4, 500 mM NaCl (4 mL/g wet
368 cells) supplemented with 5 µM leupeptin and 1 mM AEBSF, 100 µg/mL lysozyme, and 20
369 µg/mL DNase I. Subsequently cells were lysed by a single passage in a Constant System Cell
370 Cracker at 20 kPsi at 4 °C and debris was removed by centrifugation at 48.400 g for 40
371 minutes. The cytoplasmic extract was filtrated through a 0.45 µm pore filter and loaded on a 5
372 mL pre-packed Ni-NTA column (GE Healthcare) equilibrated with buffer A (50 mM Tris-
373 HCl pH 7.4, 500 mM NaCl and 20 mM imidazole). The column was then washed with 40 bed
374 volumes of buffer A and bound proteins were eluted with a linear gradient of 0-75 % buffer B
375 (50 mM Tris-HCl pH 7.4, 500 mM NaCl and 500 mM imidazole). Fractions containing Ec-
376 C1ND, as determined by SDS-PAGE, were pooled and concentrated in a 10 kDa MW cutoff
377 spin concentrator to a final volume of 5 ml. To remove minor protein contaminants, the
378 concentrated sample was injected onto the Hi-Prep[™] 26/60 Sephacryl S-100 HR column (GE
379 Healthcare) pre-equilibrated with a buffer containing 50 mM Tris-HCl pH 8.0, 150 mM NaCl.
380 Fractions containing the Ec-C1ND complex were pooled and concentrated using a 10 kDa
381 MW cutoff spin concentrator.

382

383

384 **HopQ^{AD} and HopQ^{AD}ΔID cloning, production and purification**

385 In order to obtain a soluble HopQ fragment, the HopQ gene from the *H. pylori* G27 strain
386 (accession No. CP001173 Region: 1228696..1230621) HopQ fragment ranging from residues
387 37 – 463 was produced (residues 17-444 of the mature protein), thus removing the N-terminal
388 β-strand and signal peptide, as well as the C-terminal β-domain expected to represent the TM
389 domain. In HopQ^{AD}ΔID, the amino acids 184-212 of the mature protein were replaced by two
390 glycines (Extended Data Fig.f). DNA coding sequences corresponding to the HopQ type I
391 fragments was PCR-amplified from *H. pylori* G27 genomic DNA using primers (forward:
392 GTTTAACTTTAAGAAGGAGATATACAAATGGCGGTTCAAAAAGTGAAAAACGC;
393 reverse: TCAAGCTTATTAATGATGATGATGATGGTGGGCGCCGTTATTCGTGGTTG),
394 containing 30bp overlap to the flanking target vector sequences of pPRkana-1, a derivative of
395 pPR-IBA 1 (IBA GmbH) with the ampicillin resistance cassette replaced by the kanamycin
396 resistance cassette, under a T7 promotor. In parallel, the vector was PCR-amplified using
397 primers (forward: CACCATCATCATCATTAATAAGCTTGATCCGGCTGCTAAC ;
398 reverse: GTTTAACTTTAAGAAGGAGATATACAAATG) as provided in table 1, using the
399 same overlapping sequences in reversed orientation. The forward primer additionally carried
400 the sequence for a 6x His-tag. The amplicons were seamlessly cloned using Gibson Assembly
401 (New England Biolabs GmbH). Based on codon optimized HopQ^{AD} plasmid, the HopQ^{AD}ΔID
402 constructs were cloned. The plasmids were amplified by 5' phosphorylated primers (forward:
403 GGTGACGCTCAGAACCTGCTGAC; reverse: ACCACCTTTAGAGTTCAGCGGAG)
404 replacing the ID region by two glycines, *DpnI* (NEB) digested and blunt-end ligated by T4
405 ligase (NEB).

406 *Escherichia coli* BL21(DE3) cells (NEB GmbH) were transformed with the pPRkana-1
407 constructs, grown at 37°C with 275 rpm on auto-inducing terrific broth (TRB) according to
408 Studier⁴⁴, supplemented with 2 mM MgSO₄, 100 mg/L Kanamycin-Sulfate (Carl Roth GmbH
409 + Co. KG), 0.2 g/L PPG2000 (Sigma-Aldrich) and 0.2% w/v Lactose-monohydrate (Sigma-
410 Aldrich), until an OD of 1-2 was reached. Afterwards, the temperature was lowered to 25°C
411 and auto-induced overnight, reaching a final OD of 10-15 the following morning. Cells were
412 harvested by centrifugation at 6000 g for 15 min at 4 °C using a SLA-3000 rotor in a Sorvall
413 RC-6 Plus centrifuge (Thermo Fischer). Prior to cell disruption, cells were resuspended in 10
414 mL cold NiNTA buffer A (500 mM NaCl, 100 mM Tris-HCl, 25 mM Imidazole, pH 7.4) per
415 gram of biological wet weight (BWW), supplemented with 0.1 mM AEBSF-HCl, 150 U/g

416 BWW DNase I and 5 mM MgCl₂ and dispersed with an Ultra-Turrax T25 digital (IKA GmbH
417 + Co. KG). Cell disruption was performed by high-pressure homogenization with a
418 PANDA2000 (GEA NiroSoavi) at 800-1200 bar in 3 passages at 4 °C. The cell lysate was
419 clarified by centrifugation at 25000 g for 30 min at 4 °C in a SLA-1500 rotor and remaining
420 particles removed by filtration through a 0.2 µm filter.

421 HopQ fragments were purified by consecutive nickel affinity and size exclusion
422 chromatography. Briefly, the clarified cell lysate was loaded onto a 5 mL pre-packed Ni-NTA
423 HisTrap FF crude column (GE Healthcare) pre-equilibrated with buffer A, washed with ten
424 column volumes (CV) of buffer A and the bound protein eluted with a 15 CV linear gradient
425 to 75% NiNTA buffer B (500 mM NaCl, 100 mM Tris-HCl, 500 mM Imidazole, pH 7.4).
426 Eluted peak fractions were collected, pooled and concentrated to a final concentration of 8-10
427 mg ml⁻¹ using a 10 kDa molecular-weight cutoff spin concentrator. Subsequently, 5 mL of the
428 concentrated protein were loaded onto a HiLoad 16/600 Superdex 75 pg column (GE
429 Healthcare) pre-equilibrated with Buffer C (5 mM Tris-HCl, 140 mM NaCl, pH 7.3) and
430 eluted at 1 mL/min. Finally, only protein corresponding to the monomer-peak was pooled and
431 stored at +4 °C prior to crystallization. For analyzing the multimerization state of HopQ^{AD},
432 SEC was performed on a Superdex 200 10/300 GL (GE Healthcare) with 24 mL bed volume.
433 The column was pre-equilibrated with Buffer C and subsequently, 25 µg protein injected and
434 separated with a flow rate of 0.5 mL/min.

435 The HopQ interaction domain (HopQ-ID) representing peptide was HA-tagged, synthesized
436 (EKLEAHVTTSKYQQDNQTKTTTSVIDTTNYPYDVPDYA) and HPLC purified (Peptide
437 Specialty Laboratories, Heidelberg, Germany). For cellular assays, the lyophilized peptide
438 was dissolved in sterile PBS to a concentration of 1 mM and dialysed with a 0.1-0.5 kDa
439 molecular-weight cutoff membrane against PBS to remove remaining TFA. The peptide
440 solution was stored at -20 °C until further use.

441 **Detection of the HopQ-CEACAM interaction by ELISA**

442 For detection of the interaction between CEACAM and HopQ^{AD}, recombinant C1ND (1
443 µg/mL) in PBS was coated over night at 4 °C onto a 96-well immunoplate (Nunc MaxiSorb).
444 Wells were blocked with SmartBlock (Candor) for 2 h at RT. Subsequently, HopQ fragments
445 were added in a fivefold series dilution ranging from 10 µg/mL to 0.05 ng/mL for 2h at room
446 temperature. Next, α-6xHis-HRP conjugate (clone 3D5, LifeTechnologies) was diluted
447 1:5000 and incubated for 1h at room temperature. For detection, 1-Step™ Ultra TMB-ELISA
448 Substrate Solution (LifeTechnologies) was used and the enzymatic reaction was stopped with

449 2 N H₂SO₄. Washing (3-5x) in between incubation steps was carried out with PBS / 0.05%
450 Tween20.

451 **Isothermal titration calorimetry**

452 ITC measurements were performed on a MicroCal iTC200 calorimeter (Malvern). 25 μ M
453 C1ND or EcC1ND were loaded into the cell of the calorimeter and 250 μ M HopQ^{AD} type I
454 was loaded in the syringe. All measurements were done at 25°C, with a stirring speed of 600
455 rpm and performed in 20 mM HEPES buffer (pH 7.4), 150 mM NaCl, 5% (v/v) glycerol and
456 0.05% (v/v) Tween-20. Binding data were analyzed using the MicroCal LLC ITC200
457 software.

458 **SDS-PAGE and native-PAGE for Western blot**

459 CEACAM was separated with both SDS-PAGE and native-PAGE (resp. on 15% and 7.5%
460 polyacrylamide gels) in ice-cold 25 mM Tris-HCl, 250 mM glycine buffer. Subsequently
461 samples were transferred to PVDF-membranes by wet blotting at 25 V during 60 minutes in
462 ice-cold transfer buffer (25 mM Tris-HCl, 250 mM glycine and 20% methanol). Membranes
463 were blocked during one hour in 10% milk powder (MP), 1x PBS and 0.005% Tween-20.
464 Both membranes were washed and incubated together in 5% MP, 1x PBS, 0.005% Tween-20
465 in presence of 2 μ M HopQ^{AD} type I for one hour to allow complex formation between
466 HopQ^{AD} I and CEACAM. After a washing step the C-terminal His-tag of HopQ (CEACAM is
467 strep tagged) was detected by adding consecutively mouse α -His (AbDSerotec) and goat α -
468 mouse antibody (Sigma-Aldrich) during respectively one hour and 30 minutes in 5% MP, 1x
469 PBS, 0.005% Tween-20. After a washing step the blot was developed by adding BCIP/NBT
470 substrate (5-bromo-4-chloro-3-indolyl-phosphate/nitro blue tetrazolium) (Roche) in
471 developing buffer (10 mM Tris-HCl pH 9.5, 100 mM NaCl, 50 mM MgCl₂).

472 **Bacterial pull down**

473 Bacteria were grown overnight on WC dent agar plates. Bacteria were scraped from plates,
474 suspended in PBS, and colony forming units (cfu) were estimated by optical density 600
475 readings according to a standard curve. Bacteria were washed twice with PBS and
476 2×10^8 cells/mL were incubated with soluble CEACAM-Fc or CEACAM-GFP proteins or
477 CHO cell lysates for 1 h at 37 °C with head-over-head rotation. After incubation, bacteria
478 were washed 5 times with PBS and either boiled in SDS sample buffer (62.5 mM Tris-HCl
479 [pH 6.8], 2% w/v SDS, 10% glycerol, 50 mM DTT, and 0.01% w/v bromophenol blue) prior
480 to SDS-PAGE and Western blotting or taken up in FACS buffer (PBS/0.5% BSA) for flow
481 cytometry analysis.

482 **Immunoprecipitation and Mass Spectrometry**

483 Bacteria (2×10^8) in cold PBS containing protease and phosphatase inhibitors (Roche) were
484 lysed by ultra-sonication on ice (10x, 20s). Cell debris was removed from the lysates by
485 centrifugation at 15,000 rpm for 30 min at 4 °C, followed by pre-clearing with prewashed
486 protein G-agarose (Roche Diagnostics). CEACAM1-Fc was added to the lysate (10 µg) and
487 incubated for 1 h at 4 °C. Prewashed protein G-agarose (60 µL) were added to the antibody
488 and lysate mixture and incubated 2 h at 4 °C. Beads were washed with PBS for five times to
489 remove unspecifically bound proteins. Two-thirds of the beads were separated and used for
490 mass spectrometry sample preparation. The supernatant was removed and the beads were
491 resuspended twice in 50 µL 7M urea/ 2 M thiourea solved in 20 mM Hepes (pH 7.5) for
492 denaturation of the proteins. Beads were pelleted by centrifugation and supernatants pooled
493 and transferred to a new Eppendorf tube. Subsequently, proteins were reduced in 1 mM DTT
494 for 45 min and alkylated at a final concentration of 5.5 mM iodoacetamide for 30 min in the
495 dark. The alkylation step was quenched by raising the DTT concentration to 5 mM for 30
496 min. All incubation steps were carried out at RT under vigorous shaking (Eppendorf shaker,
497 450 rpm). For digestion of the proteins 1 µL LysC (0.5 µg/µL) was added and the sample
498 incubated for 4h at RT. To reduce the urea concentration the sample was diluted 1:4 with 50
499 mM triethylammonium bicarbonate and then incubated with 1.5 µL trypsin (0.5 µg/µL) at 37
500 °C over night. Trypsin was finally inactivated by acidification with formic acid. The
501 supernatant was transferred to a new Eppendorf tube and pooled with the following wash
502 fraction of the beads with 0.1% formic acid. The sample was adjusted to pH 3 with formic
503 acid (100% v/v) and subjected to peptide desalting with a SepPak C18 column (50 mg,
504 Waters). Briefly, the column was subsequently washed with 1 mL 100% acetonitrile and 500
505 µL 80% acetonitrile, 0.5% formic acid. The column was equilibrated with 1 mL 0.1% TFA,
506 the sample was loaded and the column washed again with 1 mL 0.1% TFA. After an
507 additional wash step with 500 µL 0.5% formic acid peptides were eluted twice with 250 µL
508 80% acetonitrile, 0.5% formic acid. The organic phase was then removed by vacuum
509 centrifugation and peptides stored at -80 °C. Directly before measurement peptides were
510 resolved in 20 µL 0.1% formic acid, sonified for 5 min (water bath) and the sample afterwards
511 filtered with a prewashed and equilibrated filter (0.45 µm low protein binding filter, VWR
512 International, LLC). Measurements were performed on an LC-MS system consisting of an
513 Ultimate 3000 nano HPLC directly linked to an Orbitrap XL instrument (Thermo Scientific).
514 Samples were loaded onto a trap column (2 µm, 100 Å, 2 cm length) and separated on a 15
515 cm C18 column (2 µm, 100 Å, Thermo Scientific) during a 150 min gradient ranging from 5

516 to 30% acetonitrile, 0.1% formic acid. Survey spectra were acquired in the orbitrap with a
517 resolution of 60,000 at m/z 400. For protein identification up to five of the most intense ions
518 of the full scan were sequentially isolated and fragmented by collision induced dissociation.
519 The received data was analyzed with the Proteome Discoverer Software version 1.4 (Thermo
520 Scientific) and searched against the *H. pylori* (strain G27) database (1501 proteins) in the
521 SEQUEST algorithm. Protein N-terminal acetylation and oxidation of methionins were added
522 as variable modifications, carbamidomethylation on cysteines as static modifications. Enzyme
523 specificity was set to trypsin and mass tolerances of the precursor and fragment ions were set
524 to 10 ppm and 0.8 Da, respectively. Only peptides that fulfilled X_{corr} values of 1.5, 2.0, 2.25
525 and 2.5 for charge states +1, +2, +3 and +4 respectively were considered for data analysis.

526 **Cells, cell-bacteria co-culture and elongation phenotype quantitation assay**

527 Gastric cancer cell lines MKN45⁴⁵, KatoIII (ATCC, HTB-103), MKN28⁴⁶ and AGS (ATCC,
528 CRL-1739) were obtained from ATCC and DSMZ, authenticated by utilizing Short Tandem
529 Repeat (STR) profiling, cultured either sparse or to tight confluence in DMEM (GIBCO,
530 Invitrogen, Carlsbad CA, USA) containing 2 mM L-glutamine (GIBCO, Invitrogen, CA,
531 USA) supplemented with 10% FBS (GIBCO, Invitrogen, CA, USA) and 1% Penicillin/
532 Streptomycin (GIBCO, Invitrogen, CA, USA). All cell lines were maintained in an incubator
533 at 37°C with 5% CO₂ and 100% humidity, and were routinely mycoplasma-tested twice per
534 year by DAPI stain and PCR. Plate-grown bacteria were suspended in DMEM and washed by
535 centrifugation at 150 g for 5 min in a microcentrifuge. After resuspension in DMEM, the
536 optical density at 600 nm was determined and bacteria were added to the overnight serum-
537 deprived cells at different ratios of bacteria/cell (MOI) at 37°C to start the infection. After the
538 indicated time, cells were washed twice with PBS and then lysed with 1% NP-40 in protease
539 & phosphatase inhibitor PBS. HEK293 cells were chosen for CEACAM transfection studies
540 because the cells were found to be negative for hu-CEACAM expression, and are easily
541 transfectable. HEK cells were grown in 6-well plates containing RPMI 1640 medium
542 (Invitrogen) supplemented with 25 mM HEPES buffer and 10% heat-inactivated FBS
543 (Biochrom, Berlin, Germany) for 2 days to approximately 70% confluence. Cells were serum-
544 deprived overnight and infected with *H. pylori* at MOI 50 for the indicated time points in each
545 figure. After infection, the cells were harvested in ice-cold PBS containing 1 mM Na₃VO₄
546 (Sigma-Aldrich). Elongated AGS cells in each experiment were quantified in 5 different 0.25-
547 mm² fields using an Olympus IX50 phase contrast microscope.

548 **Transfection**

549 A CHO cell line (ATCC) permanently expressing hu-CEACAM1-4L, mouse-CEACAM1-L
550 and rat-CEACAM1-L were generated by stably transfecting cells with 4 µg pcDNA3.1-
551 huCEACAM1-4L, pcDNA3.1-huCEACAM1-4S, pcDNA3.1-msCEACAM1-L, pcDNA3.1-
552 ratCEACAM1-L plasmid (Singer), respectively, utilizing the lipofectamine 2000 procedure
553 according to the manufacturer's protocol (Invitrogen). Stable transfected cells were selected in
554 culture medium containing 1 mg/mL of Genitocinsulfat (G418, Biochrom, Berlin, Germany).
555 The surface expression of CEACAM1 in individual clones growing in log phase was
556 determined by flow cytometry (FACS calibur, BD). HEK293 cells were transfected with 4 µg
557 of the HA-tagged CEACAM constructs or luciferase reporter constructs (Clontech, Germany)
558 for 48 h with TurboFect reagent (Fermentas, Germany) according to the manufacturer's
559 instructions.

560 **Western blot**

561 An equal volume of cell lysate was loaded on 8% SDS-PAGE gels and after electrophoresis,
562 separated proteins were transferred to nitrocellulose membrane (Whatman/GE Healthcare,
563 Freiburg, Germany). Membranes were blocked in 5% non-fat milk for 1 h at room
564 temperature and incubated overnight with primary antibodies mAb 18/20 binding to
565 CEACAM1,3,5, B3-17 and C5-1X (mono-specific for hu-CEACAM1, Singer), 4/3/17
566 (binding to CEACAM1,5, Genovac), and 5C8C4 (mono-specific for hu-CEACAM5, Singer),
567 1H7-4B (mono-specific for hu-CEACAM6, Singer), 6/40c (mono-specific for hu-CEACAM8,
568 Singer), Be9.2 (α-rat-CEACAM1, kindly provided by Dr. W. Reutter, Charite, CBF,
569 Germany), mAb 11-1H (α-rat-CEACAM1ΔN, Singer), phosphotyrosine antibody PY-99
570 (Santa Cruz, LaJolla, CA, USA), α-CagAphosphotyrosine antibody PY-972⁴⁷, mouse
571 monoclonal α-CagA antibody (Austral Biologicals, San Ramon, CA, USA), mouse
572 monoclonal α-CEACAM1 (clone D14HD11Genovac/Aldevron, Freiburg,Germany) or goat
573 α-GAPDH (Santa Cruz). After washing, membranes were incubated with the secondary
574 antibody [HRP-conjugated α-mouse IgG (Promega)] and proteins were detected by ECL
575 Western Blotting Detection reagents. The quantification was done by LabImage 1D software
576 (INTAS).

577 **Flow cytometry**

578 The Fc-tagged CEACAMs (2.5 µg/mL) were incubated with *H. pylori* (OD₆₀₀=1) and
579 subsequently with FITC-conjugated goat α-human IgG (Sigma-Aldrich). After washing with

580 FACS buffer, the samples were analyzed by gating on the bacteria (based on forward and
581 sideward scatter) and measuring bacteria-associated fluorescence. In each case, 10,000 events
582 per sample were obtained. Analysis was performed with the FACS CyAn (Beckman Coulter)
583 and the data were evaluated with FlowJo software (Treestar). For the analysis of CEACAM
584 mediated HopQ binding, indicated cell types (5×10^5 in 50 μL) were incubated with 20 $\mu\text{g}/\text{mL}$
585 of *H. pylori* strain P12 derived, myc and 6x His-tagged recombinant HopQ diluted in 3%
586 FCS/PBS for 1 h on ice. After three times washing with 3% FCS/PBS samples were labeled
587 with 20 $\mu\text{g}/\text{mL}$ of mouse α -c-myc mAb (clone 9E10, AbDSerotec) and subsequently with
588 FITC conjugated goat α -mouse F(ab')₂ (Dianova, Germany). In parallel, the presence of
589 CEACAMs was controlled by staining cells utilizing the rabbit anti CEA pAb (A0115,
590 Dianova) followed by FITC conjugated goat α -rabbit F(ab')₂ (Dianova, Germany).
591 Background fluorescence was determined using isotype-matched Ig mAb. The stained cell
592 samples were examined in a FACScalibur flow cytometer (BD Biosciences, San Diego, CA)
593 and the data were analyzed utilizing the CellQuest software. Dead cells, identified by PI
594 staining, were excluded from the measurement.

595 **Immunohistochemistry and Immunofluorescence**

596 Following approval of the local ethics committee, paraffin-embedded human normal stomach,
597 gastritis and cancer samples were randomly chosen from the tissue bank of the Institut für
598 Pathologie, Klinikum Bayreuth Germany. Histological samples were excluded if tissue
599 quality was poor. After antigen retrieval with 10 mM sodium citrate buffer pH 6 in pressure
600 cooker, the sections were incubated with α -hu-CEACAM1, 5, 6 and α -rat-CEACAM1
601 antibodies (clone B3-17, 5C8C4, 1H7-4B and Be9.2, respectively). Sections were developed
602 with SignalStain DAB (Cell Signaling) following manufacturer's instructions. Sections were
603 counterstained with hematoxylin (Morphisto). The automated image acquisition was
604 performed with Olympus Virtual Slide System VS120 (Olympus, Hamburg, Germany).

605 Visualization of the co-localization of HopQ and CEACAMs co-staining of normal and
606 gastritis sections was performed utilizing HopQ-biotin followed by streptavidin-Cy3 and α -
607 hu-CEACAM1, 3, 5, 6, 8 clone 6G5j followed by Alexa 488 coupled goat anti mouse
608 antibody. The cell nuclei were stained with DAPI. DAPI and fluorescent proteins were
609 analyzed with the Leica DMI4000B microscope.

610 **Adherence assay**

611 The adherence assay was performed according to Hytonen et al ⁴⁸. Briefly, human gastric
612 epithelial cells (MKN45 and AGS) and CEACAM1-transfected CHO cells were grown in

613 antibiotic free DMEM (Gibco, Gaithersburg, MD) supplemented with 5% FCS and L-
614 glutamine (2 mM, Sigma-Aldrich) on tissue culture 96 well plates (Bioscience) in 5% CO₂
615 atmosphere for 2 days. To visualize *H. pylori* cells in adhesion assays, OD₆₀₀=1 of bacteria
616 were fluorescence labeled with CFDA-SE (Molecular Probes) and washed with PBS. CFDA-
617 SE was added at concentration of 10 μM for 30 min at 37°C under constant rotation in the
618 dark. Excess dye was removed by 3 times washing with PBS. Bacteria were resuspended in
619 PBS until further use. Labelled bacteria were co-incubated (MOI 10) with the cells at 37°C
620 with gentle agitation for 1 h. After washing with PBS (1 mL, ×3) to remove non-adherent
621 bacteria, cells were fixed in paraformaldehyde (2%, 10 min). Bacterial binding was
622 determined by measuring the percentage of cells that bound fluorescent-labeled bacteria using
623 flow cytometry analysis.

624 **IL-8 cytokine ELISA**

625 AGS cell line was infected with *H. pylori* as described already and PBS-incubated control
626 cells served as negative control. The culture supernatants were collected and stored at -20 °C
627 until assayed. IL-8 concentration in the supernatant was determined by standard ELISA with
628 commercially available assay kits (Becton Dickinson, Germany) according to described
629 procedures.

630

631 **HopQ-dependency of CagA virulence pathways**

632 If not indicated otherwise, the AGS cell line (ATCC CRL-1730) was infected with the various
633 *H. pylori* strains for 6 hours at a multiplicity of infection (MOI) of 50. The cells were then
634 harvested in ice-cold PBS in the presence of 1 mM Na₃VO₄ (Sigma-Aldrich). In each
635 experiment the number of elongated AGS cells was quantified in 10 different 0.25-mm² fields
636 using a phase contrast microscope (Olympus IX50). CagA translocation was determined using
637 the indicated antibodies detecting Tyr-phosphorylated CagA. All experiments were performed
638 in triplicates. For inhibition experiments, cells were incubated with the indicated antibodies or
639 peptides prior to infection.

640 **Confocal microscopy**

641 CHO cells were grown on chamber slides (Thermo Scientific), fixed in paraformaldehyde
642 (4%, 10 min) and blocked with PBS/5% bovine serum albumin. CFDA-SE labelled bacteria
643 (10 μM for 30 min at 37°C under constant rotation in the dark) at MOI 5 were incubated with
644 cells for 1 h at 37°C under constant rotation. After 5X PBS washing, cell membranes were

645 stained with Deep Red (Life Technology) and cell nuclei with DAPI (Life Technology).
646 Confocal images of cells were taken using a Leica SP5 confocal microscope.

647 **Crystallization and structure determination of HopQ^{AD}**

648 HopQ^{AD} was concentrated to 40 mg/mL and crystallized by sitting drop vapor diffusion at
649 20°C using 0.12 M alcohols (0.02 M 1,6-Hexanediol; 0.02 M 1-Butanol; 0.02 M 1,2-
650 Propanediol; 0.02 M 2-Propanol; 0.02 M 1,4-Butanediol; 0.02 M 1,3-Propanediol), 0.1 M Tris
651 (base)/BICINE pH 8.5, 20% v/v PEG 500 MME; 10 % w/v PEG 20000 as a crystallization
652 buffer. Crystals were loop-mounted and flash-cooled in liquid nitrogen. Data were collected at
653 100 K at beamline Proxima1 (SOLEIL, Gif-sur-Yvette, France) and were indexed, processed
654 and scaled using the XDS package⁴⁹. All crystals were in the P2₁ space group with
655 approximate unit cell dimensions of a=57.7 Å, b=57.7 Å, c=285.7 Å and beta=90.1° and four
656 copies of HopQ₄₄₂ per asymmetric unit. Phases were obtained by molecular replacement using
657 the BabA structure (PDB:5F7K)²¹ and the program phaser^{50,51}. The models were refined by
658 iterative cycles of manual rebuilding in the graphics program COOT⁵² and maximum
659 likelihood refinement using Refmac5⁵³. Extended Data Table 2 summarizes the crystal
660 parameters, data processing and structure refinement statistics.

661 **Amino acid sequence alignment**

662 The amino acid sequence alignment of the N-terminal domains of human, mouse and rat-
663 CEACAM1 and human CEACAMs (1, 5, 6 and 8) was performed using CLC main
664 Workbench (CLC bio).

665 **Luciferase reporter assays**

666 CHO-CEACAM1-L cells transfected with various luciferase reporter and control constructs
667 (Clontech) were infected with *H. pylori* for 5 h and analyzed by luciferase assay using the
668 Dual-Luciferase Reporter Assay System according to the manufacturer's instruction (Promega,
669 USA). Briefly, cells were harvested by passive lysis, the protein concentration was measured
670 with Precision Red (Cytoskeleton, USA) and the lysates were equalized by adding passive
671 lysis buffer. The luciferase activity was measured by using a Plate Luminometer (MITHRAS
672 LB940 from Berthold, Germany).

673 **Animal experiments**

674 Specific pathogen free, 120-150 g 4 weeks-old male Sprague Dawley rats, were obtained from
675 Charles River Laboratories (Sulzfeld, Germany). Animals were randomly distributed into the
676 different experimental groups by animal care takers not involved in the experiments, and

677 criteria for the exclusion of animals were pre-established. Investigator blinding was
678 performed for all assessment of outcome and data, histology was performed by an
679 independent investigator in a blinded manner. Animals were challenged twice intragastrically
680 in groups of 8 with $\sim 1 \times 10^8$ live *H. pylori* in 2 interval days. After 6 weeks infection,
681 stomachs were removed and sectioned. One part was embedded in paraffin for histological
682 analysis and another piece was weighted and homogenized to determine colony forming units
683 (CFU)/mg stomach. Serial dilutions (1/10, 1/100 and 1/1000) were plated in WC dent plates.
684 CFU were counted after 4 days.

685 The experiments were performed in the specific pathogen-free unit of Zentrum für
686 Präklinische Forschung, Klinikum r. d. Isar der TU München, according to the allowance and
687 guidelines of the ethical committee and state veterinary office (Regierung von Oberbayern,
688 55.2-1.54-2532-160-12).

689 **Statistical Analysis**

690 For in vitro experiments, normal distribution was determined by Shapiro–Wilk test. Normally
691 distributed data were analyzed with two-tailed Student *t*-test or One-way ANOVA with post
692 hoc Bonferroni test (comparing more than two groups) using Graph Pad Prism Software. Data
693 are shown as mean \pm s.e.m or S.D. for at least three independent experiments. P values <0.05
694 were considered significant. For animal studies, power calculation was performed based on
695 previous animal experiments to achieve two sided significance of 0,05 while using lowest
696 possible numbers to comply with the ethical guidelines for experimental animals. Mann-
697 Whitney U test or ANOVA Kruskal-Wallis, Dunn’s multiple comparison test were used to
698 determine statistical significances.

699 **References**

- 700
701 1 Salama, N. R., Hartung, M. L. & Muller, A. Life in the human stomach: persistence strategies of the
702 bacterial pathogen *Helicobacter pylori*. *Nature reviews. Microbiology* **11**, 385-399,
703 doi:10.1038/nrmicro3016 (2013).
- 704 2 Atherton, J. C. & Blaser, M. J. Coadaptation of *Helicobacter pylori* and humans: ancient history,
705 modern implications. *The Journal of clinical investigation* **119**, 2475-2487, doi:10.1172/JCI38605
706 (2009).
- 707 3 Montecucco, C. & Rappuoli, R. Living dangerously: how *Helicobacter pylori* survives in the human
708 stomach. *Nature reviews. Molecular cell biology* **2**, 457-466, doi:10.1038/35073084 (2001).
- 709 4 Linden, S., Mahdavi, J., Hedenbro, J., Boren, T. & Carlstedt, I. Effects of pH on *Helicobacter pylori*
710 binding to human gastric mucins: identification of binding to non-MUC5AC mucins. *The Biochemical*
711 *journal* **384**, 263-270, doi:10.1042/BJ20040402 (2004).
- 712 5 Ilver, D. *et al.* *Helicobacter pylori* adhesin binding fucosylated histo-blood group antigens revealed by
713 retagging. *Science* **279**, 373-377 (1998).
- 714 6 Mahdavi, J. *et al.* *Helicobacter pylori* SabA adhesin in persistent infection and chronic inflammation.
715 *Science* **297**, 573-578, doi:10.1126/science.1069076 (2002).
- 716 7 Solnick, J. V., Hansen, L. M., Salama, N. R., Boonjakuakul, J. K. & Syvanen, M. Modification of
717 *Helicobacter pylori* outer membrane protein expression during experimental infection of rhesus
718 macaques. *Proceedings of the National Academy of Sciences of the United States of America* **101**, 2106-
719 2111, doi:10.1073/pnas.0308573100 (2004).
- 720 8 Hammarstrom, S. The carcinoembryonic antigen (CEA) family: structures, suggested functions and
721 expression in normal and malignant tissues. *Seminars in cancer biology* **9**, 67-81,
722 doi:10.1006/scbi.1998.0119 (1999).
- 723 9 Obrink, B. On the role of CEACAM1 in cancer. *Lung cancer* **60**, 309-312,
724 doi:10.1016/j.lungcan.2008.03.020 (2008).
- 725 10 Gray-Owen, S. D. & Blumberg, R. S. CEACAM1: contact-dependent control of immunity. *Nature*
726 *reviews. Immunology* **6**, 433-446, doi:10.1038/nri1864 (2006).
- 727 11 Voges, M., Bachmann, V., Kammerer, R., Gophna, U. & Hauck, C. R. CEACAM1 recognition by
728 bacterial pathogens is species-specific. *BMC microbiology* **10**, 117, doi:10.1186/1471-2180-10-117
729 (2010).
- 730 12 Heneghan, M. A. *et al.* Effect of host Lewis and ABO blood group antigen expression on *Helicobacter*
731 *pylori* colonisation density and the consequent inflammatory response. *FEMS immunology and medical*
732 *microbiology* **20**, 257-266 (1998).
- 733 13 Virji, M., Watt, S. M., Barker, S., Makepeace, K. & Doyonnas, R. The N-domain of the human CD66a
734 adhesion molecule is a target for Opa proteins of *Neisseria meningitidis* and *Neisseria gonorrhoeae*.
735 *Molecular microbiology* **22**, 929-939 (1996).
- 736 14 Hill, D. J. & Virji, M. A novel cell-binding mechanism of *Moraxella catarrhalis* ubiquitous surface
737 protein UspA: specific targeting of the N-domain of carcinoembryonic antigen-related cell adhesion
738 molecules by UspA1. *Molecular microbiology* **48**, 117-129 (2003).
- 739 15 Kuespert, K., Roth, A. & Hauck, C. R. *Neisseria meningitidis* has two independent modes of
740 recognizing its human receptor CEACAM1. *PLoS one* **6**, e14609, doi:10.1371/journal.pone.0014609
741 (2011).
- 742 16 Peek, R. M. *Helicobacter pylori* infection and disease: from humans to animal models. *Disease models*
743 *& mechanisms* **1**, 50-55, doi:10.1242/dmm.000364 (2008).
- 744 17 Icatlo, F. C., Goshima, H., Kimura, N. & Kodama, Y. Acid-dependent adherence of *Helicobacter pylori*
745 urease to diverse polysaccharides. *Gastroenterology* **119**, 358-367 (2000).
- 746 18 Cao, P. & Cover, T. L. Two different families of hopQ alleles in *Helicobacter pylori*. *Journal of clinical*
747 *microbiology* **40**, 4504-4511 (2002).
- 748 19 Ohno, T. *et al.* Relationship between *Helicobacter pylori* hopQ genotype and clinical outcome in Asian
749 and Western populations. *J Gastroenterol Hepatol* **24**, 462-468, doi:10.1111/j.1440-1746.2008.05762.x
750 (2009).
- 751 20 Alm, R. A. *et al.* Comparative genomics of *Helicobacter pylori*: analysis of the outer membrane protein
752 families. *Infection and immunity* **68**, 4155-4168 (2000).
- 753 21 Moonens, K. *et al.* Structural Insights into Polymorphic ABO Glycan Binding by *Helicobacter pylori*.
754 *Cell host & microbe* **19**, 55-66, doi:10.1016/j.chom.2015.12.004 (2016).
- 755 22 Rossez, Y. *et al.* The lacdiNac-specific adhesin LabA mediates adhesion of *Helicobacter pylori* to
756 human gastric mucosa. *The Journal of infectious diseases* **210**, 1286-1295, doi:10.1093/infdis/jiu239
757 (2014).

- 758 23 Singer, B. B. *et al.* Deregulation of the CEACAM expression pattern causes undifferentiated cell
759 growth in human lung adenocarcinoma cells. *PloS one* **5**, e8747, doi:10.1371/journal.pone.0008747
760 (2010).
- 761 24 Muenzner, P., Bachmann, V., Zimmermann, W., Hentschel, J. & Hauck, C. R. Human-restricted
762 bacterial pathogens block shedding of epithelial cells by stimulating integrin activation. *Science* **329**,
763 1197-1201, doi:10.1126/science.1190892 (2010).
- 764 25 Slevogt, H. *et al.* CEACAM1 inhibits Toll-like receptor 2-triggered antibacterial responses of human
765 pulmonary epithelial cells. *Nature immunology* **9**, 1270-1278, doi:10.1038/ni.1661 (2008).
- 766 26 Belogolova, E. *et al.* Helicobacter pylori outer membrane protein HopQ identified as a novel T4SS-
767 associated virulence factor. *Cell Microbiol* **15**, 1896-1912, doi:10.1111/cmi.12158 (2013).
- 768 27 Mahler, M. *et al.* Experimental Helicobacter pylori infection induces antral-predominant, chronic active
769 gastritis in hispid cotton rats (Sigmodon hispidus). *Helicobacter* **10**, 332-344, doi:10.1111/j.1523-
770 5378.2005.00320.x (2005).
- 771 28 Chang, Y. J. *et al.* Mechanisms for Helicobacter pylori CagA-induced cyclin D1 expression that affect
772 cell cycle. *Cell Microbiol* **8**, 1740-1752, doi:10.1111/j.1462-5822.2006.00743.x (2006).
- 773 29 Muenzner, P., Naumann, M., Meyer, T. F. & Gray-Owen, S. D. Pathogenic Neisseria trigger expression
774 of their carcinoembryonic antigen-related cellular adhesion molecule 1 (CEACAM1; previously
775 CD66a) receptor on primary endothelial cells by activating the immediate early response transcription
776 factor, nuclear factor-kappaB. *The Journal of biological chemistry* **276**, 24331-24340,
777 doi:10.1074/jbc.M006883200 (2001).
- 778 30 Olbermann, P. *et al.* A global overview of the genetic and functional diversity in the Helicobacter pylori
779 cag pathogenicity island. *PLoS genetics* **6**, e1001069, doi:10.1371/journal.pgen.1001069 (2010).
- 780 31 Suerbaum, S. & Josenhans, C. Helicobacter pylori evolution and phenotypic diversification in a
781 changing host. *Nature reviews. Microbiology* **5**, 441-452, doi:10.1038/nrmicro1658 (2007).
- 782 32 Baltrus, D. A. *et al.* The complete genome sequence of Helicobacter pylori strain G27. *Journal of*
783 *bacteriology* **191**, 447-448, doi:10.1128/JB.01416-08 (2009).
- 784 33 Arnold, I. C. *et al.* Tolerance rather than immunity protects from Helicobacter pylori-induced gastric
785 preneoplasia. *Gastroenterology* **140**, 199-209, doi:10.1053/j.gastro.2010.06.047 (2011).
- 786 34 Lee, A. *et al.* A standardized mouse model of Helicobacter pylori infection: introducing the Sydney
787 strain. *Gastroenterology* **112**, 1386-1397 (1997).
- 788 35 Lundin, A. *et al.* The NudA protein in the gastric pathogen Helicobacter pylori is an ubiquitous and
789 constitutively expressed dinucleoside polyphosphate hydrolase. *J Biol Chem* **278**, 12574-12578,
790 doi:10.1074/jbc.M212542200 (2003).
- 791 36 Atherton, J. C. *et al.* Mosaicism in vacuolating cytotoxin alleles of Helicobacter pylori. Association of
792 specific vacA types with cytotoxin production and peptic ulceration. *The Journal of biological*
793 *chemistry* **270**, 17771-17777 (1995).
- 794 37 Cover, T. L., Dooley, C. P. & Blaser, M. J. Characterization of and human serologic response to
795 proteins in Helicobacter pylori broth culture supernatants with vacuolizing cytotoxin activity. *Infect*
796 *Immun* **58**, 603-610 (1990).
- 797 38 Backert, S., Muller, E. C., Jungblut, P. R. & Meyer, T. F. Tyrosine phosphorylation patterns and size
798 modification of the Helicobacter pylori CagA protein after translocation into gastric epithelial cells.
799 *Proteomics* **1**, 608-617, doi:10.1002/1615-9861(200104)1:4<608::AID-PROT608>3.0.CO;2-G (2001).
- 800 39 Vermoote, M. *et al.* Genome sequence of Helicobacter suis supports its role in gastric pathology. *Vet*
801 *Res* **42**, 51, doi:10.1186/1297-9716-42-51 (2011).
- 802 40 Haesebrouck, F. *et al.* Non-Helicobacter pylori Helicobacter species in the human gastric mucosa: a
803 proposal to introduce the terms H. heilmannii sensu lato and sensu stricto. *Helicobacter* **16**, 339-340,
804 doi:10.1111/j.1523-5378.2011.00849.x (2011).
- 805 41 Schott, T., Kondadi, P. K., Hanninen, M. L. & Rossi, M. Comparative genomics of Helicobacter pylori
806 and the human-derived Helicobacter bizzozeronii CIII-1 strain reveal the molecular basis of the
807 zoonotic nature of non-pylori gastric Helicobacter infections in humans. *BMC Genomics* **12**, 534,
808 doi:10.1186/1471-2164-12-534 (2011).
- 809 42 Tegtmeier, N. *et al.* Characterisation of worldwide Helicobacter pylori strains reveals genetic
810 conservation and essentiality of serine protease HtrA. *Molecular microbiology* **99**, 925-944,
811 doi:10.1111/mmi.13276 (2016).
- 812 43 Singer, B. B. *et al.* Soluble CEACAM8 interacts with CEACAM1 inhibiting TLR2-triggered immune
813 responses. *PLoS One* **9**, e94106, doi:10.1371/journal.pone.0094106 (2014).
- 814 44 Studier, F. W. Protein production by auto-induction in high density shaking cultures. *Protein expression*
815 *and purification* **41**, 207-234 (2005).
- 816 45 Hojo, H. & Onishi, Y. [Case suspected to be atypical diffuse myeloma]. *Nihon rinsho. Japanese journal*
817 *of clinical medicine* **35**, 2659-2662 (1977).

818 46 Romano, M., Razandi, M., Sekhon, S., Krause, W. J. & Ivey, K. J. Human cell line for study of damage
819 to gastric epithelial cells in vitro. *The Journal of laboratory and clinical medicine* **111**, 430-440 (1988).
820 47 Mueller, D. *et al.* c-Src and c-Abl kinases control hierarchic phosphorylation and function of the CagA
821 effector protein in Western and East Asian *Helicobacter pylori* strains. *The Journal of clinical*
822 *investigation* **122**, 1553-1566, doi:10.1172/JCI61143 (2012).
823 48 Hytonen, J., Haataja, S. & Finne, J. Use of flow cytometry for the adhesion analysis of *Streptococcus*
824 *pyogenes* mutant strains to epithelial cells: investigation of the possible role of surface pullulanase and
825 cysteine protease, and the transcriptional regulator Rgg. *BMC Microbiol* **6**, 18, doi:10.1186/1471-2180-
826 6-18 (2006).
827 49 Krauth-Siegel, R. L. *et al.* Crystallization and preliminary crystallographic analysis of trypanothione
828 reductase from *Trypanosoma cruzi*, the causative agent of Chagas' disease. *FEBS letters* **317**, 105-108
829 (1993).
830 50 Winn, M. D. *et al.* Overview of the CCP4 suite and current developments. *Acta crystallographica.*
831 *Section D, Biological crystallography* **67**, 235-242, doi:10.1107/S0907444910045749 (2011).
832 51 McCoy, A. J. *et al.* Phaser crystallographic software. *Journal of applied crystallography* **40**, 658-674,
833 doi:10.1107/S0021889807021206 (2007).
834 52 Emsley, P., Lohkamp, B., Scott, W. G. & Cowtan, K. Features and development of Coot. *Acta*
835 *crystallographica. Section D, Biological crystallography* **66**, 486-501,
836 doi:10.1107/S0907444910007493 (2010).
837 53 Murshudov, G. N. *et al.* REFMAC5 for the refinement of macromolecular crystal structures. *Acta*
838 *crystallographica. Section D, Biological crystallography* **67**, 355-367,
839 doi:10.1107/S0907444911001314 (2011).
840

841

842 **Acknowledgments**

843 We thank Jeannette Koch, Judith Lind, Birgit Maranca-Hüwel and Bärbel Gobs-Hevelke for
844 their excellent technical support; Carolin Konrad, Johannes Fischer for support with rat
845 experiments and Marie Roskrow for fruitful discussion and revision. KM and HR
846 acknowledge use of the Soleil synchrotron, Gif-sur-Yvette, France under proposal 20131370
847 and support by VIB and the Flanders Science Foundation (FWO) through the Odysseus
848 program, a postdoctoral fellowship and Hercules funds UABR/09/005. This work was
849 supported by the German Centre for Infection Research, partner site Munich, to MG, by the
850 BMBF 01EO1002 to E.K., the Mercator Research Center Ruhr An2012-0070 to BBS, the
851 German Science Foundation CRC-796 (B10) and CRC-1181 (A04) to SB, the Collaborative
852 Research Center/Transregio 124, Project A5 to HS.

853

854 **Author Contribution**

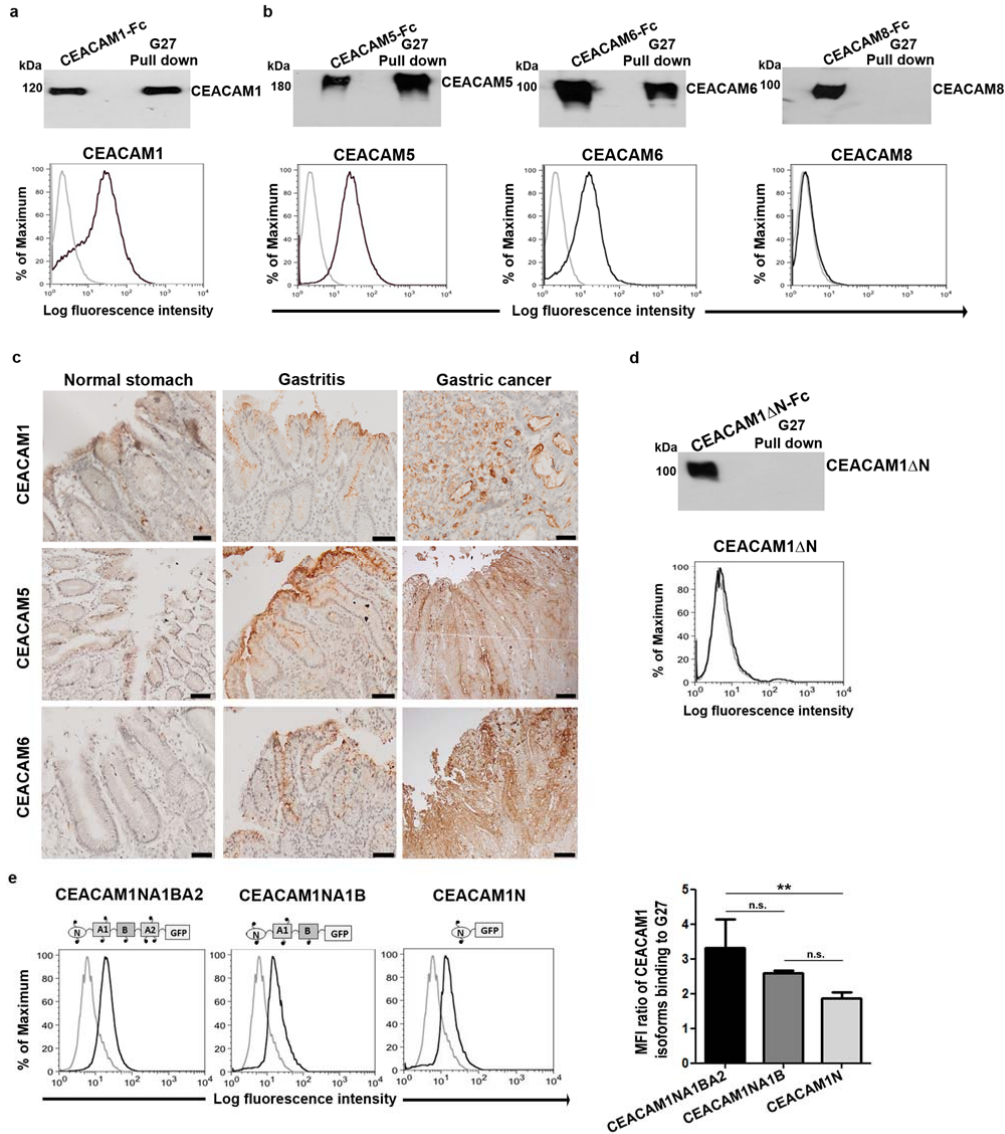
855 A.J., T.K., K.M., N.T., B.K., N.B., A.S. and B.B.S performed the experiments, B.B.S, R.H.,
856 V.K., E.K., H.S. and C.R.H. provided reagents and tools, A.J., B.B.S, H.R., D.B., R.M.-L.,
857 S.B. and M.G. conceived the experiments, analyzed the data and wrote the manuscript. All
858 authors read and approved the final manuscript.

859

860 **Author information**

861 Reprints and permissions information is available at www.nature.com/reprints. M.G., B.K.
862 and T.K. are employees and Shareholders of Imevax GmbH. M.G., A.J., B.S., S.B. and T.K.
863 are named as inventors on a patent application regarding HopQ. The other authors declare no
864 conflict of interest. Correspondence and requests for materials should be addressed to
865 markus.gerhard@tum.de.

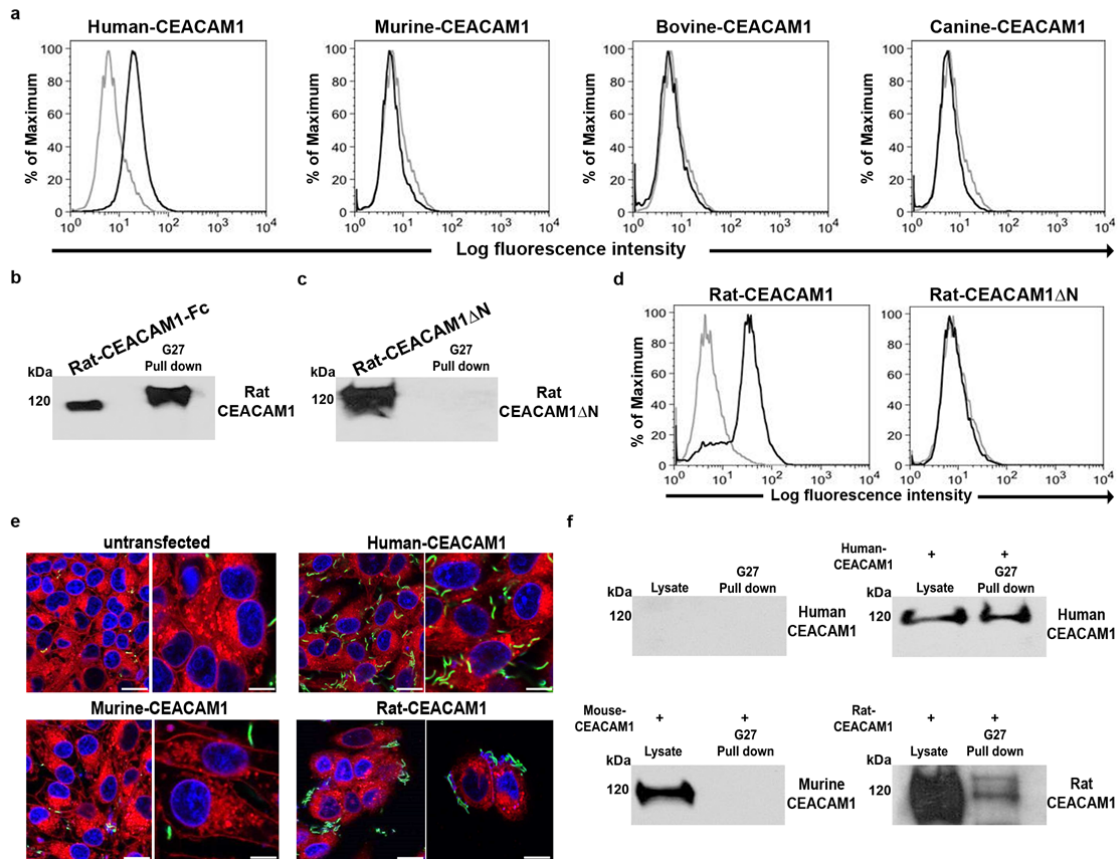
Gerhard Fig. 1



866

867 **Figure 1** *H. pylori* employs the N-terminal domain of hu-CEACAM1 and binds
 868 **CEACAM5 and CEACAM6 but not CEACAM8**. *H. pylori* G27 strain binding to human
 869 CEACAM1-Fc (a) and human CEACAM5-Fc, CEACAM6-Fc or CEACAM8-Fc (b) was
 870 analyzed by pull down experiments followed by western blot analysis and flow cytometry
 871 (n=3). (c) CEACAM1, CEACAM5 and CEACAM6 expression detected by
 872 immunohistochemistry in human normal stomach, gastritis and gastric cancer samples. Scale
 873 bars, 50 μm. (d) Binding of *H. pylori* to human CEACAM1ΔN-Fc (lacking the complete N-
 874 domain) detected by western blot after pull down or by flow cytometry. One representative
 875 experiment of 4 is shown. (e) *H. pylori* binding to CEACAM variants analyzed by flow
 876 cytometry. Mean Fluorescence Intensity (MFI) ratios (mean, S.D.) are shown (n=4). One-way
 877 ANOVA, *P* value= 0.009, n. s.: not significant.

Gerhard Fig. 2

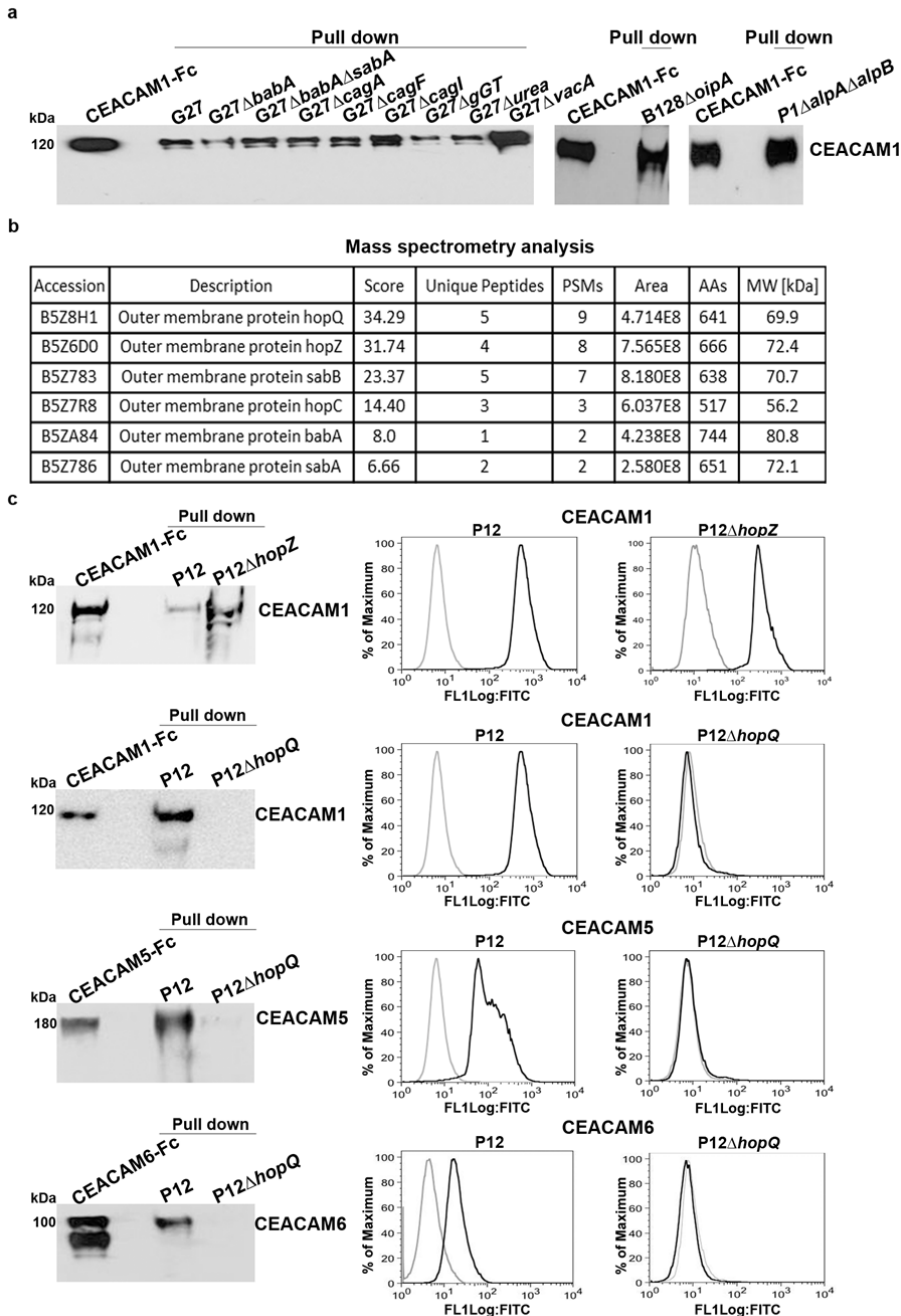


878

879

880 **Figure 2** *H. pylori* binding to CEACAM1 orthologues. (a) *H. pylori* G27 strain binding to
 881 human, murine, bovine and canine CEACAM1 determined by flow cytometry. (b) and (c) *H.*
 882 *pylori* (G27) binding to rat-CEACAM1-Fc (b) and rat-CEACAM1ΔN-Fc (c) detected by
 883 western blot after bacterial pull down. (d) Binding of G27 *H. pylori* strain to rat-CEACAM1
 884 and rat-CEACAM1ΔN detected by flow cytometry. (e) Representative confocal images of *H.*
 885 *pylori* binding to human, rat and mouse CEACAM1-expressing CHO cells. Untransfected
 886 CHO served as control. Scale bars: left panels, 25 μm, right panels, 10 μm. (f) *H. pylori* G27
 887 pull down of whole cell lysates of untransfected, human-, mouse- and rat CEACAM1-
 888 transfected CHO cells. CEACAM1 was detected using species-specific CEACAM1
 889 antibodies, as indicated. Representative experiments are shown (n=3).

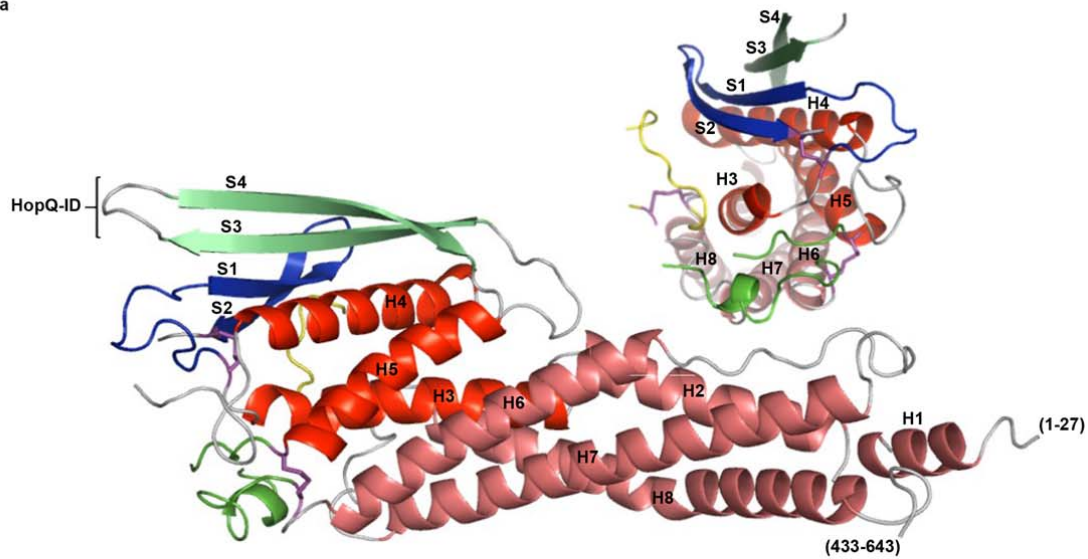
Gerhard Fig. 3



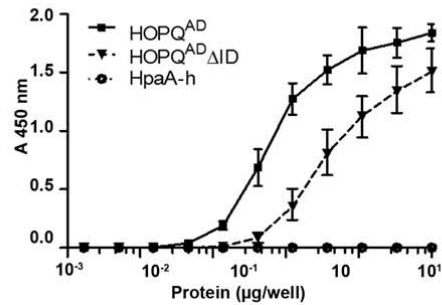
890

891 **Figure 3** *H. pylori* binds to CEACAM1 via HopQ. (a) Human CEACAM1 detected by
 892 western blot after pull down of various *H. pylori* G27 knockout strains incubated with human
 893 CEACAM1-Fc. (b) Candidate outer membrane proteins of *H. pylori* strain G27 binding to
 894 human CEACAM1-Fc (for complete MS table see Suppl. Table 1). (c) *H. pylori* strains P12,
 895 P12ΔhopQ and P12ΔhopZ binding to hu-CEACAM1-, CEACAM5- and CEACAM6-Fc
 896 detected by western blot and FACS analysis after pull down. Representative experiments are
 897 shown (n=3).

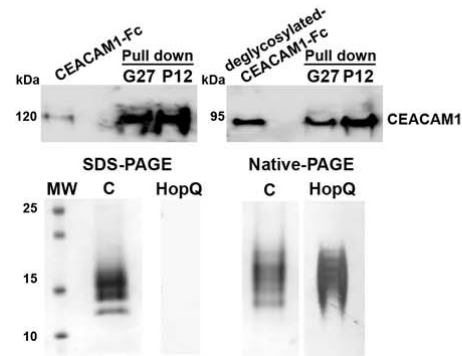
a



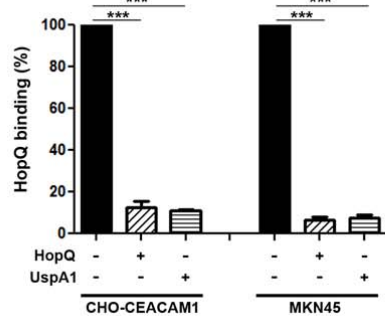
b



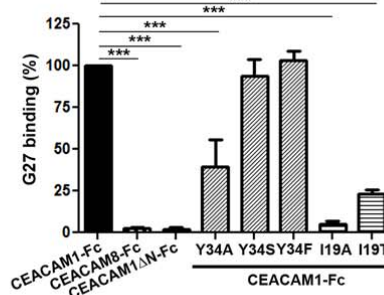
c



d



e



898

899 **Figure 4. X-ray structure and binding properties of the HopQ adhesin domain.**900 Ribbon representation of the HopQ^{AD} showing the 3+4-helix bundle topology (colored red

901 and brick, respectively). Three Cys pairs (Cys102-Cys131, Cys237-Cys269 and Cys361-

902 Cys384) conserved in most Hop family members pinch off extended loops are colored blue,

903 yellow and green. HopQ-ID; green, β-hairpin insertion. (b) ELISA titers of HopQ^{AD} or mutant904 HopQ^{AD} lacking the HopQ-ID (HopQ^{AD}ΔID) binding to increasing concentrations of C1-N905 domain (C1ND) (*n*=4, mean, S.D.). (c) Upper panel, pull down experiments of *H. pylori*

906 strains incubated with de-glycosylated human CEACAM1-Fc. Lower panel, SDS and native

907 page of C1ND stained with Coomassie-blue (“C”) or with HopQ^{AD} in a far western blot
908 (“HopQ”) experiment. (d) HopQ binding (%) to CEACAM1 in CHO and MKN45 cells after
909 pre-incubation with recombinant HopQ or UspA1, respectively. Mean, S.D. of three
910 independent experiments are shown. (e) *H. pylori* G27 binding (%) to CEACAM1,
911 CEACAM1ΔN and different CEACAM1 variants. CEACAM8 was used as negative control.
912 Mean, S.D. of three independent experiments are shown. One-way ANOVA with Bonferroni’s
913 correction for multiple comparisons. ***P≤0.001.

914

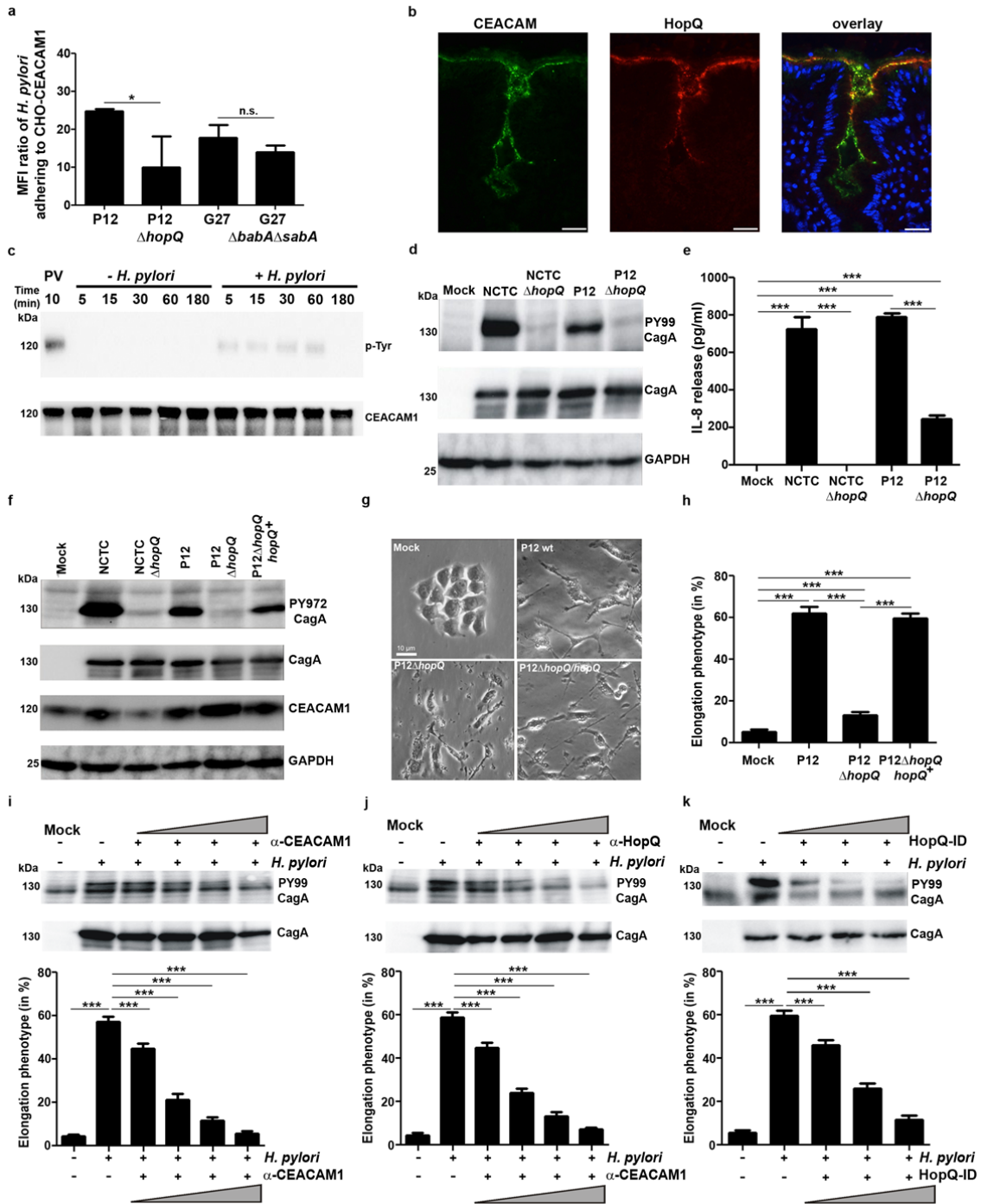
915

916

917

918

Gerhard Fig. 5

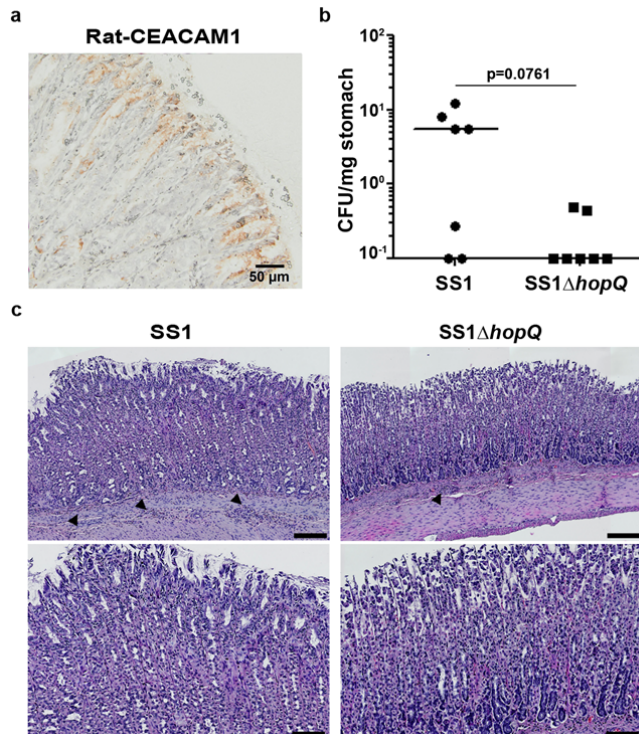


919

920 **Figure 5 Deletion of *hopQ* in *H. pylori* leads to reduced bacterial cell adhesion and**
 921 **abrogates CagA delivery, IL-8 release and cell elongation. (a) *H. pylori* binding to CHO-**
 922 **hu-CEACAM1-L cells detected by flow cytometry analysis (n=3). Means \pm S.D. are shown.**
 923 **Two-tailed *t*-test, * $P \leq 0.03$. (b) Immunofluorescence detection of apical CEACAM**
 924 **expression (green) and HopQ binding (red) in the gastric epithelium from human gastritis**
 925 **biopsies. Scale bar 25 μ m. (c) CEACAM1 Tyr-phosphorylation and total CEACAM1 levels in**

926 uninfected and *H. pylori*-infected CHO-CEACAM1-L cells. Pervanadate (PV) treatment
927 served as positive control. (d) CagA phosphorylation detected in lysates of AGS cells after
928 infection with *H. pylori* P12, NCTC11637 and corresponding isogenic *hopQ* mutants (e)
929 Secreted IL-8 by AGS cells after infection with the indicated *H. pylori* strains (mean, S.D. of
930 three independent experiments are shown). One-way ANOVA with Bonferroni's correction for
931 multiple comparisons. *** $P \leq 0.001$. (f) CagA phosphorylation and CEACM1 levels in HA-
932 tagged HEK293-hu-CEACAM1 transfectants infected with indicated *H. pylori* strains. (g)
933 Representative phase contrast micrographs of AGS cells infected for 6 h with P12, P12 Δ *hopQ*
934 or P12 Δ *hopQhopQ*⁺ re-expressing wt *hopQ* gene. (h) Quantification of elongation phenotype
935 induced in AGS cells after infection with the indicated *H. pylori* strains. Data (mean, S.D.) of
936 three independent experiments are shown. One-way ANOVA with Bonferroni's correction for
937 multiple comparisons. *** $P \leq 0.001$. (i) CagA phosphorylation and quantification of the
938 elongation phenotype (five different 0.25-mm² fields) after *H. pylori* P12 infection of AGS
939 cells pre-treated with 2, 5, 10 or 20 μ g of α -CEACAM Ab (lanes 3-6). Data (mean, S.D.) of
940 three independent experiments are shown. One-way ANOVA with Bonferroni's correction for
941 multiple comparisons. *** $P \leq 0.001$. (j) CagA phosphorylation and quantification of the
942 elongation phenotype after infection of AGS with wild type *H. pylori* pre-treated with 2, 5, 10
943 or 20 μ g of α -HopQ (lanes 3-6) Data (mean, S.D.) of three independent experiments are
944 shown. One-way ANOVA with Bonferroni's correction for multiple comparisons.
945 *** $P \leq 0.001$. (k) CagA phosphorylation in *H. pylori*-infected AGS cells pre-incubated with a
946 HopQ-derived peptide (1 μ M, 2.5 μ M and 5 μ M) corresponding to the HopQ-ID (aa 189-
947 220). Cell elongation (mean, S.D.) from 3 independent experiments is shown. One-way
948 ANOVA with Bonferroni's correction for multiple comparisons. *** $P \leq 0.001$.
949

Gerhard Fig. 6



950

951 **Figure 6** *H. pylori* colonization of rat stomach depends on HopQ. (a) CEACAM1
952 expression in rat stomach. (b) *H. pylori* colony forming units (CFU) per mg stomach of male
953 Sprague dawley rats after 6 weeks infection. Horizontal bars indicate medians. Mann-Whitney
954 U test. (c) Hematoxylin/eosin staining of infected rat stomachs. Representative images of
955 same stomach regions are shown. Scale bar 100µm (upper panels) and 200µm (lower panels).
956 Arrows denote inflammatory cells.

1 ***H. pylori* adhesin HopQ engages in a virulence-enhancing interaction with**
2 **human CEACAMs**
3
4
5

6 Anahita Javaheri^{1,15,‡}, Tobias Kruse^{2,‡}, Kristof Moonens^{3,4,‡}, Ayla Debraekeleer^{3,4}, Raquel
7 Mejías-Luque^{1,15}, Isabell Asche⁵, Nicole Tegtmeyer⁵, Behnam Kalali^{1,2}, Nina C. Bach⁶,
8 Stephan A. Sieber⁶, Darryl J. Hill⁷, Verena Königer⁸, Christof R. Hauck⁹, Roman
9 Moskalenko¹⁰, Rainer Haas⁸, Dirk H. Busch¹, Esther Klaile^{11,12}, Hortense Slevogt¹¹, Alexej
10 Schmidt^{13,14}, Steffen Backert⁵, Han Remaut^{3,4,‡}, Bernhard B. Singer^{12‡} and Markus
11 Gerhard^{1,2,15‡*}

12
13
14
15 **Affiliations:**

16 ¹Institute for Medical Microbiology, Immunology and Hygiene; Technische Universität
17 München; Munich, 81675, Germany,

18 ²Imevax GmbH, 81675 Munich

19 ³Structural and Molecular Microbiology, Structural Biology Research Center, VIB, Pleinlaan 2, 1050
20 Brussels, Belgium

21 ⁴Structural Biology Brussels, Vrije Universiteit Brussel, Pleinlaan 2, 1050 Brussels, Belgium

22 ⁵Friedrich Alexander University Erlangen, Department of Biology, Division of Microbiology,
23 Erlangen, Germany

24 ⁶Center for Integrated Protein Science Munich, Department Chemie, Institute of Advanced Studies,
25 Technische Universität München, 85747 Garching, Germany

26 ⁷School of Cellular & Molecular Medicine, University of Bristol, BS8 ITD, Bristol, UK

27 ⁸Max von Pettenkofer-Institut für Hygiene und Medizinische Mikrobiologie, Department of
28 Bacteriology, Ludwig-Maximilians-Universität, D-80336 Munich, Germany

29 ⁹Lehrstuhl für Zellbiologie, Universität Konstanz, Konstanz, Germany

30 ¹⁰Department of Pathology, Sumy State University, Sumy 40000, Ukraine

31 ¹¹Septomics Research Centre, Jena University Hospital, 07745 Jena, Germany.

32 ¹²Center for Sepsis Control and Care (CSCC), Jena University Hospital, 07747 Jena, Germany

33 ¹³Institute of Anatomy, Medical Faculty, University Duisburg-Essen, 45122 Essen, Germany

34 ¹⁴Department of Medical Biosciences, Pathology, Umeå University, SE-901 85 Umeå, Sweden

35 ¹⁵German Center for Infection Research, Partner Site Munich, Munich, Germany

36 *Correspondence to: markus.gerhard@tum.de

37 ‡ These authors contributed equally to this work

38 **Summary:** *Helicobacter pylori* specifically colonizes the human gastric epithelium and is the
39 major causative agent for ulcer disease and gastric cancer development. Here we identified
40 members of the carcinoembryonic antigen-related cell adhesion molecule (CEACAM) family
41 as novel receptors of *H. pylori* and show that HopQ is the surface-exposed adhesin that
42 specifically binds human CEACAM1, CEACAM3, CEACAM5 and CEACAM6. HopQ -
43 CEACAM binding is glycan-independent and targeted to the N-domain. *H. pylori* binding
44 induces CEACAM1 mediated signaling, and the HopQ-CEACAM1 interaction enables
45 translocation of the virulence factor CagA into host cells, and enhances the release of pro-
46 inflammatory mediators such as interleukin-8. Based on the crystal structure of HopQ, we
47 found that a β -hairpin insertion (HopQ-ID) in HopQ's extracellular 3+4 helix bundle domain
48 is important for CEACAM binding. A peptide derived from this domain competitively
49 inhibits HopQ-mediated activation of the Cag virulence pathway, as genetic or antibody-
50 mediated abrogation of the HopQ function **shows**. Together, our data imply the HopQ-
51 CEACAM1 interaction as potentially promising novel therapeutic target to combat *H. pylori*-
52 associated diseases.

53

54 *Helicobacter pylori* (*H. pylori*) is one of the most prevalent human pathogens,
55 colonizing half of the world's population. Chronic inflammation elicited by this bacterium is
56 the main cause of gastric cancer¹. During co-evolution with its human host over more than
57 60,000 years², the bacterium has acquired numerous adaptations for the long-term survival
58 within its unique niche, the stomach. This includes the ability to buffer the extreme acidity of
59 this environment, the interference with cellular signaling pathways, the evasion of the human
60 immune response and a strong adhesive property to host cells³. Specifically, *H. pylori*
61 persistence is facilitated by the binding of BabA and SabA adhesins to the human blood group
62 antigen Leb and the sLex antigen, respectively⁴⁻⁶. However, adhesion to blood group antigens
63 is not universal, is dynamically regulated during the course of infection and can also be turned
64 off⁷. We observed that *H. pylori* was capable of binding to human gastric epithelium of non-
65 secretors. Therefore, we hypothesized that the bacterium might be able to interact with other
66 cell surface receptors to ensure persistent colonization.

67 We here show that the *H. pylori* adhesin HopQ specifically interacts with human
68 carcinoembryonic antigen-related cell adhesion molecules (CEACAMs). CEACAMs embrace
69 a group of immunoglobulin superfamily-related glycoproteins with a wide tissue distribution.
70 CEACAM1 can be expressed in leukocytes, endothelial and epithelial cells, CEACAM3 and
71 CEACAM8 in granulocytes, CEACAM5 and CEACAM7 in epithelial cells and CEACAM6
72 in epithelia and granulocytes. In epithelial cells, transmembrane anchored CEACAM1 as well
73 as glycosylphosphatidylinositol-linked CEACAM5, CEACAM6 and CEACAM7 localize to
74 the apical membrane⁸. CEACAMs modulate diverse cellular functions such as cell adhesion,
75 differentiation, proliferation, and cell survival. Some CEACAMs were recognized as valuable
76 tumor markers due to their enlarged expression in the malignant tissue and increased sera
77 level⁹. In recent years, CEACAMs have also emerged as immunomodulatory mediators¹⁰.
78 Interestingly, in humans, several CEACAMs have been found to specifically interact with
79 bacteria such as *Neisseria*, *Haemophilus influenzae*, *Moraxella catarrhalis*, and *Escherichia*
80 *coli*¹¹.

81

82 ***H. pylori* binds to CEACAMs expressed in human stomach**

83 Based on the observation that *H. pylori* efficiently colonizes individuals in the absence of
84 Lewis blood group antigens¹² on the one hand, and the increased expression of members of
85 the carcinoembryonic antigen-related cell adhesion molecule family (CEACAMs) in gastric
86 tumors, we hypothesized that *H. pylori* may employ CEACAMs as receptors. Using pull
87 down and flow cytometric approaches we found a robust interaction of the *H. pylori* strain

88 G27 with recombinant human CEACAM1-Fc (Fig. 1a), comparable to that of *Moraxella*
89 *catarrhalis* (Extended Data Fig. 1a and b). As negative control, *Moraxella lacunata* did not
90 bind to human CEACAM1, nor did *Campylobacter jejuni*, a pathogen closely related to *H.*
91 *pylori* (Extended Data Fig. 1a and b). When testing for CEACAM specificity, we observed a
92 clear interaction of *H. pylori* also with CEACAM3, 5 and 6, but not with CEACAM8 (Fig.1b
93 and Extended Data Fig. 1c and d). Importantly, all *H. pylori* strains tested bound to these
94 CEACAMs (Extended Data Fig.1f and g) including well-characterized reference strains
95 (26695, J99) and the mouse-adapted strain SS1. However, binding strength differed among
96 strains, with some preferentially binding to CEACAM1, and others to CEACAM5 and/or
97 CEACAM6 (Extended Data Fig. 1f and g). We then analyzed the expression profiles of
98 CEACAM1, CEACAM5 and CEACAM6 in normal and inflamed human stomach tissues and
99 gastric cancer. If at all low levels of CEACAM1 and CEACAM5 were expressed at the apical
100 side of epithelial cells, and their expression, as well as that of CEACAM6, was up-regulated
101 upon gastritis and in gastric tumors (Fig. 1c and Extended Data Fig. 1e). During infection, *H.*
102 *pylori*-induced responses may thus lead to increased expression of its CEACAM-receptors.
103 Adhesins from other bacteria were shown to specifically bind to the N-domain of human
104 CEACAM1^{13,14}. Similarly, we found that lack of the CEACAM1 N-domain abolished *H.*
105 *pylori* binding completely (Fig. 1d). While for the interaction of *Neisseria meningitidis* with
106 CEACAM1 the N-domain was necessary but not sufficient for binding¹⁵, we observed binding
107 of *H. pylori* to all tested CEACAM1 isoforms containing the N-domain, as well as to the N-
108 domain alone (Fig. 1e). However, binding to the N-domain alone was weaker than to the N-
109 A1-B CEACAM1 variant, which bound less than the N-A1-B-A2 variant (Fig. 1e and
110 Extended Data Fig.1j), suggesting that these domains stabilize the CEACAM1-*H.pylori*
111 interaction. Comparison of the respective N-domains indicated several residues conserved in
112 CEACAM1, 5, and 6 but not in CEACAM8 (Extended Data Fig. 1h).

113

114 **Species specificity of *Helicobacter* – CEACAM interaction**

115 Although, murine and Mongolian gerbil models are routinely used to study gastric infection
116 with *H. pylori*, the bacterium has been described so far to be naturally transmitted to only
117 humans and non-human primates. Although CEACAMs are found in most mammalian
118 species, and have a high degree of conservation, we found *H. pylori* to bind selectively to
119 human, but not to mouse, bovine or canine CEACAM1 orthologues (Fig. 2a). However, we
120 were surprised to find a strong interaction of *H. pylori* with rat-CEACAM1 (Fig. 2b and d).
121 This interaction was also mediated through the N-domain of rat-CEACAM1 (Fig. 2c and d).

122 To substantiate these findings, we transfected human, mouse or rat-CEACAM1 into CHO
123 cells, to which *H. pylori* does not adhere otherwise. Using confocal laser scanning
124 microscopy, we observed *de novo* adhesion of *H. pylori* to CHO cells expressing human and
125 rat, but not mouse CEACAM1 (Fig. 2e), which could be confirmed by pull down and Western
126 blotting of lysates from transfected cells (Fig. 2f and Extended Data Fig. 2d). This finding
127 makes *H. pylori* the first pathogen for which its CEACAM binding is not restricted to one
128 species. Comparing the protein sequences of the CEACAM1-N domains, several amino acids
129 conserved in human and rat differ in mouse (i.e. asn10, glu26, asn42, tyr48, pro59, thr66,
130 asn77, val79, val89, ile90, glu103, tyr108) (Extended Data Fig. 2a). In addition, our findings
131 of the lack of binding to mouse CEACAM1 may explain the differences seen in pathology
132 between infected mice and humans¹⁶.

133 The genus *Helicobacter* comprises several other spp. i.e. *H. felis*, *suis*, and *bizzozeronii* as
134 well as the human pathogenic *H. bilis* and *H. heilmannii*. When assessing the interaction of
135 these *Helicobacters* with human CEACAMs, only *H. bilis* bound to human CEACAM1, 5 and
136 6 (Extended Data Fig.2b and c). As *H. pylori*, *H. bilis* interacted with the N-domain of hu-
137 CEACAM1 (Extended Data Fig.2b and c). This interaction may explain how *H. bilis* manages
138 to colonize human bile ducts, where high levels of constitutively expressed CEACAM1 are
139 present.

140

141 **HopQ is the *Helicobacter* adhesin interacting with CEACAMs**

142 In order to identify the CEACAM-binding partner in *Helicobacter*, we initially screened a
143 number of *Helicobacter* mutants devoid of defined virulence factors that have been shown to
144 be implicated in various modes of host cell interaction (BabA, SabA, AlpA/B, VacA, gGT,
145 urease and the **cagPAI**)^{5,6,17}. All of these mutants still bound to hu-CEACAM1 (Fig. 3a).
146 Therefore we established an immunoprecipitation approach (Extended Data Fig. 3a) using *H.*
147 *pylori* lysate and recombinant hu-CEACAM1-Fc coupled to protein G. Mass spectrometric
148 analysis of the co-precipitate identified two highly conserved *H. pylori* outer membrane
149 proteins as candidate CEACAM1 adhesins: HopQ and HopZ (Fig. 3b). Unlike a *hopZ* mutant,
150 a *hopQ* deletion mutant was devoid of CEACAM1 binding (Fig. 3c). Importantly, the *hopQ*
151 mutant was also unable to bind to CEACAM5 and 6 (Fig.3c).

152 Next we tested the binding of recombinant HopQ to different gastric cancer cell lines and
153 found that HopQ interacted with AGS and MKN45 both endogenously expressing
154 CEACAMs (Extended Data Fig.3b). HopQ did not bind to the CEACAM negative cell line
155 MKN28. Utilizing our CHO transfectants, we found that the recombinant HopQ interacted

156 preferentially with CEACAM1 and 5, and to lesser extent to CEACAM3 and 6. No binding
157 was observed to CHO cells expressing either CEACAM4, 7, or 8 (Extended Data Fig. 3c).
158 HopQ is a member of a *H. pylori*-specific family of outer membrane proteins, and shows no
159 significant homology to other CEACAM-binding adhesins from other Gram-negative
160 bacteria, i.e. Opa proteins or UspA1 from *Neisseria meningitidis* and *Neisseria gonorrhoeae*
161 or *Moraxella catarrhalis*, respectively, and is therefore a novel bacterial factor hijacking
162 CEACAMs. Like Opa and UspA1^{13,14}, HopQ targets the N-terminal domain in CEACAMs,
163 an interaction we found to require folded protein (see below) and was dependent on
164 CEACAM sequence, resulting in specificity for human CEACAM1, 3, 5 and 6. The *H. pylori*
165 *hopQ* gene (*omp27*; HP1177 in the *H. pylori* reference strain 26695) exhibits genetic diversity
166 that represents two allelic families¹⁸, type-I and type-II (Extended Data Fig. 3d), of which the
167 type-I allele is found more frequently in *cag*(+)/*s1-vacA* type strains. Both alleles share 75 to
168 80% nucleotide sequences and exhibit a homology of 70% at the amino acid level¹⁸.
169 Importantly, *hopQ* genotype shows a geographic variation, with the *hopQ* type-I alleles more
170 prevalent in Asian compared to Western strains; and was also found to correlate with strain
171 virulence, with type-I alleles associated with higher inflammation and gastric atrophy¹⁹.

172

173 **Structure and binding properties of the HopQ adhesin domain**

174 HopQ belongs to a paralogous family of *H. pylori* outer membrane proteins (Hop's), to which
175 also the blood group antigen binding adhesins BabA and SabA belong^{5,6,17,20}. To gain insight
176 into its structure-function relationship we determined the binding properties and X-ray
177 structure of a HopQ fragment corresponding to its predicted extracellular domain (residues
178 17-444 of the mature protein; HopQ^{AD}; Fig. 4a). HopQ^{AD} showed strong, dose dependent
179 binding to the N-terminal domain of human CEACAM1 (C1ND; residues 35-142) in ELISA
180 (Fig. 4b) and isothermal titration calorimetry (ITC) revealed a 1:1 stoichiometry with a
181 dissociation constant of 296±40 nM (Extended Data Fig. 4a). The HopQ^{AD} X-ray structure
182 shows that, like BabA and SabA, the HopQ ectodomain adopts a 3+4-helix bundle topology,
183 though lacks the extended coiled-coil “stem” domain that connects the ectodomain to the
184 transmembrane region (Fig. 4a and Extended Data Fig.4d). In BabA, the carbohydrate binding
185 site resides fully in a 4-stranded β-domain that is inserted between helices 4 and 5²¹ (Extended
186 Data Fig.4d). In HopQ, a 2-stranded β-hairpin is found in this position (residues 180-218).
187 Removal of the β-hairpin resulted in a soluble protein that showed a ~10 fold reduction of
188 CEACAM1 binding affinity (Fig. 4b and Extended Data Fig. 4c), indicating that although the

189 HopQ insertion domain is implicated in binding, it does not comprise the full binding site as
190 found in BabA (Fig. 4b).

191 The hitherto characterized Hop adhesins are lectins^{5,6,17,22}. Instead, *H. pylori* was seen to
192 retain binding to CEACAM1 upon enzymatic deglycosylation, and Far Western analysis
193 revealed that HopQ^{AD} specifically bound folded, but not denatured C1ND (Fig. 4c),
194 suggesting HopQ-CEACAM binding relies on protein-protein rather than glycan-dependent
195 interactions. Indeed, ITC binding profiles of HopQ^{AD} titrated with non-glycosylated *E. coli*
196 expressed C1ND (Ec-C1ND) revealed an equimolar interaction with a dissociation constant of
197 417±48 nM (Extended Data Fig. 4b), showing that CEACAM N-glycosylation only provides
198 a minor stabilizing contribution to the HopQ-CEACAM interaction. To further map the HopQ
199 binding site, we pre-incubated CEACAM1 with the *M. catarrhalis* adhesin UspA1, and found
200 that this prevented binding by *H. pylori* (Fig. 4d), suggesting that both adhesins have
201 overlapping binding epitopes. In further support, mutation of CEACAM1 residues Y34 or I91
202 within the UspA1 binding epitope reduced or nearly abrogated CEACAM1 binding by *H.*
203 *pylori* (Fig. 4e). Interestingly, I91 is conserved in rat but mutated to T in mouse CEACAM1,
204 possibly explaining the observed species specificity in HopQ binding (Extended Data Fig. 2a,
205 see above).

206

207 **HopQ – CEACAM1 interaction triggers cell responses**

208 Available animal models only partially replicate the *H. pylori* pathogenesis observed in its
209 human host and mouse CEACAMs did not support HopQ binding. Therefore, to further
210 investigate how HopQ may influence adhesion and cellular responses, we sought to establish
211 cellular pathogenesis models in which the HopQ-CEACAM mediated adhesion could be
212 analyzed. According to Singer et al.²³, we characterized various gastric cell lines typically
213 employed for *H. pylori in vitro* experiments regarding their expression of CEACAMs, and
214 observed that MKN45, KatoIII and AGS did express CEACAM1, CEACAM5 and
215 CEACAM6, whereas MKN28 showed no presence of CEACAMs (Extended Data Fig.5a and
216 b). In parallel, CHO cells were stably transfected with CEACAM1-L (containing the
217 immunoreceptor tyrosine-based inhibition motif (ITIM). Upon infection with *H. pylori* wild-
218 type strain P12 and its isogenic *hopQ* deletion mutant, we observed a significantly reduced
219 adherence to CHO-CEACAM1-L, MKN45 and AGS cells when *hopQ* was not present, while
220 strains deficient in the adhesins BabA and SabA showed only slightly reduced adhesion (Fig.
221 5a and Extended Data Fig.5c). HopQ binding was also studied in human gastric biopsies from
222 *H. pylori* infected individuals. Here, we detected that HopQ bound to the apical side human

223 gastric epithelium and co-localized with CEACAM in biopsies from *H. pylori* infected
224 individuals (Fig. 5b and Extended Data Fig. 5d), while no binding was observed in
225 CEACAM1 negative samples from normal stomach (not shown). In CHO-CEACAM1-L
226 cells, we observed tyrosine-phosphorylation of the CEACAM1 ITIM domain upon exposure
227 to *H. pylori*, which was apparent within 5 minutes, and was maintained for up to 1 hour
228 (Fig.5c). Phosphorylation of the CEACAM1 ITIM domain is a well-known initial event
229 triggering SHP1/2 recruitment inducing downstream signaling cascades^{24,25}. Contact-
230 dependent signaling through CEACAMs is a common means of modulating immune
231 responses related to infection, inflammation and cancer¹⁰, and these immune-dampening
232 cascades likely reflect the multiple independent emergence of non-homologous CEACAM-
233 interacting proteins in diverse mucosal Gram-negative pathogens including *Neisseria*,
234 *Haemophilus*, *Escherichia*, *Salmonella*, *Moraxella* sp.^{13,14}. For *H. pylori*, interaction with
235 human CEACAM1 through HopQ may represent a critical parameter for immuno-modulatory
236 signaling during colonization and chronic infection of man.

237 Additionally, *hopQ* mutant *H. pylori* strains showed an almost complete loss of *cagPAI*-
238 dependent CagA translocation (Fig. 5d) and strongly reduced IL-8 induction (Fig.5e), while
239 loss of other known adhesins had no effect on CagA delivery (Extended Data Fig.5e and f).
240 This is in line with a previous study showing that in AGS gastric cancer cells, a *hopQ* mutant
241 *H. pylori* strain exhibited reduced ability to activate NF-κB and altered translocation of
242 CagA²⁶. In contrast to our findings, Belogolova et al. did not observe reduced adherence of a
243 *hopQ* mutant *H. pylori* P12 strain, which could be due to the observed growth dependent
244 expression of CEACAMs in these cells.

245 To corroborate our data in an independent model and compensate for potential clonal effects
246 in stably transfected cells, we transiently transfected HEK293 cells with human CEACAM (1-
247 L,3,4,5,6,7,8) expression plasmids. Infection of these cells confirmed the defect in CagA
248 translocation observed in CHO-CEACAM1-L cells, which was restored upon
249 complementation of the *hopQ* mutant strain (P12Δ*hopQ**hopQ*⁺) (Fig.5f and Extended Data
250 Fig.5g). Also, cellular elongation, the so called “hummingbird phenotype”, was significantly
251 reduced upon deletion of *hopQ* (Fig. 5g and h). Further, we observed that *H. pylori* modulates
252 important host transcription factors such as Myc or STAT3, in a *hopQ*-dependent fashion
253 (Extended Data Fig. 5h). Our results reveal that HopQ-CEACAM binding leads to direct and
254 indirect alterations in host cell signaling cascades, and start to shed light on these HopQ-
255 associated virulence landscapes. Given the importance of these signaling events for gastric
256 carcinogenesis, we explored if the CEACAM-HopQ interaction could be targeted in order to

257 prevent CagA translocation and downstream effects. Indeed, incubation of the cells with an α -
258 CEACAM1 antibody, α -HopQ antiserum or a HopQ-derived peptide corresponding to the
259 Hop-ID (aa 189-220) reduced CagA translocation in a dose dependent manner (Fig. 5i-k), but
260 not corresponding controls (Extended Data Fig. 5h). These data demonstrate that the HopQ-
261 CEACAM1 interaction is necessary for successful translocation of the oncoprotein CagA into
262 epithelial cells as well as modulation of inflammatory signaling, and that interference with
263 this interaction can prevent CagA translocation, giving an indication of the translational
264 potential of HopQ targeting for *H. pylori* vaccination or immunotherapy.

265

266 **Deletion of *hopQ* abrogates colonization in a rat model of *H. pylori* infection**

267 As we have found binding of HopQ to human and rat, but not to mouse CEACAM, we finally
268 determined the role of HopQ *in vivo*, using a rat model of *H. pylori* infection. Having
269 observed that CEACAM1 was expressed in normal rat stomach (Fig. 6a and Extended Data
270 Fig. 6b), we infected rats with the mouse adapted strain SS1, able to bind human and rat
271 CEACAM1 (Extended Data Fig. 6a). While the wild type SS1 was able to efficiently colonize
272 rats, albeit at lower levels compared to the mouse, (Fig. 6b) , the *hopQ* deficient SS1 strain
273 was not able to colonize rats at detectable levels, and could not induce an inflammatory
274 response in comparison to the wild type SS1 strain (Fig. 6b and c). Therefore, in this model,
275 HopQ seems also to serve as an important factor to mediate *H. pylori* colonization. While
276 infection of rats with *H. pylori* has been described²⁷, our finding may allow the establishment
277 of an animal model for studying *H. pylori* infection that better replicates the prevailing
278 virulence pathways.

279

280 Discussion

281 The here identified CEACAM-binding property provides *H. pylori* a means of
282 epithelial adherence in addition to the Lewis antigens used by the BabA and SabA
283 adhesins^{5,6,17}. While over-expression of CEACAMs in gastrointestinal tumors is well
284 described, their up-regulation during *H. pylori*-induced inflammation in the stomach has not
285 been reported so far, suggesting the pathogen has the ability to shape its own adhesive niche.
286 A similar phenomenon has also been observed for the inflammation-induced up-regulation of
287 sialylated antigens that form the receptors for the SabA adhesin⁶. A plausible route to
288 CEACAM modulation is through the transcription factors NF- κ B and AP1, both of which are
289 induced during *H. pylori* infection²⁸ and are known to regulate CEACAM expression²⁹.
290 Though HopQ-dependent adherence may appear redundant to that of other adhesins like
291 BabA, SabA or LabA, HopQ specializes on human CEACAMs and is required for *cagPAI*
292 functionality. From the perspective of host-pathogen (i.e. human-*H. pylori*) co-evolution, the
293 primary function of HopQ may lie in immune-modulation through CEACAM binding, and
294 HopQ's indirect effects on other virulence cascades elicited by *H. pylori* such as that induced
295 by increased CagA delivery may not have been initially "intended". The *cagPAI* was acquired
296 by ancestral *H. pylori* in a single event that occurred before modern humans migrated out of
297 East Africa around 58,000 years ago³⁰. Thus, it is likely that the employment of CEACAM1
298 ligation by *H. pylori* occurred much earlier to support colonization and to modulate immune
299 responses. This assumption is supported by the fact that all fully sequenced *H. pylori* strains
300 bear *hopQ* (Extended Data Fig.3d), indicating that this is an essential outer membrane protein
301 of *H. pylori*. Upon occurrence of type-I *H. pylori* strains by *cagPAI* acquisition more than
302 60,000 years ago³⁰ this ancient survival strategy was further implemented into a mechanism
303 supporting pathogenicity, and thus may have contributed to the switch from commensal to
304 pathogenic *H. pylori*³¹. Pathogenicity might even be further aggravated by our observation
305 that CEACAMs are strongly up-regulated during gastritis, which further potentiates binding
306 of *H. pylori* to epithelial cells and specifically facilitates CagA/*cagPAI* interaction with the
307 host cells.

308 Taken together, the finding that *H. pylori* employs CEACAMs not only for bacterial
309 adherence but also to induce cellular signaling may lead to a better understanding of the
310 pathogenic mechanisms of these bacteria and might lead to novel therapeutic approaches to
311 more effectively combat this highly prevalent infection and the associated gastric pathology.

312

313

314

315 **Materials and Methods**

316

317 **Bacteria and bacterial growth conditions**

318 The *H. pylori* strains G27³², PMSS1³³, SS1³⁴, J99 (ATCC, 700824), 2808³⁵, 26695 (ATCC,
319 70039), TX30³⁶, 60190³⁷, P12³⁸, NCTC11637 (ATCC, 43504), Ka89 and *H. bilis*
320 (ATCC43879) were grown on Wilkins–Chalgren blood agar plates under microaerobic
321 conditions (10% CO₂, 5% O₂, 8.5% N₂, and 37°C). *H. suis*³⁹ and *H. heilmannii*⁴⁰ were grown
322 on Brucella agar and *H. felis* (ATCC 49179) and *H. bizzozeronii*⁴¹ on brain-heart infusion
323 (BHI) agar supplemented with 10% horse blood. *Moraxella catarrhalis* (ATCC, 25238)
324 provided by C. R. Hauck (Konstanz Research School Chemical Biology, University of
325 Konstanz, Germany), *Moraxella Lacunata* (ATCC 17967) and *Campylobacter jejuni* (ATCC,
326 33560) were cultured on brain–heart infusion (BHI) agar supplemented with 5% heated horse
327 blood overnight at 37°C in a CO₂ incubator. The generation of an isogenic Δ *hopQ* mutant has
328 been done by replacement of the entire gene by a chloramphenicol resistance cassette. For
329 genetic complementation of *hopQ*, the 1,926 bp gene fragment of *H. pylori* strain P12 was
330 amplified by PCR. This fragment was cloned into the complementation vector pSB1001 using
331 the AphA3 cassette for selection. This fusion construct was introduced in the plasticity region
332 of strain P12 Δ *hopQ* (between ORFs HP0999 and HP1000) using a strategy as described⁴².

333 **Production of CEACAM proteins**

334 The cDNA, which encodes the extracellular domains of human CEACAM1-Fc (consisting of
335 N-A1-B1-A2 domains), human CEACAM1dN-Fc (consisting of A1-B1-A2, lacking the first
336 143 amino acids of the N-terminal IgV-like domain), rat CEACAM1-Fc (consisting of N-A1-
337 B1-A2), rat CEACAM1dN-Fc (consisting of A1-B1-A2), human CEACAM3-Fc (consisting
338 of N), human CEACAM6-Fc (consisting of N-A-B), human CEACAM8-Fc (consisting of N-
339 A-B), respectively, were fused to a human heavy chain Fc-domain and cloned into the
340 pcDNA3.1(+) expression vector (Invitrogen, San Diego, CA), sequenced and stably
341 transfected into HEK293 (ATCC CRL-1573) cells as described⁴³. The Fc chimeric CEACAM-
342 Fc proteins were accumulated in serum-free Pro293s-CDM medium (Lonza) and were
343 recovered by Protein A/G-Sepharose affinity Chromatography (Pierce). Proteins were
344 analyzed by SDS-PAGE and stained by Coomassie blue demonstrating an equal amount and
345 integrity of the produced fusion proteins (Extended Data Fig. 1i). Recombinant-human
346 CEACAM5-Fc was ordered from Sino Biological Inc. The GFP-tagged CEACAMs (human-
347 CEACAM1 and its variants, mouse-CEACAM1, bovine-CEACAM1 and canine-CEACAM1)

348 were provided by Dr. C. R. Hauck (University Konstanz, Germany). For production of the
349 recombinant human CEACAM1 N-Domain (C1ND), the annotated domain (residues 35-142
350 of CEACAM1, Uniprot ID: P13688) was first backtranslated using the Gene
351 Optimizer[®] (LifeTechnologies) and the leader sequence of the Igk-chain as well as a C-
352 terminal Strep-Tag II was added. The gene was synthesized and seamlessly cloned into
353 pCDNA3.4-TOPO (LifeTechnologies). Protein was produced in a 2 L culture of Expi293
354 cells according to the Expi293 expression system instructions (LifeTechnologies).
355 The resulting supernatant was concentrated and diafiltered against ten volumes of 1x
356 SAC buffer (100 mM Tris-HCl, 140 mM NaCl, 1 mM EDTA, pH 8.0) by crossflow-
357 filtration, using a Hydrosart 5 kDa molecular-weight cutoff membrane (Sartorius). The
358 retentate was loaded onto a StrepTrap HP column (GE Healthcare) and eluted with 1x SAC
359 supplemented with 2.5 mM D-Desthiobiotin (IBA). The protein was stored at +4°C.

360 For the bacterial expression of the C1ND (Ec-C1ND) the amino acid sequence (residues 35-
361 142 of CEACAM1, Uniprot ID: P13688) was codon optimized for expression in *E. coli*,
362 synthesized by GeneArt *de novo* gene synthesis (Life Technologies), and cloned with a C-
363 terminal His6 tag in the pDEST[™]14 vector using Gateway technology (Invitrogen). *E. coli*
364 C43(DE3) cells were transformed with the resulting construct and grown in LB supplemented
365 with 100 µg/mL ampicillin at 37°C while shaking. At OD₆₀₀=1 Ec-C1ND expression was
366 induced with 1 mM IPTG overnight at 30°C. Cells were collected by centrifugation at 6.238 g
367 for 15 minutes at 4°C and resuspended in 50mM Tris-HCl pH 7.4, 500 mM NaCl (4 mL/g wet
368 cells) supplemented with 5 µM leupeptin and 1 mM AEBSF, 100 µg/mL lysozyme, and 20
369 µg/mL DNase I. Subsequently cells were lysed by a single passage in a Constant System Cell
370 Cracker at 20 kPsi at 4 °C and debris was removed by centrifugation at 48.400 g for 40
371 minutes. The cytoplasmic extract was filtrated through a 0.45 µm pore filter and loaded on a 5
372 mL pre-packed Ni-NTA column (GE Healthcare) equilibrated with buffer A (50 mM Tris-
373 HCl pH 7.4, 500 mM NaCl and 20 mM imidazole). The column was then washed with 40 bed
374 volumes of buffer A and bound proteins were eluted with a linear gradient of 0-75 % buffer B
375 (50 mM Tris-HCl pH 7.4, 500 mM NaCl and 500 mM imidazole). Fractions containing Ec-
376 C1ND, as determined by SDS-PAGE, were pooled and concentrated in a 10 kDa MW cutoff
377 spin concentrator to a final volume of 5 ml. To remove minor protein contaminants, the
378 concentrated sample was injected onto the Hi-Prep[™] 26/60 Sephacryl S-100 HR column (GE
379 Healthcare) pre-equilibrated with a buffer containing 50 mM Tris-HCl pH 8.0, 150 mM NaCl.
380 Fractions containing the Ec-C1ND complex were pooled and concentrated using a 10 kDa
381 MW cutoff spin concentrator.

382

383

384 **HopQ^{AD} and HopQ^{AD}ΔID cloning, production and purification**

385 In order to obtain a soluble HopQ fragment, the HopQ gene from the *H. pylori* G27 strain
386 (accession No. CP001173 Region: 1228696..1230621) HopQ fragment ranging from residues
387 37 – 463 was produced (residues 17-444 of the mature protein), thus removing the N-terminal
388 β-strand and signal peptide, as well as the C-terminal β-domain expected to represent the TM
389 domain. In HopQ^{AD}ΔID, the amino acids 184-212 of the mature protein were replaced by two
390 glycines (Extended Data Fig.f). DNA coding sequences corresponding to the HopQ type I
391 fragments was PCR-amplified from *H. pylori* G27 genomic DNA using primers (forward:
392 GTTTAACTTTAAGAAGGAGATATACAAATGGCGGTTCAAAAAGTGAAAAACGC;
393 reverse: TCAAGCTTATTAATGATGATGATGATGGTGGGCGCCGTTATTCGTGGTTG),
394 containing 30bp overlap to the flanking target vector sequences of pPRkana-1, a derivative of
395 pPR-IBA 1 (IBA GmbH) with the ampicillin resistance cassette replaced by the kanamycin
396 resistance cassette, under a T7 promotor. In parallel, the vector was PCR-amplified using
397 primers (forward: CACCATCATCATCATTAATAAGCTTGATCCGGCTGCTAAC ;
398 reverse: GTTTAACTTTAAGAAGGAGATATACAAATG) as provided in table 1, using the
399 same overlapping sequences in reversed orientation. The forward primer additionally carried
400 the sequence for a 6x His-tag. The amplicons were seamlessly cloned using Gibson Assembly
401 (New England Biolabs GmbH). Based on codon optimized HopQ^{AD} plasmid, the HopQ^{AD}ΔID
402 constructs were cloned. The plasmids were amplified by 5' phosphorylated primers (forward:
403 GGTGACGCTCAGAACCTGCTGAC; reverse: ACCACCTTTAGAGTTCAGCGGAG)
404 replacing the ID region by two glycines, *DpnI* (NEB) digested and blunt-end ligated by T4
405 ligase (NEB).

406 *Escherichia coli* BL21(DE3) cells (NEB GmbH) were transformed with the pPRkana-1
407 constructs, grown at 37°C with 275 rpm on auto-inducing terrific broth (TRB) according to
408 Studier⁴⁴, supplemented with 2 mM MgSO₄, 100 mg/L Kanamycin-Sulfate (Carl Roth GmbH
409 + Co. KG), 0.2 g/L PPG2000 (Sigma-Aldrich) and 0.2% w/v Lactose-monohydrate (Sigma-
410 Aldrich), until an OD of 1-2 was reached. Afterwards, the temperature was lowered to 25°C
411 and auto-induced overnight, reaching a final OD of 10-15 the following morning. Cells were
412 harvested by centrifugation at 6000 g for 15 min at 4 °C using a SLA-3000 rotor in a Sorvall
413 RC-6 Plus centrifuge (Thermo Fischer). Prior to cell disruption, cells were resuspended in 10
414 mL cold NiNTA buffer A (500 mM NaCl, 100 mM Tris-HCl, 25 mM Imidazole, pH 7.4) per
415 gram of biological wet weight (BWW), supplemented with 0.1 mM AEBSF-HCl, 150 U/g

416 BWW DNase I and 5 mM MgCl₂ and dispersed with an Ultra-Turrax T25 digital (IKA GmbH
417 + Co. KG). Cell disruption was performed by high-pressure homogenization with a
418 PANDA2000 (GEA NiroSoavi) at 800-1200 bar in 3 passages at 4 °C. The cell lysate was
419 clarified by centrifugation at 25000 g for 30 min at 4 °C in a SLA-1500 rotor and remaining
420 particles removed by filtration through a 0.2 µm filter.

421 HopQ fragments were purified by consecutive nickel affinity and size exclusion
422 chromatography. Briefly, the clarified cell lysate was loaded onto a 5 mL pre-packed Ni-NTA
423 HisTrap FF crude column (GE Healthcare) pre-equilibrated with buffer A, washed with ten
424 column volumes (CV) of buffer A and the bound protein eluted with a 15 CV linear gradient
425 to 75% NiNTA buffer B (500 mM NaCl, 100 mM Tris-HCl, 500 mM Imidazole, pH 7.4).
426 Eluted peak fractions were collected, pooled and concentrated to a final concentration of 8-10
427 mg ml⁻¹ using a 10 kDa molecular-weight cutoff spin concentrator. Subsequently, 5 mL of the
428 concentrated protein were loaded onto a HiLoad 16/600 Superdex 75 pg column (GE
429 Healthcare) pre-equilibrated with Buffer C (5 mM Tris-HCl, 140 mM NaCl, pH 7.3) and
430 eluted at 1 mL/min. Finally, only protein corresponding to the monomer-peak was pooled and
431 stored at +4 °C prior to crystallization. For analyzing the multimerization state of HopQ^{AD},
432 SEC was performed on a Superdex 200 10/300 GL (GE Healthcare) with 24 mL bed volume.
433 The column was pre-equilibrated with Buffer C and subsequently, 25 µg protein injected and
434 separated with a flow rate of 0.5 mL/min.

435 The HopQ interaction domain (HopQ-ID) representing peptide was HA-tagged, synthesized
436 (EKLEAHVTTSKYQQDNQTKTTTSVIDTTNYPYDVPDYA) and HPLC purified (Peptide
437 Specialty Laboratories, Heidelberg, Germany). For cellular assays, the lyophilized peptide
438 was dissolved in sterile PBS to a concentration of 1 mM and dialysed with a 0.1-0.5 kDa
439 molecular-weight cutoff membrane against PBS to remove remaining TFA. The peptide
440 solution was stored at -20 °C until further use.

441 **Detection of the HopQ-CEACAM interaction by ELISA**

442 For detection of the interaction between CEACAM and HopQ^{AD}, recombinant C1ND (1
443 µg/mL) in PBS was coated over night at 4 °C onto a 96-well immunoplate (Nunc MaxiSorb).
444 Wells were blocked with SmartBlock (Candor) for 2 h at RT. Subsequently, HopQ fragments
445 were added in a fivefold series dilution ranging from 10 µg/mL to 0.05 ng/mL for 2h at room
446 temperature. Next, α-6xHis-HRP conjugate (clone 3D5, LifeTechnologies) was diluted
447 1:5000 and incubated for 1h at room temperature. For detection, 1-Step™ Ultra TMB-ELISA
448 Substrate Solution (LifeTechnologies) was used and the enzymatic reaction was stopped with

449 2 N H₂SO₄. Washing (3-5x) in between incubation steps was carried out with PBS / 0.05%
450 Tween20.

451 **Isothermal titration calorimetry**

452 ITC measurements were performed on a MicroCal iTC200 calorimeter (Malvern). 25 μ M
453 C1ND or EcC1ND were loaded into the cell of the calorimeter and 250 μ M HopQ^{AD} type I
454 was loaded in the syringe. All measurements were done at 25°C, with a stirring speed of 600
455 rpm and performed in 20 mM HEPES buffer (pH 7.4), 150 mM NaCl, 5% (v/v) glycerol and
456 0.05% (v/v) Tween-20. Binding data were analyzed using the MicroCal LLC ITC200
457 software.

458 **SDS-PAGE and native-PAGE for Western blot**

459 CEACAM was separated with both SDS-PAGE and native-PAGE (resp. on 15% and 7.5%
460 polyacrylamide gels) in ice-cold 25 mM Tris-HCl, 250 mM glycine buffer. Subsequently
461 samples were transferred to PVDF-membranes by wet blotting at 25 V during 60 minutes in
462 ice-cold transfer buffer (25 mM Tris-HCl, 250 mM glycine and 20% methanol). Membranes
463 were blocked during one hour in 10% milk powder (MP), 1x PBS and 0.005% Tween-20.
464 Both membranes were washed and incubated together in 5% MP, 1x PBS, 0.005% Tween-20
465 in presence of 2 μ M HopQ^{AD} type I for one hour to allow complex formation between
466 HopQ^{AD} I and CEACAM. After a washing step the C-terminal His-tag of HopQ (CEACAM is
467 strep tagged) was detected by adding consecutively mouse α -His (AbDSerotec) and goat α -
468 mouse antibody (Sigma-Aldrich) during respectively one hour and 30 minutes in 5% MP, 1x
469 PBS, 0.005% Tween-20. After a washing step the blot was developed by adding BCIP/NBT
470 substrate (5-bromo-4-chloro-3-indolyl-phosphate/nitro blue tetrazolium) (Roche) in
471 developing buffer (10 mM Tris-HCl pH 9.5, 100 mM NaCl, 50 mM MgCl₂).

472 **Bacterial pull down**

473 Bacteria were grown overnight on WC dent agar plates. Bacteria were scraped from plates,
474 suspended in PBS, and colony forming units (cfu) were estimated by optical density 600
475 readings according to a standard curve. Bacteria were washed twice with PBS and
476 2×10^8 cells/mL were incubated with soluble CEACAM-Fc or CEACAM-GFP proteins or
477 CHO cell lysates for 1 h at 37 °C with head-over-head rotation. After incubation, bacteria
478 were washed 5 times with PBS and either boiled in SDS sample buffer (62.5 mM Tris-HCl
479 [pH 6.8], 2% w/v SDS, 10% glycerol, 50 mM DTT, and 0.01% w/v bromophenol blue) prior
480 to SDS-PAGE and Western blotting or taken up in FACS buffer (PBS/0.5% BSA) for flow
481 cytometry analysis.

482 **Immunoprecipitation and Mass Spectrometry**

483 Bacteria (2×10^8) in cold PBS containing protease and phosphatase inhibitors (Roche) were
484 lysed by ultra-sonication on ice (10x, 20s). Cell debris was removed from the lysates by
485 centrifugation at 15,000 rpm for 30 min at 4 °C, followed by pre-clearing with prewashed
486 protein G-agarose (Roche Diagnostics). CEACAM1-Fc was added to the lysate (10 µg) and
487 incubated for 1 h at 4 °C. Prewashed protein G-agarose (60 µL) were added to the antibody
488 and lysate mixture and incubated 2 h at 4 °C. Beads were washed with PBS for five times to
489 remove unspecifically bound proteins. Two-thirds of the beads were separated and used for
490 mass spectrometry sample preparation. The supernatant was removed and the beads were
491 resuspended twice in 50 µL 7M urea/ 2 M thiourea solved in 20 mM Hepes (pH 7.5) for
492 denaturation of the proteins. Beads were pelleted by centrifugation and supernatants pooled
493 and transferred to a new Eppendorf tube. Subsequently, proteins were reduced in 1 mM DTT
494 for 45 min and alkylated at a final concentration of 5.5 mM iodoacetamide for 30 min in the
495 dark. The alkylation step was quenched by raising the DTT concentration to 5 mM for 30
496 min. All incubation steps were carried out at RT under vigorous shaking (Eppendorf shaker,
497 450 rpm). For digestion of the proteins 1 µL LysC (0.5 µg/µL) was added and the sample
498 incubated for 4h at RT. To reduce the urea concentration the sample was diluted 1:4 with 50
499 mM triethylammonium bicarbonate and then incubated with 1.5 µL trypsin (0.5 µg/µL) at 37
500 °C over night. Trypsin was finally inactivated by acidification with formic acid. The
501 supernatant was transferred to a new Eppendorf tube and pooled with the following wash
502 fraction of the beads with 0.1% formic acid. The sample was adjusted to pH 3 with formic
503 acid (100% v/v) and subjected to peptide desalting with a SepPak C18 column (50 mg,
504 Waters). Briefly, the column was subsequently washed with 1 mL 100% acetonitrile and 500
505 µL 80% acetonitrile, 0.5% formic acid. The column was equilibrated with 1 mL 0.1% TFA,
506 the sample was loaded and the column washed again with 1 mL 0.1% TFA. After an
507 additional wash step with 500 µL 0.5% formic acid peptides were eluted twice with 250 µL
508 80% acetonitrile, 0.5% formic acid. The organic phase was then removed by vacuum
509 centrifugation and peptides stored at -80 °C. Directly before measurement peptides were
510 resolved in 20 µL 0.1% formic acid, sonified for 5 min (water bath) and the sample afterwards
511 filtered with a prewashed and equilibrated filter (0.45 µm low protein binding filter, VWR
512 International, LLC). Measurements were performed on an LC-MS system consisting of an
513 Ultimate 3000 nano HPLC directly linked to an Orbitrap XL instrument (Thermo Scientific).
514 Samples were loaded onto a trap column (2 µm, 100 Å, 2 cm length) and separated on a 15
515 cm C18 column (2 µm, 100 Å, Thermo Scientific) during a 150 min gradient ranging from 5

516 to 30% acetonitrile, 0.1% formic acid. Survey spectra were acquired in the orbitrap with a
517 resolution of 60,000 at m/z 400. For protein identification up to five of the most intense ions
518 of the full scan were sequentially isolated and fragmented by collision induced dissociation.
519 The received data was analyzed with the Proteome Discoverer Software version 1.4 (Thermo
520 Scientific) and searched against the *H. pylori* (strain G27) database (1501 proteins) in the
521 SEQUEST algorithm. Protein N-terminal acetylation and oxidation of methionins were added
522 as variable modifications, carbamidomethylation on cysteines as static modifications. Enzyme
523 specificity was set to trypsin and mass tolerances of the precursor and fragment ions were set
524 to 10 ppm and 0.8 Da, respectively. Only peptides that fulfilled X_{corr} values of 1.5, 2.0, 2.25
525 and 2.5 for charge states +1, +2, +3 and +4 respectively were considered for data analysis.

526 **Cells, cell-bacteria co-culture and elongation phenotype quantitation assay**

527 Gastric cancer cell lines MKN45⁴⁵, KatoIII (ATCC, HTB-103), MKN28⁴⁶ and AGS (ATCC,
528 CRL-1739) were obtained from ATCC and DSMZ, authenticated by utilizing Short Tandem
529 Repeat (STR) profiling, cultured either sparse or to tight confluence in DMEM (GIBCO,
530 Invitrogen, Carlsbad CA, USA) containing 2 mM L-glutamine (GIBCO, Invitrogen, CA,
531 USA) supplemented with 10% FBS (GIBCO, Invitrogen, CA, USA) and 1% Penicillin/
532 Streptomycin (GIBCO, Invitrogen, CA, USA). All cell lines were maintained in an incubator
533 at 37°C with 5% CO₂ and 100% humidity, and were routinely mycoplasma-tested twice per
534 year by DAPI stain and PCR. Plate-grown bacteria were suspended in DMEM and washed by
535 centrifugation at 150 g for 5 min in a microcentrifuge. After resuspension in DMEM, the
536 optical density at 600 nm was determined and bacteria were added to the overnight serum-
537 deprived cells at different ratios of bacteria/cell (MOI) at 37°C to start the infection. After the
538 indicated time, cells were washed twice with PBS and then lysed with 1% NP-40 in protease
539 & phosphatase inhibitor PBS. HEK293 cells were chosen for CEACAM transfection studies
540 because the cells were found to be negative for hu-CEACAM expression, and are easily
541 transfectable. HEK cells were grown in 6-well plates containing RPMI 1640 medium
542 (Invitrogen) supplemented with 25 mM HEPES buffer and 10% heat-inactivated FBS
543 (Biochrom, Berlin, Germany) for 2 days to approximately 70% confluence. Cells were serum-
544 deprived overnight and infected with *H. pylori* at MOI 50 for the indicated time points in each
545 figure. After infection, the cells were harvested in ice-cold PBS containing 1 mM Na₃VO₄
546 (Sigma-Aldrich). Elongated AGS cells in each experiment were quantified in 5 different 0.25-
547 mm² fields using an Olympus IX50 phase contrast microscope.

548 **Transfection**

549 A CHO cell line (ATCC) permanently expressing hu-CEACAM1-4L, mouse-CEACAM1-L
550 and rat-CEACAM1-L were generated by stably transfecting cells with 4 µg pcDNA3.1-
551 huCEACAM1-4L, pcDNA3.1-huCEACAM1-4S, pcDNA3.1-msCEACAM1-L, pcDNA3.1-
552 ratCEACAM1-L plasmid (Singer), respectively, utilizing the lipofectamine 2000 procedure
553 according to the manufacturer's protocol (Invitrogen). Stable transfected cells were selected in
554 culture medium containing 1 mg/mL of Genitocinsulfat (G418, Biochrom, Berlin, Germany).
555 The surface expression of CEACAM1 in individual clones growing in log phase was
556 determined by flow cytometry (FACS calibur, BD). HEK293 cells were transfected with 4 µg
557 of the HA-tagged CEACAM constructs or luciferase reporter constructs (Clontech, Germany)
558 for 48 h with TurboFect reagent (Fermentas, Germany) according to the manufacturer's
559 instructions.

560 **Western blot**

561 An equal volume of cell lysate was loaded on 8% SDS-PAGE gels and after electrophoresis,
562 separated proteins were transferred to nitrocellulose membrane (Whatman/GE Healthcare,
563 Freiburg, Germany). Membranes were blocked in 5% non-fat milk for 1 h at room
564 temperature and incubated overnight with primary antibodies mAb 18/20 binding to
565 CEACAM1,3,5, B3-17 and C5-1X (mono-specific for hu-CEACAM1, Singer), 4/3/17
566 (binding to CEACAM1,5, Genovac), and 5C8C4 (mono-specific for hu-CEACAM5, Singer),
567 1H7-4B (mono-specific for hu-CEACAM6, Singer), 6/40c (mono-specific for hu-CEACAM8,
568 Singer), Be9.2 (α-rat-CEACAM1, kindly provided by Dr. W. Reutter, Charite, CBF,
569 Germany), mAb 11-1H (α-rat-CEACAM1ΔN, Singer), phosphotyrosine antibody PY-99
570 (Santa Cruz, LaJolla, CA, USA), α-CagAphosphotyrosine antibody PY-972⁴⁷, mouse
571 monoclonal α-CagA antibody (Austral Biologicals, San Ramon, CA, USA), mouse
572 monoclonal α-CEACAM1 (clone D14HD11Genovac/Aldevron, Freiburg,Germany) or goat
573 α-GAPDH (Santa Cruz). After washing, membranes were incubated with the secondary
574 antibody [HRP-conjugated α-mouse IgG (Promega)] and proteins were detected by ECL
575 Western Blotting Detection reagents. The quantification was done by LabImage 1D software
576 (INTAS).

577 **Flow cytometry**

578 The Fc-tagged CEACAMs (2.5 µg/mL) were incubated with *H. pylori* (OD₆₀₀=1) and
579 subsequently with FITC-conjugated goat α-human IgG (Sigma-Aldrich). After washing with

580 FACS buffer, the samples were analyzed by gating on the bacteria (based on forward and
581 sideward scatter) and measuring bacteria-associated fluorescence. In each case, 10,000 events
582 per sample were obtained. Analysis was performed with the FACS CyAn (Beckman Coulter)
583 and the data were evaluated with FlowJo software (Treestar). For the analysis of CEACAM
584 mediated HopQ binding, indicated cell types (5×10^5 in 50 μL) were incubated with 20 $\mu\text{g}/\text{mL}$
585 of *H. pylori* strain P12 derived, myc and 6x His-tagged recombinant HopQ diluted in 3%
586 FCS/PBS for 1 h on ice. After three times washing with 3% FCS/PBS samples were labeled
587 with 20 $\mu\text{g}/\text{mL}$ of mouse α -c-myc mAb (clone 9E10, AbDSerotec) and subsequently with
588 FITC conjugated goat α -mouse F(ab')₂ (Dianova, Germany). In parallel, the presence of
589 CEACAMs was controlled by staining cells utilizing the rabbit anti CEA pAb (A0115,
590 Dianova) followed by FITC conjugated goat α -rabbit F(ab')₂ (Dianova, Germany).
591 Background fluorescence was determined using isotype-matched Ig mAb. The stained cell
592 samples were examined in a FACScalibur flow cytometer (BD Biosciences, San Diego, CA)
593 and the data were analyzed utilizing the CellQuest software. Dead cells, identified by PI
594 staining, were excluded from the measurement.

595 **Immunohistochemistry and Immunofluorescence**

596 Following approval of the local ethics committee, paraffin-embedded human normal stomach,
597 gastritis and cancer samples were randomly chosen from the tissue bank of the Institut für
598 Pathologie, Klinikum Bayreuth Germany. Histological samples were excluded if tissue
599 quality was poor. After antigen retrieval with 10 mM sodium citrate buffer pH 6 in pressure
600 cooker, the sections were incubated with α -hu-CEACAM1, 5, 6 and α -rat-CEACAM1
601 antibodies (clone B3-17, 5C8C4, 1H7-4B and Be9.2, respectively). Sections were developed
602 with SignalStain DAB (Cell Signaling) following manufacturer's instructions. Sections were
603 counterstained with hematoxylin (Morphisto). The automated image acquisition was
604 performed with Olympus Virtual Slide System VS120 (Olympus, Hamburg, Germany).

605 **Visualization of the co-localization of HopQ and CEACAMs co-staining of normal and**
606 **gastritis sections was performed utilizing HopQ-biotin followed by streptavidin-Cy3 and α -**
607 **hu-CEACAM1, 3, 5, 6, 8 clone 6G5j followed by Alexa 488 coupled goat anti mouse**
608 **antibody. The cell nuclei were stained with DAPI. DAPI and fluorescent proteins were**
609 **analyzed with the Leica DMI4000B microscope.**

610 **Adherence assay**

611 The adherence assay was performed according to Hytonen et al ⁴⁸. Briefly, human gastric
612 epithelial cells (MKN45 and AGS) and CEACAM1-transfected CHO cells were grown in

613 antibiotic free DMEM (Gibco, Gaithersburg, MD) supplemented with 5% FCS and L-
614 glutamine (2 mM, Sigma-Aldrich) on tissue culture 96 well plates (Bioscience) in 5% CO₂
615 atmosphere for 2 days. To visualize *H. pylori* cells in adhesion assays, OD₆₀₀=1 of bacteria
616 were fluorescence labeled with CFDA-SE (Molecular Probes) and washed with PBS. CFDA-
617 SE was added at concentration of 10 μM for 30 min at 37°C under constant rotation in the
618 dark. Excess dye was removed by 3 times washing with PBS. Bacteria were resuspended in
619 PBS until further use. Labelled bacteria were co-incubated (MOI 10) with the cells at 37°C
620 with gentle agitation for 1 h. After washing with PBS (1 mL, ×3) to remove non-adherent
621 bacteria, cells were fixed in paraformaldehyde (2%, 10 min). Bacterial binding was
622 determined by measuring the percentage of cells that bound fluorescent-labeled bacteria using
623 flow cytometry analysis.

624 **IL-8 cytokine ELISA**

625 AGS cell line was infected with *H. pylori* as described already and PBS-incubated control
626 cells served as negative control. The culture supernatants were collected and stored at -20 °C
627 until assayed. IL-8 concentration in the supernatant was determined by standard ELISA with
628 commercially available assay kits (Becton Dickinson, Germany) according to described
629 procedures.

630

631 **HopQ-dependency of CagA virulence pathways**

632 If not indicated otherwise, the AGS cell line (ATCC CRL-1730) was infected with the various
633 *H. pylori* strains for 6 hours at a multiplicity of infection (MOI) of 50. The cells were then
634 harvested in ice-cold PBS in the presence of 1 mM Na₃VO₄ (Sigma-Aldrich). In each
635 experiment the number of elongated AGS cells was quantified in 10 different 0.25-mm² fields
636 using a phase contrast microscope (Olympus IX50). CagA translocation was determined using
637 the indicated antibodies detecting Tyr-phosphorylated CagA. All experiments were performed
638 in triplicates. For inhibition experiments, cells were incubated with the indicated antibodies or
639 peptides prior to infection.

640 **Confocal microscopy**

641 CHO cells were grown on chamber slides (Thermo Scientific), fixed in paraformaldehyde
642 (4%, 10 min) and blocked with PBS/5% bovine serum albumin. CFDA-SE labelled bacteria
643 (10 μM for 30 min at 37°C under constant rotation in the dark) at MOI 5 were incubated with
644 cells for 1 h at 37°C under constant rotation. After 5X PBS washing, cell membranes were

645 stained with Deep Red (Life Technology) and cell nuclei with DAPI (Life Technology).
646 Confocal images of cells were taken using a Leica SP5 confocal microscope.

647 **Crystallization and structure determination of HopQ^{AD}**

648 HopQ^{AD} was concentrated to 40 mg/mL and crystallized by sitting drop vapor diffusion at
649 20°C using 0.12 M alcohols (0.02 M 1,6-Hexanediol; 0.02 M 1-Butanol; 0.02 M 1,2-
650 Propanediol; 0.02 M 2-Propanol; 0.02 M 1,4-Butanediol; 0.02 M 1,3-Propanediol), 0.1 M Tris
651 (base)/BICINE pH 8.5, 20% v/v PEG 500 MME; 10 % w/v PEG 20000 as a crystallization
652 buffer. Crystals were loop-mounted and flash-cooled in liquid nitrogen. Data were collected at
653 100 K at beamline Proxima1 (SOLEIL, Gif-sur-Yvette, France) and were indexed, processed
654 and scaled using the XDS package⁴⁹. All crystals were in the P2₁ space group with
655 approximate unit cell dimensions of a=57.7 Å, b=57.7 Å, c=285.7 Å and beta=90.1° and four
656 copies of HopQ₄₄₂ per asymmetric unit. Phases were obtained by molecular replacement using
657 the BabA structure (PDB:5F7K)²¹ and the program phaser^{50,51}. The models were refined by
658 iterative cycles of manual rebuilding in the graphics program COOT⁵² and maximum
659 likelihood refinement using Refmac5⁵³. Extended Data Table 2 summarizes the crystal
660 parameters, data processing and structure refinement statistics.

661 **Amino acid sequence alignment**

662 The amino acid sequence alignment of the N-terminal domains of human, mouse and rat-
663 CEACAM1 and human CEACAMs (1, 5, 6 and 8) was performed using CLC main
664 Workbench (CLC bio).

665 **Luciferase reporter assays**

666 CHO-CEACAM1-L cells transfected with various luciferase reporter and control constructs
667 (Clontech) were infected with *H. pylori* for 5 h and analyzed by luciferase assay using the
668 Dual-Luciferase Reporter Assay System according to the manufacturer's instruction (Promega,
669 USA). Briefly, cells were harvested by passive lysis, the protein concentration was measured
670 with Precision Red (Cytoskeleton, USA) and the lysates were equalized by adding passive
671 lysis buffer. The luciferase activity was measured by using a Plate Luminometer (MITHRAS
672 LB940 from Berthold, Germany).

673 **Animal experiments**

674 Specific pathogen free, 120-150 g 4 weeks-old male Sprague Dawley rats, were obtained from
675 Charles River Laboratories (Sulzfeld, Germany). Animals were randomly distributed into the
676 different experimental groups by animal care takers not involved in the experiments, and

677 criteria for the exclusion of animals were pre-established. Investigator blinding was
678 performed for all assessment of outcome and data, histology was performed by an
679 independent investigator in a blinded manner. Animals were challenged twice intragastrically
680 in groups of 8 with $\sim 1 \times 10^8$ live *H. pylori* in 2 interval days. After 6 weeks infection,
681 stomachs were removed and sectioned. One part was embedded in paraffin for histological
682 analysis and another piece was weighted and homogenized to determine colony forming units
683 (CFU)/mg stomach. Serial dilutions (1/10, 1/100 and 1/1000) were plated in WC dent plates.
684 CFU were counted after 4 days.

685 The experiments were performed in the specific pathogen-free unit of Zentrum für
686 Präklinische Forschung, Klinikum r. d. Isar der TU München, according to the allowance and
687 guidelines of the ethical committee and state veterinary office (Regierung von Oberbayern,
688 55.2-1.54-2532-160-12).

689 **Statistical Analysis**

690 For in vitro experiments, normal distribution was determined by Shapiro–Wilk test. Normally
691 distributed data were analyzed with two-tailed Student *t*-test or One-way ANOVA with post
692 hoc Bonferroni test (comparing more than two groups) using Graph Pad Prism Software. Data
693 are shown as mean \pm s.e.m or S.D. for at least three independent experiments. P values <0.05
694 were considered significant. For animal studies, power calculation was performed based on
695 previous animal experiments to achieve two sided significance of 0,05 while using lowest
696 possible numbers to comply with the ethical guidelines for experimental animals. Mann-
697 Whitney U test or ANOVA Kruskal-Wallis, Dunn’s multiple comparison test were used to
698 determine statistical significances.

699 **References**

- 700
701 1 Salama, N. R., Hartung, M. L. & Muller, A. Life in the human stomach: persistence strategies of the
702 bacterial pathogen *Helicobacter pylori*. *Nature reviews. Microbiology* **11**, 385-399,
703 doi:10.1038/nrmicro3016 (2013).
- 704 2 Atherton, J. C. & Blaser, M. J. Coadaptation of *Helicobacter pylori* and humans: ancient history,
705 modern implications. *The Journal of clinical investigation* **119**, 2475-2487, doi:10.1172/JCI38605
706 (2009).
- 707 3 Montecucco, C. & Rappuoli, R. Living dangerously: how *Helicobacter pylori* survives in the human
708 stomach. *Nature reviews. Molecular cell biology* **2**, 457-466, doi:10.1038/35073084 (2001).
- 709 4 Linden, S., Mahdavi, J., Hedenbro, J., Boren, T. & Carlstedt, I. Effects of pH on *Helicobacter pylori*
710 binding to human gastric mucins: identification of binding to non-MUC5AC mucins. *The Biochemical*
711 *journal* **384**, 263-270, doi:10.1042/BJ20040402 (2004).
- 712 5 Ilver, D. *et al.* *Helicobacter pylori* adhesin binding fucosylated histo-blood group antigens revealed by
713 retagging. *Science* **279**, 373-377 (1998).
- 714 6 Mahdavi, J. *et al.* *Helicobacter pylori* SabA adhesin in persistent infection and chronic inflammation.
715 *Science* **297**, 573-578, doi:10.1126/science.1069076 (2002).
- 716 7 Solnick, J. V., Hansen, L. M., Salama, N. R., Boonjakuakul, J. K. & Syvanen, M. Modification of
717 *Helicobacter pylori* outer membrane protein expression during experimental infection of rhesus
718 macaques. *Proceedings of the National Academy of Sciences of the United States of America* **101**, 2106-
719 2111, doi:10.1073/pnas.0308573100 (2004).
- 720 8 Hammarstrom, S. The carcinoembryonic antigen (CEA) family: structures, suggested functions and
721 expression in normal and malignant tissues. *Seminars in cancer biology* **9**, 67-81,
722 doi:10.1006/scbi.1998.0119 (1999).
- 723 9 Obrink, B. On the role of CEACAM1 in cancer. *Lung cancer* **60**, 309-312,
724 doi:10.1016/j.lungcan.2008.03.020 (2008).
- 725 10 Gray-Owen, S. D. & Blumberg, R. S. CEACAM1: contact-dependent control of immunity. *Nature*
726 *reviews. Immunology* **6**, 433-446, doi:10.1038/nri1864 (2006).
- 727 11 Voges, M., Bachmann, V., Kammerer, R., Gophna, U. & Hauck, C. R. CEACAM1 recognition by
728 bacterial pathogens is species-specific. *BMC microbiology* **10**, 117, doi:10.1186/1471-2180-10-117
729 (2010).
- 730 12 Heneghan, M. A. *et al.* Effect of host Lewis and ABO blood group antigen expression on *Helicobacter*
731 *pylori* colonisation density and the consequent inflammatory response. *FEMS immunology and medical*
732 *microbiology* **20**, 257-266 (1998).
- 733 13 Virji, M., Watt, S. M., Barker, S., Makepeace, K. & Doyonnas, R. The N-domain of the human CD66a
734 adhesion molecule is a target for Opa proteins of *Neisseria meningitidis* and *Neisseria gonorrhoeae*.
735 *Molecular microbiology* **22**, 929-939 (1996).
- 736 14 Hill, D. J. & Virji, M. A novel cell-binding mechanism of *Moraxella catarrhalis* ubiquitous surface
737 protein UspA: specific targeting of the N-domain of carcinoembryonic antigen-related cell adhesion
738 molecules by UspA1. *Molecular microbiology* **48**, 117-129 (2003).
- 739 15 Kuespert, K., Roth, A. & Hauck, C. R. *Neisseria meningitidis* has two independent modes of
740 recognizing its human receptor CEACAM1. *PLoS one* **6**, e14609, doi:10.1371/journal.pone.0014609
741 (2011).
- 742 16 Peek, R. M. *Helicobacter pylori* infection and disease: from humans to animal models. *Disease models*
743 *& mechanisms* **1**, 50-55, doi:10.1242/dmm.000364 (2008).
- 744 17 Icatlo, F. C., Goshima, H., Kimura, N. & Kodama, Y. Acid-dependent adherence of *Helicobacter pylori*
745 urease to diverse polysaccharides. *Gastroenterology* **119**, 358-367 (2000).
- 746 18 Cao, P. & Cover, T. L. Two different families of hopQ alleles in *Helicobacter pylori*. *Journal of clinical*
747 *microbiology* **40**, 4504-4511 (2002).
- 748 19 Ohno, T. *et al.* Relationship between *Helicobacter pylori* hopQ genotype and clinical outcome in Asian
749 and Western populations. *J Gastroenterol Hepatol* **24**, 462-468, doi:10.1111/j.1440-1746.2008.05762.x
750 (2009).
- 751 20 Alm, R. A. *et al.* Comparative genomics of *Helicobacter pylori*: analysis of the outer membrane protein
752 families. *Infection and immunity* **68**, 4155-4168 (2000).
- 753 21 Moonens, K. *et al.* Structural Insights into Polymorphic ABO Glycan Binding by *Helicobacter pylori*.
754 *Cell host & microbe* **19**, 55-66, doi:10.1016/j.chom.2015.12.004 (2016).
- 755 22 Rossez, Y. *et al.* The lacdiNac-specific adhesin LabA mediates adhesion of *Helicobacter pylori* to
756 human gastric mucosa. *The Journal of infectious diseases* **210**, 1286-1295, doi:10.1093/infdis/jiu239
757 (2014).

- 758 23 Singer, B. B. *et al.* Deregulation of the CEACAM expression pattern causes undifferentiated cell
759 growth in human lung adenocarcinoma cells. *PloS one* **5**, e8747, doi:10.1371/journal.pone.0008747
760 (2010).
- 761 24 Muenzner, P., Bachmann, V., Zimmermann, W., Hentschel, J. & Hauck, C. R. Human-restricted
762 bacterial pathogens block shedding of epithelial cells by stimulating integrin activation. *Science* **329**,
763 1197-1201, doi:10.1126/science.1190892 (2010).
- 764 25 Slevogt, H. *et al.* CEACAM1 inhibits Toll-like receptor 2-triggered antibacterial responses of human
765 pulmonary epithelial cells. *Nature immunology* **9**, 1270-1278, doi:10.1038/ni.1661 (2008).
- 766 26 Belogolova, E. *et al.* Helicobacter pylori outer membrane protein HopQ identified as a novel T4SS-
767 associated virulence factor. *Cell Microbiol* **15**, 1896-1912, doi:10.1111/cmi.12158 (2013).
- 768 27 Mahler, M. *et al.* Experimental Helicobacter pylori infection induces antral-predominant, chronic active
769 gastritis in hispid cotton rats (Sigmodon hispidus). *Helicobacter* **10**, 332-344, doi:10.1111/j.1523-
770 5378.2005.00320.x (2005).
- 771 28 Chang, Y. J. *et al.* Mechanisms for Helicobacter pylori CagA-induced cyclin D1 expression that affect
772 cell cycle. *Cell Microbiol* **8**, 1740-1752, doi:10.1111/j.1462-5822.2006.00743.x (2006).
- 773 29 Muenzner, P., Naumann, M., Meyer, T. F. & Gray-Owen, S. D. Pathogenic Neisseria trigger expression
774 of their carcinoembryonic antigen-related cellular adhesion molecule 1 (CEACAM1; previously
775 CD66a) receptor on primary endothelial cells by activating the immediate early response transcription
776 factor, nuclear factor-kappaB. *The Journal of biological chemistry* **276**, 24331-24340,
777 doi:10.1074/jbc.M006883200 (2001).
- 778 30 Olbermann, P. *et al.* A global overview of the genetic and functional diversity in the Helicobacter pylori
779 cag pathogenicity island. *PLoS genetics* **6**, e1001069, doi:10.1371/journal.pgen.1001069 (2010).
- 780 31 Suerbaum, S. & Josenhans, C. Helicobacter pylori evolution and phenotypic diversification in a
781 changing host. *Nature reviews. Microbiology* **5**, 441-452, doi:10.1038/nrmicro1658 (2007).
- 782 32 Baltrus, D. A. *et al.* The complete genome sequence of Helicobacter pylori strain G27. *Journal of*
783 *bacteriology* **191**, 447-448, doi:10.1128/JB.01416-08 (2009).
- 784 33 Arnold, I. C. *et al.* Tolerance rather than immunity protects from Helicobacter pylori-induced gastric
785 preneoplasia. *Gastroenterology* **140**, 199-209, doi:10.1053/j.gastro.2010.06.047 (2011).
- 786 34 Lee, A. *et al.* A standardized mouse model of Helicobacter pylori infection: introducing the Sydney
787 strain. *Gastroenterology* **112**, 1386-1397 (1997).
- 788 35 Lundin, A. *et al.* The NudA protein in the gastric pathogen Helicobacter pylori is an ubiquitous and
789 constitutively expressed dinucleoside polyphosphate hydrolase. *J Biol Chem* **278**, 12574-12578,
790 doi:10.1074/jbc.M212542200 (2003).
- 791 36 Atherton, J. C. *et al.* Mosaicism in vacuolating cytotoxin alleles of Helicobacter pylori. Association of
792 specific vacA types with cytotoxin production and peptic ulceration. *The Journal of biological*
793 *chemistry* **270**, 17771-17777 (1995).
- 794 37 Cover, T. L., Dooley, C. P. & Blaser, M. J. Characterization of and human serologic response to
795 proteins in Helicobacter pylori broth culture supernatants with vacuolizing cytotoxin activity. *Infect*
796 *Immun* **58**, 603-610 (1990).
- 797 38 Backert, S., Muller, E. C., Jungblut, P. R. & Meyer, T. F. Tyrosine phosphorylation patterns and size
798 modification of the Helicobacter pylori CagA protein after translocation into gastric epithelial cells.
799 *Proteomics* **1**, 608-617, doi:10.1002/1615-9861(200104)1:4<608::AID-PROT608>3.0.CO;2-G (2001).
- 800 39 Vermoote, M. *et al.* Genome sequence of Helicobacter suis supports its role in gastric pathology. *Vet*
801 *Res* **42**, 51, doi:10.1186/1297-9716-42-51 (2011).
- 802 40 Haesebrouck, F. *et al.* Non-Helicobacter pylori Helicobacter species in the human gastric mucosa: a
803 proposal to introduce the terms H. heilmannii sensu lato and sensu stricto. *Helicobacter* **16**, 339-340,
804 doi:10.1111/j.1523-5378.2011.00849.x (2011).
- 805 41 Schott, T., Kondadi, P. K., Hanninen, M. L. & Rossi, M. Comparative genomics of Helicobacter pylori
806 and the human-derived Helicobacter bizzozeronii CIII-1 strain reveal the molecular basis of the
807 zoonotic nature of non-pylori gastric Helicobacter infections in humans. *BMC Genomics* **12**, 534,
808 doi:10.1186/1471-2164-12-534 (2011).
- 809 42 Tegtmeier, N. *et al.* Characterisation of worldwide Helicobacter pylori strains reveals genetic
810 conservation and essentiality of serine protease HtrA. *Molecular microbiology* **99**, 925-944,
811 doi:10.1111/mmi.13276 (2016).
- 812 43 Singer, B. B. *et al.* Soluble CEACAM8 interacts with CEACAM1 inhibiting TLR2-triggered immune
813 responses. *PLoS One* **9**, e94106, doi:10.1371/journal.pone.0094106 (2014).
- 814 44 Studier, F. W. Protein production by auto-induction in high density shaking cultures. *Protein expression*
815 *and purification* **41**, 207-234 (2005).
- 816 45 Hojo, H. & Onishi, Y. [Case suspected to be atypical diffuse myeloma]. *Nihon rinsho. Japanese journal*
817 *of clinical medicine* **35**, 2659-2662 (1977).

818 46 Romano, M., Razandi, M., Sekhon, S., Krause, W. J. & Ivey, K. J. Human cell line for study of damage
819 to gastric epithelial cells in vitro. *The Journal of laboratory and clinical medicine* **111**, 430-440 (1988).
820 47 Mueller, D. *et al.* c-Src and c-Abl kinases control hierarchic phosphorylation and function of the CagA
821 effector protein in Western and East Asian *Helicobacter pylori* strains. *The Journal of clinical*
822 *investigation* **122**, 1553-1566, doi:10.1172/JCI61143 (2012).
823 48 Hytonen, J., Haataja, S. & Finne, J. Use of flow cytometry for the adhesion analysis of *Streptococcus*
824 *pyogenes* mutant strains to epithelial cells: investigation of the possible role of surface pullulanase and
825 cysteine protease, and the transcriptional regulator Rgg. *BMC Microbiol* **6**, 18, doi:10.1186/1471-2180-
826 6-18 (2006).
827 49 Krauth-Siegel, R. L. *et al.* Crystallization and preliminary crystallographic analysis of trypanothione
828 reductase from *Trypanosoma cruzi*, the causative agent of Chagas' disease. *FEBS letters* **317**, 105-108
829 (1993).
830 50 Winn, M. D. *et al.* Overview of the CCP4 suite and current developments. *Acta crystallographica.*
831 *Section D, Biological crystallography* **67**, 235-242, doi:10.1107/S0907444910045749 (2011).
832 51 McCoy, A. J. *et al.* Phaser crystallographic software. *Journal of applied crystallography* **40**, 658-674,
833 doi:10.1107/S0021889807021206 (2007).
834 52 Emsley, P., Lohkamp, B., Scott, W. G. & Cowtan, K. Features and development of Coot. *Acta*
835 *crystallographica. Section D, Biological crystallography* **66**, 486-501,
836 doi:10.1107/S0907444910007493 (2010).
837 53 Murshudov, G. N. *et al.* REFMAC5 for the refinement of macromolecular crystal structures. *Acta*
838 *crystallographica. Section D, Biological crystallography* **67**, 355-367,
839 doi:10.1107/S0907444911001314 (2011).
840

841

842 **Acknowledgments**

843 We thank Jeannette Koch, Judith Lind, Birgit Maranca-Hüwel and Bärbel Gobs-Hevelke for
844 their excellent technical support; Carolin Konrad, Johannes Fischer for support with rat
845 experiments and Marie Roskrow for fruitful discussion and revision. KM and HR
846 acknowledge use of the Soleil synchrotron, Gif-sur-Yvette, France under proposal 20131370
847 and support by VIB and the Flanders Science Foundation (FWO) through the Odysseus
848 program, a postdoctoral fellowship and Hercules funds UABR/09/005. This work was
849 supported by the German Centre for Infection Research, partner site Munich, to MG, by the
850 BMBF 01EO1002 to E.K., the Mercator Research Center Ruhr An2012-0070 to BBS, the
851 German Science Foundation CRC-796 (B10) and CRC-1181 (A04) to SB, the Collaborative
852 Research Center/Transregio 124, Project A5 to HS.

853

854 **Author Contribution**

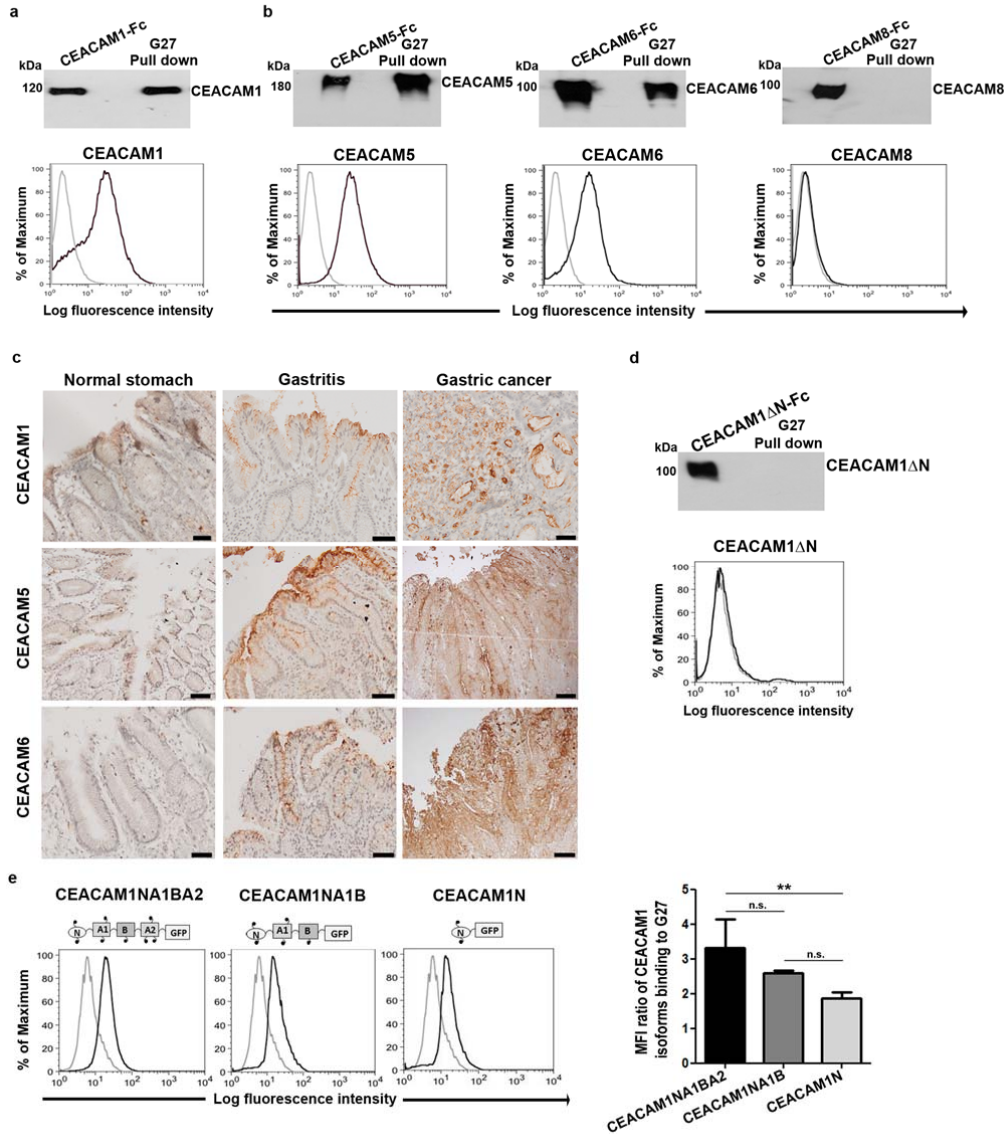
855 A.J., T.K., K.M., N.T., B.K., N.B., A.S. and B.B.S performed the experiments, B.B.S, R.H.,
856 V.K., E.K., H.S. and C.R.H. provided reagents and tools, A.J., B.B.S, H.R., D.B., R.M.-L.,
857 S.B. and M.G. conceived the experiments, analyzed the data and wrote the manuscript. All
858 authors read and approved the final manuscript.

859

860 **Author information**

861 Reprints and permissions information is available at www.nature.com/reprints. M.G., B.K.
862 and T.K. are employees and Shareholders of Imevax GmbH. M.G., A.J., B.S., S.B. and T.K.
863 are named as inventors on a patent application regarding HopQ. The other authors declare no
864 conflict of interest. Correspondence and requests for materials should be addressed to
865 markus.gerhard@tum.de.

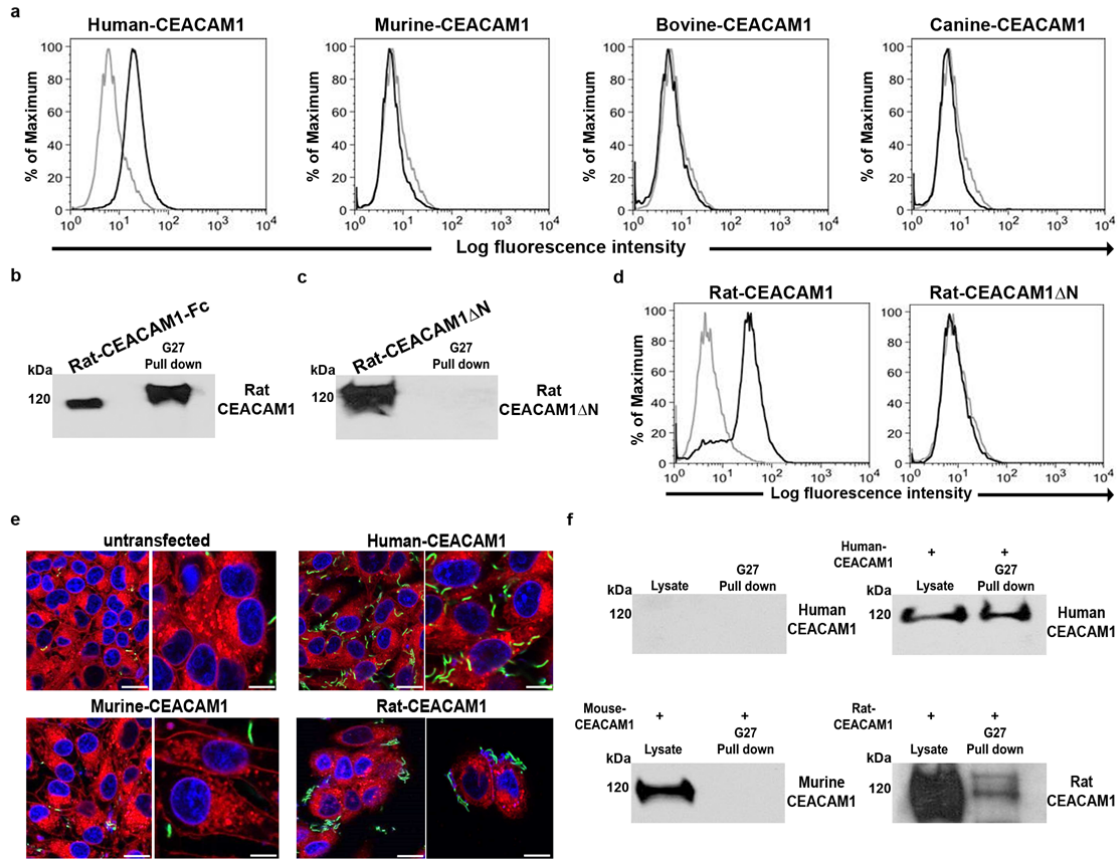
Gerhard Fig. 1



866

867 **Figure 1** *H. pylori* employs the N-terminal domain of hu-CEACAM1 and binds
 868 **CEACAM5 and CEACAM6 but not CEACAM8**. *H. pylori* G27 strain binding to human
 869 CEACAM1-Fc (a) and human CEACAM5-Fc, CEACAM6-Fc or CEACAM8-Fc (b) was
 870 analyzed by pull down experiments followed by western blot analysis and flow cytometry
 871 (n=3). (c) CEACAM1, CEACAM5 and CEACAM6 expression detected by
 872 immunohistochemistry in human normal stomach, gastritis and gastric cancer samples. Scale
 873 bars, 50 μm. (d) Binding of *H. pylori* to human CEACAM1ΔN-Fc (lacking the complete N-
 874 domain) detected by western blot after pull down or by flow cytometry. One representative
 875 experiment of 4 is shown. (e) *H. pylori* binding to CEACAM variants analyzed by flow
 876 cytometry. Mean Fluorescence Intensity (MFI) ratios (mean, S.D.) are shown (n=4). One-way
 877 ANOVA, *P* value= 0.009, n. s.: not significant.

Gerhard Fig. 2

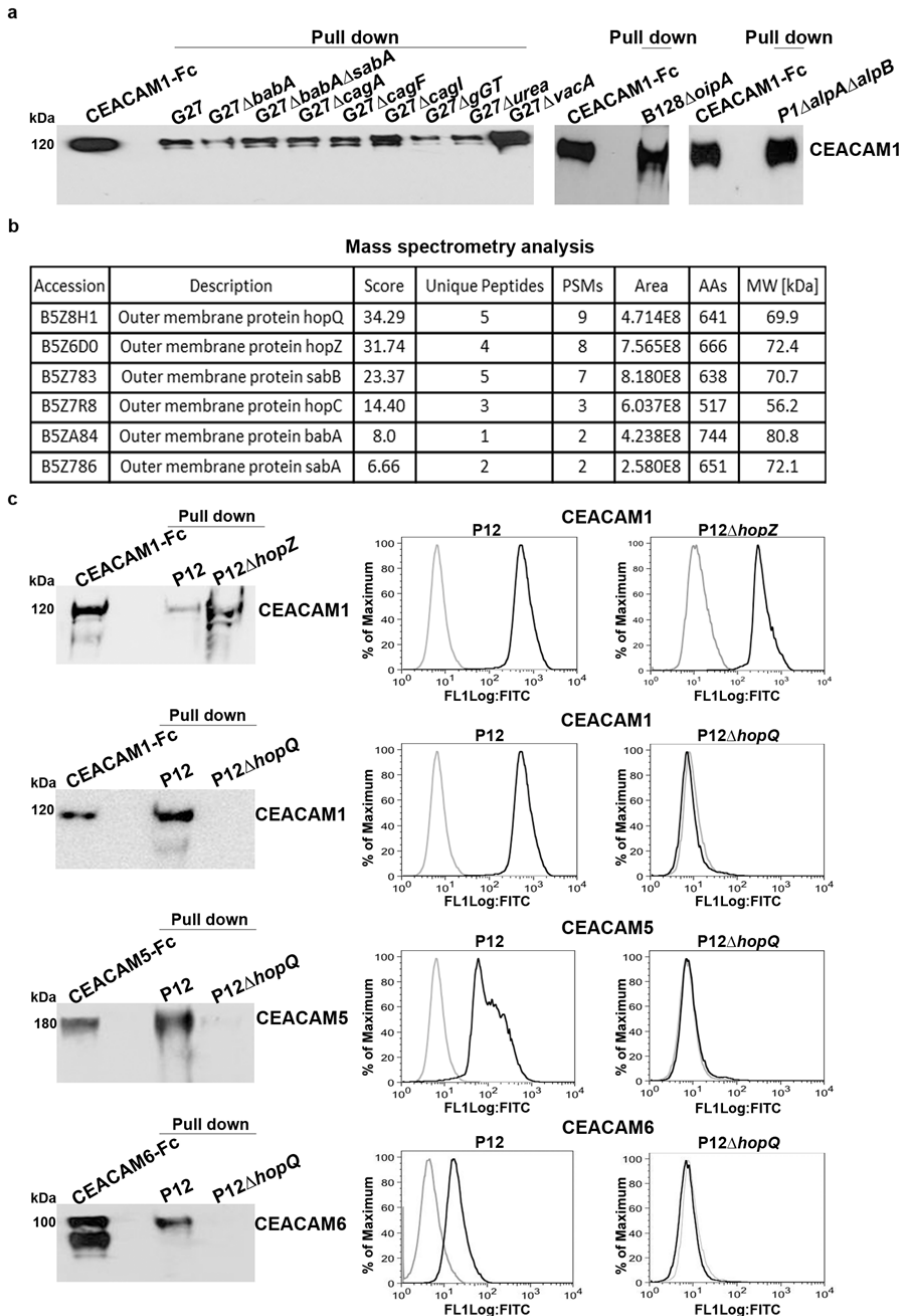


878

879

880 **Figure 2 *H. pylori* binding to CEACAM1 orthologues.** (a) *H. pylori* G27 strain binding to
 881 human, murine, bovine and canine CEACAM1 determined by flow cytometry. (b) and (c) *H.*
 882 *pylori* (G27) binding to rat-CEACAM1-Fc (b) and rat-CEACAM1ΔN-Fc (c) detected by
 883 western blot after bacterial pull down. (d) Binding of G27 *H. pylori* strain to rat-CEACAM1
 884 and rat-CEACAM1ΔN detected by flow cytometry. (e) Representative confocal images of *H.*
 885 *pylori* binding to human, rat and mouse CEACAM1-expressing CHO cells. Untransfected
 886 CHO served as control. Scale bars: left panels, 25 μm, right panels, 10 μm. (f) *H. pylori* G27
 887 pull down of whole cell lysates of untransfected, human-, mouse- and rat CEACAM1-
 888 transfected CHO cells. CEACAM1 was detected using species-specific CEACAM1
 889 antibodies, as indicated. Representative experiments are shown (n=3).

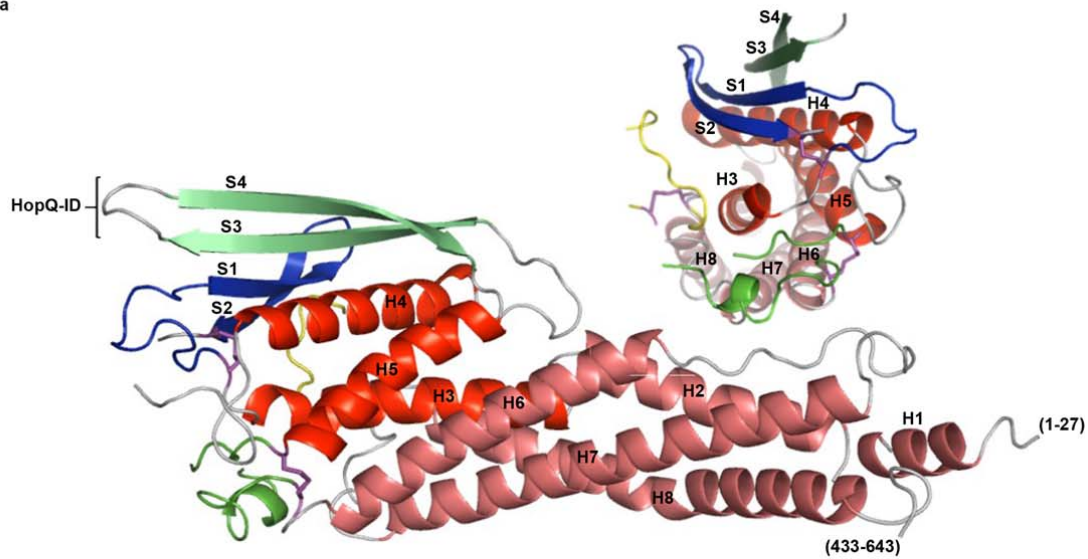
Gerhard Fig. 3



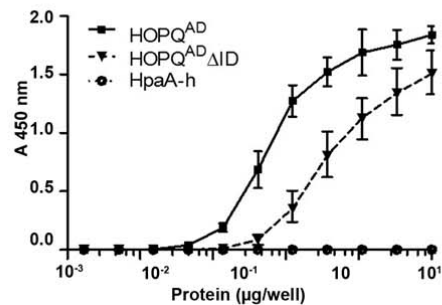
890

891 **Figure 3 *H. pylori* binds to CEACAM1 via HopQ.** (a) Human CEACAM1 detected by
 892 western blot after pull down of various *H. pylori* G27 knockout strains incubated with human
 893 CEACAM1-Fc. (b) Candidate outer membrane proteins of *H. pylori* strain G27 binding to
 894 human CEACAM1-Fc (for complete MS table see Suppl. Table 1). (c) *H. pylori* strains P12,
 895 P12ΔhopQ and P12ΔhopZ binding to hu-CEACAM1-, CEACAM5- and CEACAM6-Fc
 896 detected by western blot and FACS analysis after pull down. Representative experiments are
 897 shown (n=3).

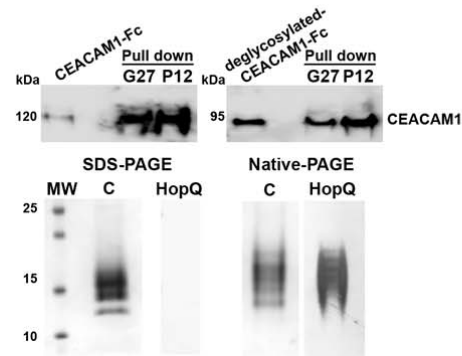
a



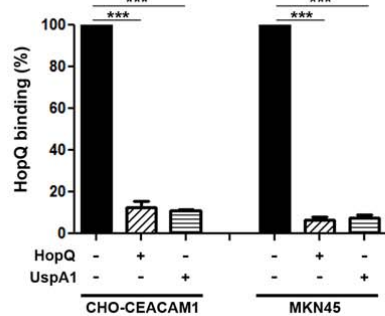
b



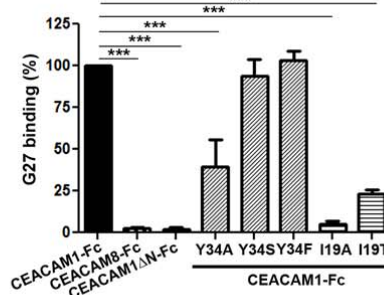
c



d



e



898

899 **Figure 4. X-ray structure and binding properties of the HopQ adhesin domain.**900 Ribbon representation of the HopQ^{AD} showing the 3+4-helix bundle topology (colored red

901 and brick, respectively). Three Cys pairs (Cys102-Cys131, Cys237-Cys269 and Cys361-

902 Cys384) conserved in most Hop family members pinch off extended loops are colored blue,

903 yellow and green. HopQ-ID; green, β -hairpin insertion. (b) ELISA titers of HopQ^{AD} or mutant904 HopQ^{AD} lacking the HopQ-ID (HopQ^{AD} Δ ID) binding to increasing concentrations of C1-N905 domain (C1ND) ($n=4$, mean, S.D.). (c) Upper panel, pull down experiments of *H. pylori*

906 strains incubated with de-glycosylated human CEACAM1-Fc. Lower panel, SDS and native

907 page of C1ND stained with Coomassie-blue (“C”) or with HopQ^{AD} in a far western blot
908 (“HopQ”) experiment. (d) HopQ binding (%) to CEACAM1 in CHO and MKN45 cells after
909 pre-incubation with recombinant HopQ or UspA1, respectively. Mean, S.D. of three
910 independent experiments are shown. (e) *H. pylori* G27 binding (%) to CEACAM1,
911 CEACAM1ΔN and different CEACAM1 variants. CEACAM8 was used as negative control.
912 Mean, S.D. of three independent experiments are shown. One-way ANOVA with Bonferroni’s
913 correction for multiple comparisons. ***P≤0.001.

914

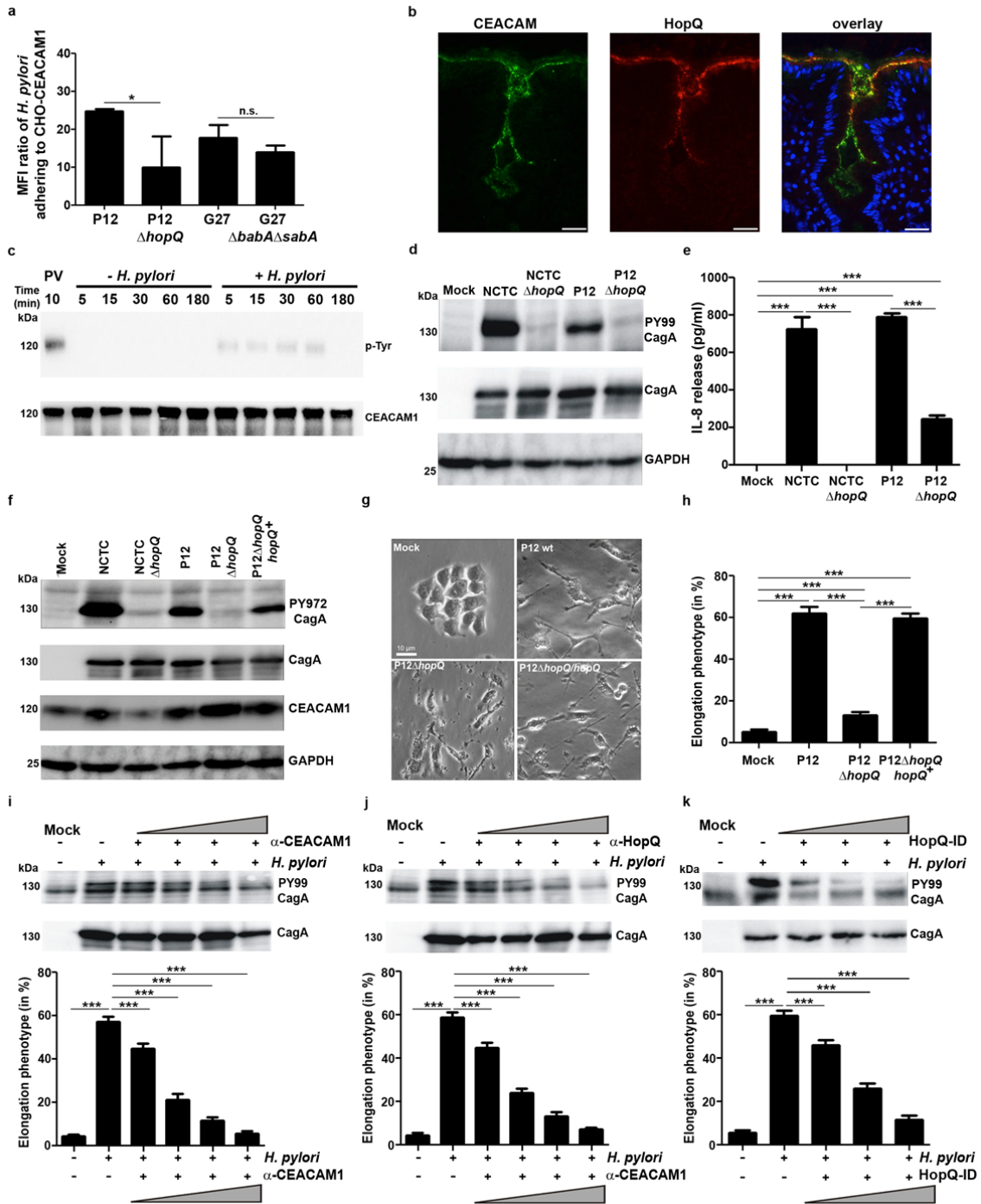
915

916

917

918

Gerhard Fig. 5

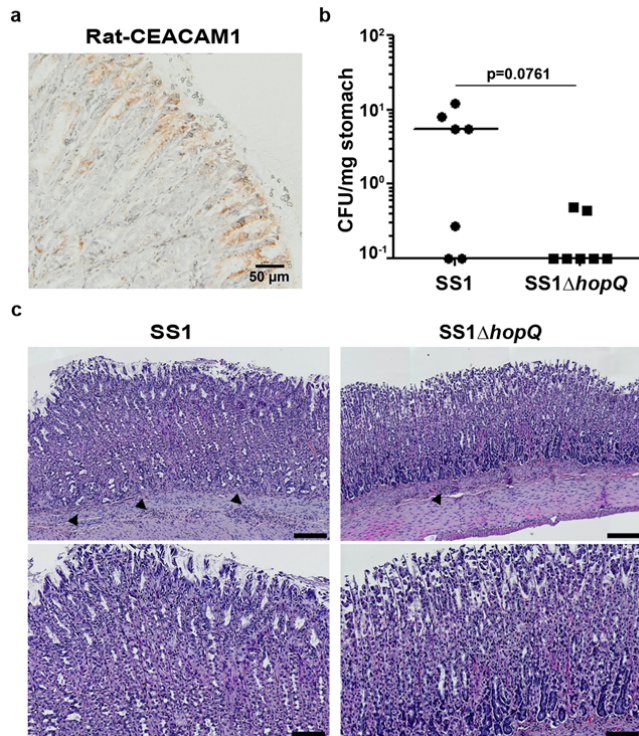


919

920 **Figure 5 Deletion of *hopQ* in *H. pylori* leads to reduced bacterial cell adhesion and**
 921 **abrogates CagA delivery, IL-8 release and cell elongation. (a) *H. pylori* binding to CHO-**
 922 **hu-CEACAM1-L cells detected by flow cytometry analysis (n=3). Means \pm S.D. are shown.**
 923 **Two-tailed *t*-test, * $P \leq 0.03$. (b) Immunofluorescence detection of apical CEACAM**
 924 **expression (green) and HopQ binding (red) in the gastric epithelium from human gastritis**
 925 **biopsies. Scale bar 25 μ m. (c) CEACAM1 Tyr-phosphorylation and total CEACAM1 levels in**

926 uninfected and *H. pylori*-infected CHO-CEACAM1-L cells. Pervanadate (PV) treatment
927 served as positive control. (d) CagA phosphorylation detected in lysates of AGS cells after
928 infection with *H. pylori* P12, NCTC11637 and corresponding isogenic *hopQ* mutants (e)
929 Secreted IL-8 by AGS cells after infection with the indicated *H. pylori* strains (mean, S.D. of
930 three independent experiments are shown). One-way ANOVA with Bonferroni's correction for
931 multiple comparisons. ***P≤0.001. (f) CagA phosphorylation and CEACM1 levels in HA-
932 tagged HEK293-hu-CEACAM1 transfectants infected with indicated *H. pylori* strains. (g)
933 Representative phase contrast micrographs of AGS cells infected for 6 h with P12, P12Δ*hopQ*
934 or P12Δ*hopQhopQ*⁺ re-expressing wt *hopQ* gene. (h) Quantification of elongation phenotype
935 induced in AGS cells after infection with the indicated *H. pylori* strains. Data (mean, S.D.) of
936 three independent experiments are shown. One-way ANOVA with Bonferroni's correction for
937 multiple comparisons. ***P≤0.001. (i) CagA phosphorylation and quantification of the
938 elongation phenotype (five different 0.25-mm² fields) after *H. pylori* P12 infection of AGS
939 cells pre-treated with 2, 5, 10 or 20 μg of α-CEACAM Ab (lanes 3-6). Data (mean, S.D.) of
940 three independent experiments are shown. One-way ANOVA with Bonferroni's correction for
941 multiple comparisons. ***P≤0.001. (j) CagA phosphorylation and quantification of the
942 elongation phenotype after infection of AGS with wild type *H. pylori* pre-treated with 2, 5, 10
943 or 20 μg of α-HopQ (lanes 3-6) Data (mean, S.D.) of three independent experiments are
944 shown. One-way ANOVA with Bonferroni's correction for multiple comparisons.
945 ***P≤0.001. (k) CagA phosphorylation in *H. pylori*-infected AGS cells pre-incubated with a
946 HopQ-derived peptide (1 μM, 2.5 μM and 5 μM) corresponding to the HopQ-ID (aa 189-
947 220). Cell elongation (mean, S.D.) from 3 independent experiments is shown. One-way
948 ANOVA with Bonferroni's correction for multiple comparisons. ***P≤0.001.
949

Gerhard Fig. 6



950

951 **Figure 6** *H. pylori* colonization of rat stomach depends on HopQ. (a) CEACAM1
952 expression in rat stomach. (b) *H. pylori* colony forming units (CFU) per mg stomach of male
953 Sprague dawley rats after 6 weeks infection. Horizontal bars indicate medians. Mann-Whitney
954 U test. (c) Hematoxylin/eosin staining of infected rat stomachs. Representative images of
955 same stomach regions are shown. Scale bar 100µm (upper panels) and 200µm (lower panels).
956 Arrows denote inflammatory cells.